FOR UNRESTRICTED DISTRIBUTION

DATE ______________________ WNES

468 054

7907200305

WESTINGHOUSE CLASS 3

WCAP-9405

STUDY OF REACTOR VESSEL UPPER HEAD REGION FLUID TEMPERATURE

R. H. McFetridge

D. C. Garner

December 1978

APPROVED: [signature] T. M. Anderson, Manager
Nuclear Safety Department

APPROVED: [signature] J. D. Nastasy, Manager
Reactor Internals and Drive Line Equipment

Work performed under Shop Order YYHX-25

WESTINGHOUSE ELECTRIC CORPORATION
Nuclear Energy Systems
P. O. Box 355
Pittsburgh, Pennsylvania 15230

468 065

ACKNOWLEDGMENT

The authors would like to thank each of the utilities participating in the plant measurement program for their assistance in obtaining and transmitting the data on a timely basis.

We also acknowledge the work performed on the 1/5-scale model at the Westinghouse R and D Center by D. T. Beecher, C. J. Kapral, R. D. Hamacher, N. J. Wilds and G. Miklos.

We would like to particularly acknowledge J. M. Makiel of the Westinghouse R and D Center for his assistance during the design, construction, and testing phases of the 1/5-scale model test and for providing descriptions of the test facility and testing procedures.

TABLE OF CONTENTS

468 067

TABLE OF CONTENTS (cont)

468 068

LIST OF ILLUSTRATIONS

LIST OF ILLUSTRATIONS (cont)

468 070

LIST OF ILLUSTRATIONS (cont)

468 071

LIST OF TABLES

468 072

SECTION 1
BACKGROUND INFORMATION ON INCREASED TEMPERATURE OF VESSEL UPPER HEAD FLUID TEMPERATURE

During the design development of the Westinghouse 4-loop plant with upper head injection (UHI), it became apparent that the percentage of flow directed into the vessel head to achieve a head fluid temperature equal to vessel inlet temperature would have to be increased over that of current standard 4-loop plants. This assessment was due to the fact that upper internals support columns in plants with UHI have flow paths which provide direct communication between the vessel head plenum and the upper core plate region. Using the best analytical techniques available at the time, a decision was made to divert 0.9 percent of the total coolant flow into the vessel head plenum to achieve the vessel inlet temperature (T_{cold}) in this zone.

Testing of a 1/7-scale UHI plant model was begun. This test was structured principally as a reactor internals vibration test program to qualify the new design in that regard. During the last phase of this testing, static pressure taps were installed in six RCC guide tubes to verify that a nonuniform distribution of guide tube pressure existed with a magnitude capable of sustaining the flow of hot fluid into the head. With the limited UHI pressure data obtained from this test, some verification of the analytical techniques and guide tube pressure distributions assumed for the flow analysis was achieved.

However, it was realized that other analytical models could also support the test data. At this point, development of other anlalytical models was initiated to better predict the results of the 1/7 scale UHI tests. In addition, planning for further testing was begun to more accurately assess upper head fluid temperature and flow conditions. It was decided to equip eleven RCC guide tubes with static pressure taps in the 1/7-scale, 14-foot core, 4-loop flow model test. (Essentially, one complete quadrant of guide tubes was instrumented.)

A new analytical model was subsequently developed for predicting the upper head fluid temperature of all 2-, 3-, and 4-loop designs. When applied, the new hydraulic prediction model indicated that more vessel head cooling flow was theoretically required, (in varying degrees, depending on plant type), to achieve a T_{cold} condition in the vessel upper head. The need for experimental and operating plant data became more important to verify these new findings. However, no mechanical equipment problems had been experienced or were foreseen for normal operation, nor was any assessment made of the possible implications associated with SAR accident analyses.

The availability of data on upper head fluid temperatures in operating plants was investigated. Investigation showed that one plant (Connecticut Yankee) had one thermocouple installed in the vessel upper head plenum which could yield the fluid temperature in this region. Data obtained for this point indicated that the fluid temperature in the vessel head at 100 percent power was in the range of [ ]^{b,c,e} percent of the difference between vessel inlet and outlet temperature, i.e., [ ].^{b,c,e} Since this reading represented only one data point, further verification and additional data were required. It was decided that further verification would be obtained from the previously mentioned experimental confirmation of the guide tube pressure distribution from the 14-foot, 4-loop, 1/7-scale model test. (Subsequent application of th the analytical prediction model to the Connecticut Yankee plant configruation indicated that the head fluid temperature would be [ ]^{b,c,e} percent of the difference between vessel inlet and outlet temperature, i.e., [ ]^{b,c,e}

Data from the 1/7-scale, 14-foot core, 4-loop model test were obtained, reduced, and analyzed. Test data supported the basic techniques in the analytical prediction model, verifying that the pressure profile associated with the guide tubes is sufficient to cause a flow of water that exits from the core up through RCC guide tubes in the central portion of the array with a return path down through the peripheral RCC guide tubes. This influx of T_{hot} water causes the vessel head fluid temperature to become somewhat greater than vessel inlet temperature. A more detailed description of the flow paths, pressure gradients, and analytical model is given in section 2 of this report.

With the flow paths and static pressure distribution phenomena thus acceptably substantiated and with minor modifications to the analytical prediction model, investigation of other implications of possible effects on LOCA/ECCS and other accident analyses were begun using the new predicted elevated vessel upper head fluid temperatures. The analysis revealed peak cladding temperature penalties (in varying degree, dependent on plant type) and larger pressure gradients across the reactor internals upper support plate. These results were brought to the attention of the Westinghouse Water Reactor Division Safety Review Committee on August 4, 1976, and resulted in the notification of customers and the NRC of an unreviewed safety question on August 5, 1976.

An action plan was formulated to expand the data bases by: (1) obtaining more temperature readings for fluid temperature in the vessel heads of operating plants; and (2) performing subscale model testing. The remainder of this report presents the results obtained when the expanded data base was used.

468 074

SECTION 2
ANALYTICAL MODEL FOR UPPER HEAD TEMPERATURE CALCULATION

2-1. INTRODUCTION

An analytical model for estimating upper head region fluid temperature during normal operation has been developed. To estimate the upper head region fluid temperature with the analytical model, numerous boundary conditions must be known. The boundary conditions used are based on experimental data obtained from a series of three hydraulic tests conducted at the Westinghouse Forest Hills facility.

This section contains a description of the analytical method and test programs, a summary of the pertinent test results, and correlates the test data as a set of design curves. Discussion of comparisons between the predicted and measured results are presented in this report under the 1/5-scale model and in-plant measurement program sections.

2-2. DESCRIPTION OF ANALYTICAL MODEL

To determine the mean temperature of the fluid in the upper head region of the reactor, the temperature and flow rate of all fluid crossing the boundary of the region must be known. Figure 2-1 depicts the various flow paths into or out of the upper head region. There are three potential flow paths by which flow crosses the upper head region boundary in a reactor. These paths are the head cooling spray nozzles, the support columns, and the guide tubes. In plants equipped with upper head injection (UHI), all three flow paths are present. For plants without UHI, the support columns are not a flow path. The following discussion is applicable to the UHI plant. Therefore, for designs without UHI, reference to support columns should be neglected.

The geometry of a typical head cooling spray nozzle is shown in figure 2-2. The head cooling spray nozzle is a flow path between the downcomer region and the upper head region. The temperature of the flow which enters the head via this path corresponds to the cold leg value (i.e., T_{cold}).

468 075

13465-1

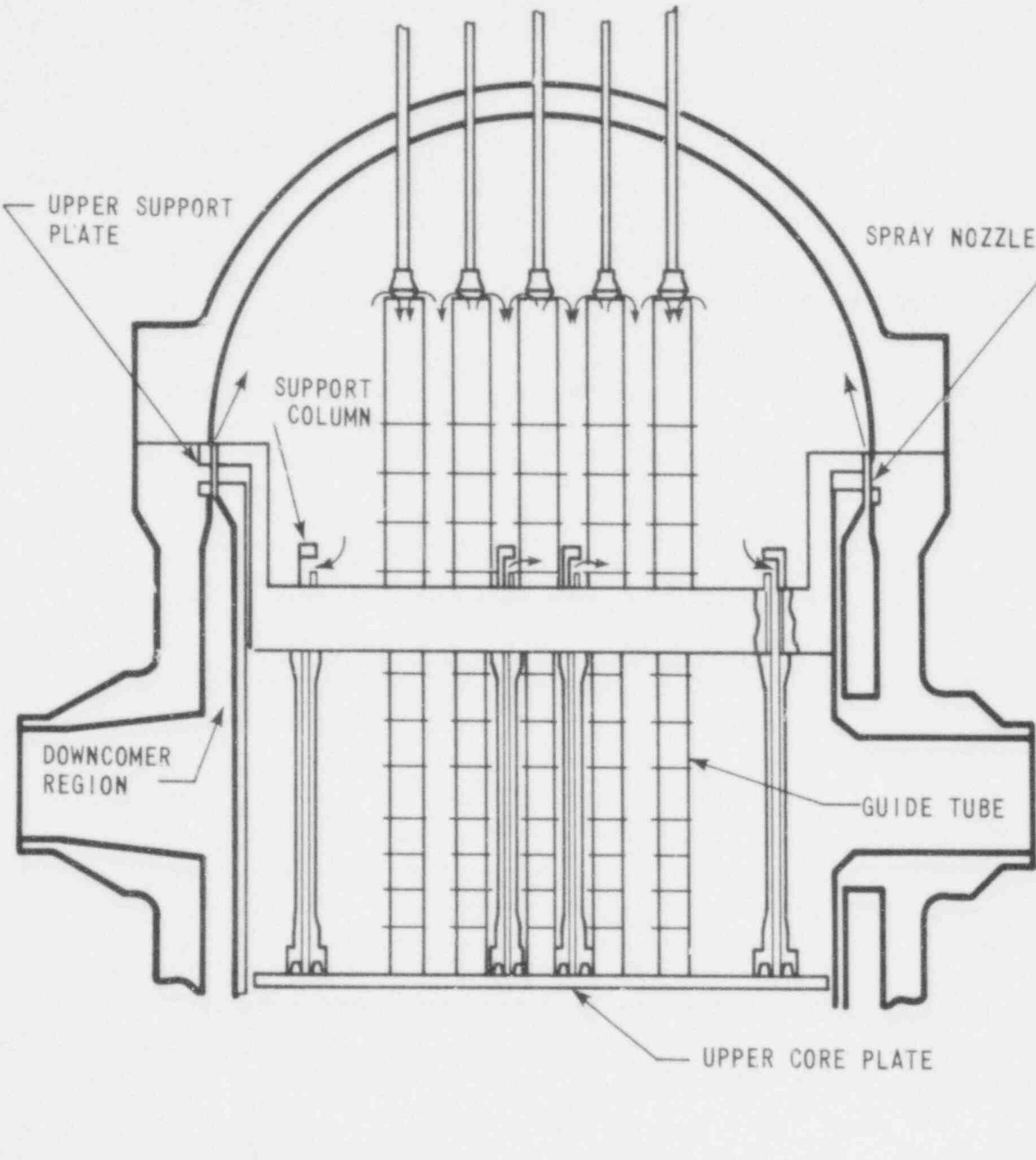

Figure 2-1. Reactor Upper Head Region Flow Paths

468 076

13465-2

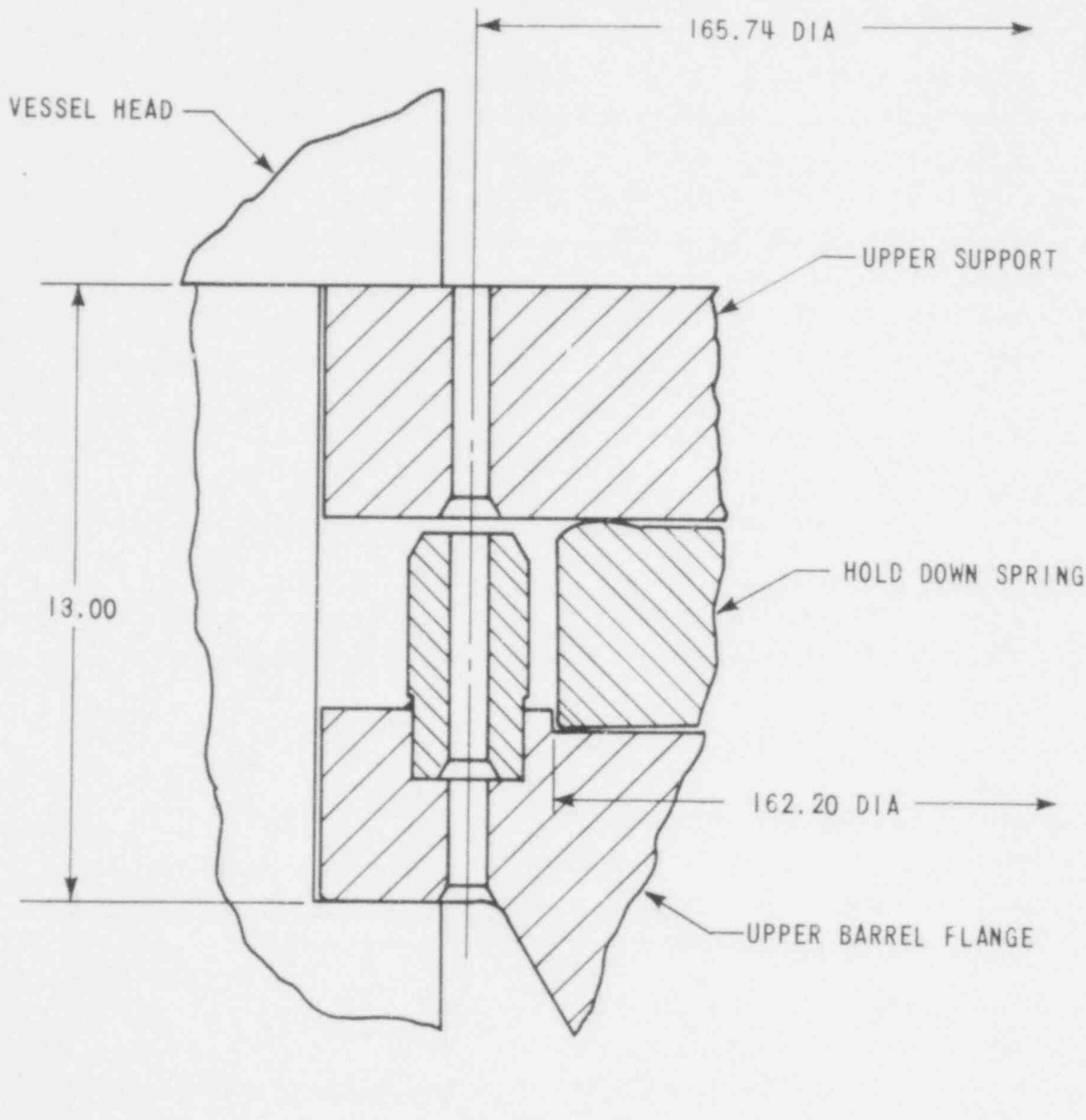

Figure 2-2. Typical Head Cooling Spray Nozzle

468 077

The amount of flow entering the head region via this path is accurately known. Fluid may also be exchanged between the upper plenum region (i.e., the portion of the reactor between the upper core plate and the upper support plate) and the upper head region via the support columns and guide tubes. It can be seen from figure 2-1 that the support columns and guide tubes are dispersed in the upper plenum region from the center to the periphery. Because of nonuniform pressure distribution at the upper core plate elevation, the pressure in the support columns and guide tubes varies from location to location. Based on experimental data obtained from scale-model flow testing, which will be discussed in a later section, the pressure in any support column or guide tube is a function of the distance from the hot leg outlet nozzle to that column or tube. The support column or guide tube pressure increases as the distance from the outlet nozzle increases. These support column and guide tube pressure variations create the potential for flow to either enter or exit the upper head region via the support columns or guide tubes. Any flow which enters the upper head region via the support columns and guide tubes is at a temperature approximately equal to the hot leg value (i.e., T_{hot}). Flow that exits the upper head region via the support columns or guide tubes is assumed to have a fluid temperature corresponding to the mixed mean temperature of the fluid entering the upper head region via the support columns, guide tubes, and head cooling spray nozzles. This assumption is based on the following:

- The upper head cooling flow exits from the nozzle as a high-momentum jet (V=61 ft/sec) that produces substantial entrainment and mixing.
- The flows exiting the guide tubes and support columns are also jets (V<4.5 ft/sec and V<7.6 ft/sec, respectively) thus producing substantial entrainment and mixing.
- Stratification due to density gradients should be minimal, as the directions of the flows oppose the density gradient (i.e., the cold flow is jetting upward and the hot flow is jetting laterally or downward).

As a consequence of the above inlet flow velocities and directions, the flow pattern in the head is considered to resemble a toroidal vortex with flow upward near the surface of the head and downward near the centerline of the vessel. Thermal stratification is considered to be negligible and the head fluid is considered as a "mixed mean temperature."

Due to the relatively large volume and low velocities in the upper head region, except for variations due to the elevation at which the flow enters or exits the flow paths, the pressure of the region is assumed to be uniform. A graphic summary of the above discussion is shown in figure 2-3.

468 078

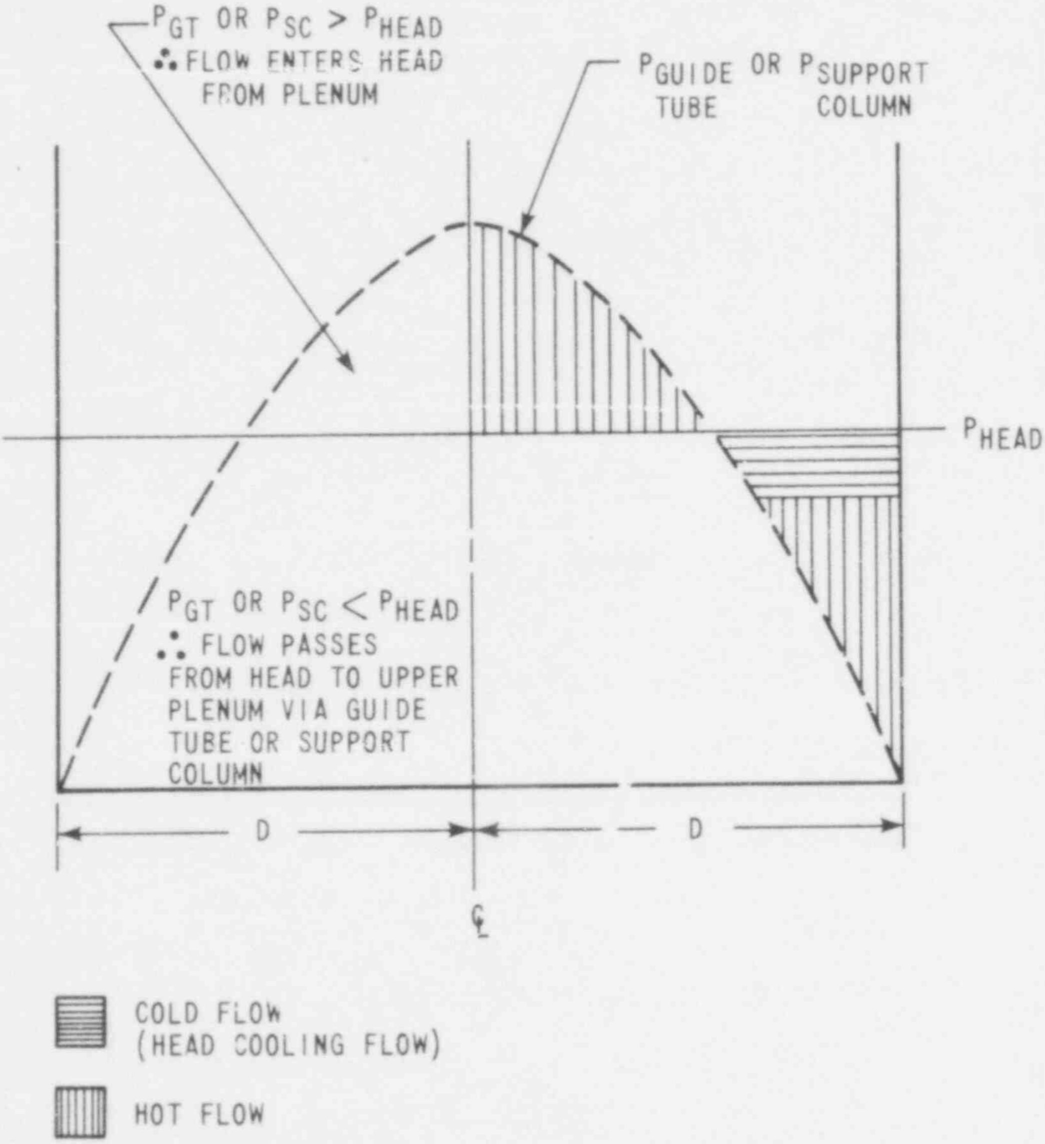

Figure 2-3. Effect of Non-Uniform Guide Tube and Support Column Pressure Distribution on Upper Head Region

468 079

Based on the experimental support column and guide tube pressure distributions and the head cooling spray nozzle flow rate, it is possible to determine the mixed mean fluid temperature of the upper head region as outlined in the following steps:

1. Assume an upper head region pressure.

2. For each support column and guide tube location, calculate the pressure differential between the upper head region and that support column or guide tube. If the pressure differential is positive, flow will enter the upper head region. If the pressure differential is negative, flow will exit the upper head region.

3. Determine the total amount of hot leg temperature flow entering the upper head region via the support columns and guide tubes by summing the flows of all the support columns and guide tubes with a positive pressure differential. The flow rate calculation is based on the experimentally determined support column and guide tube hydraulic characteristics, the pressure differential calculated in Step (2) above, and the vessel hot leg nozzle density according to the following equation

$$W_{T_{\text{flow into head}}} = \sum_{i=1}^{n} \sqrt{\frac{(P_{SC_i} - P_{head})\ (2gc)\ (144)\ \rho_{T_{hot}}}{K_{SC}}}\ (A_{SC_i})$$

$$+ \sum_{i=1}^{m} \sqrt{\frac{(P_{GT_i} - P_{head})\ (2gc)\ (144)\ \rho_{T_{hot}}}{K_{CT}}}\ (A_{GT_i})$$

4. Determine the mixed mean fluid temperature and density of the upper head region by calculating the mean temperature of the head cooling spray nozzle flow and the core outlet flow entering the head via the guide tubes and support columns. The following equations are employed

$$h_{\substack{\text{hot flow}\\ \text{into head}}} = f\ (t_{hot},\ 2250\ \text{psia})$$

$$h_{\substack{\text{spray}\\ \text{nozzle}\\ \text{flow}\\ \text{into head}}} = f\ (t_{cold},\ 2250\ \text{psia})$$

468 080

$$h_{\substack{\text{mixed}\\\text{mean head}}} = \frac{(h_{t_{\substack{\text{hot flow}\\\text{into head}}}})(W_{t_{\substack{\text{hot flow}\\\text{into head}}}}) + (h_{\substack{\text{spray nozzle}\\\text{flow into head}}})(W_{\substack{\text{spray nozzle}\\\text{flow into head}}})}{(W_{t_{\substack{\text{hot flow}\\\text{into head}}}} + W_{\substack{\text{spray nozzle}\\\text{flow into head}}})}$$

$$t_{\substack{\text{mixed}\\\text{mean head}}} = f\,(h_{\substack{\text{mixed}\\\text{mean head}}}, 2250 \text{ psia})$$

$$\rho_{\substack{\text{mixed}\\\text{mean head}}} = f\,(t_{\substack{\text{mixed}\\\text{mean head}}}, 2250 \text{ psia})$$

where,

h = enthalpy, Btu/lb_m

t = temperature

W = mass flow rate, lb_m/sec

g_c = gravitational constant, $32.174 \dfrac{lb_m \cdot ft}{lb_f - sec^2}$

P = pressure, psi

ρ = fluid density, lb_m/ft^3

K = hydraulic loss coefficient

A = flow area, ft^2

and subscripts are as follows

head refers to head region

SC refers to support column

GT refers to guide tube

T refers to "total"

5. Determine the total amount of mixed mean head temperature fluid exiting the upper head region via the support columns and guide tubes by summing the flows of all the support columns and guide tubes with a negative pressure differential. The flow rate calculation is based on the experimentally determined support column and guide tube

468 081

hydraulic characteristics, the pressure differential calculated in Step (2), and the upper head region mixed mean fluid temperature according to the following equation

$$W_{T_{\substack{\text{mixed mean temp.}\\ \text{exiting head}}}} = \sum_{i=1}^{J} \sqrt{\frac{(P_{head} - P_{SC_i})(2g_c)(144)\ \rho_{\substack{\text{mixed}\\ \text{mean head}}}}{K_{SC}}}\ (A_{SC_i})$$

$$+ \sum_{i=1}^{K} \sqrt{\frac{(P_{head} - P_{GT_i})(2gc)(144)\ \rho_{\substack{\text{mixed}\\ \text{mean head}}}}{K_{GT}}}\ (A_{GT_i})$$

6. Determine if mass is conserved by adding the head cooling nozzle flow results from Step (4) and subtract result of Step (5). If the result of this operation is zero, the flow patterns and flow rates have been determined along with the corresponding mixed mean temperature of the upper head region. The above operation expressed arithmetically is

Flow Into Head Region = Flow Out of Head Region

$$0 = W_{\substack{\text{head cooling}\\ \text{spray nozzle}}} + W_{T_{\substack{\text{hot flow}\\ \text{into head}}}} - W_{T_{\substack{\text{mixed mean temp.}\\ \text{exiting head}}}}$$

7. If the result of Step (6) is not zero, assume a new value of the upper head region pressure and repeat Steps (2) through (6).

2-3. DESCRIPTION OF EXPERIMENTAL TESTING RELATED TO GUIDE TUBE, SUPPORT COLUMN, AND UPPER PLENUM-UPPER HEAD REGION HYDRAULIC CHARACTERISTICS

To assess the hydraulic characteristics of guide tubes, support column, and the interaction between the upper plenum and upper head region of a UHI reactor, experimental data were obtained from three independent tests. The three tests performed were:

- UHI Flow Distribution Test.
- 1/7-Scale UHI Upper Internals Test.
- 1/7-Scale 414 Flow Test.

A brief description of each test and a discussion of the information obtained is presented.

468 082

2-4. UHI Flow Distribution Test

The test facility shown in figure 2-4 was designed to facilitate isothermal hydraulic testing of a full-scale 17 x 17 fuel assembly guide tube and UHI support column enclosed in a common test vessel to demonstrate the compatibility of their hydraulic characteristics. The tests were performed at low-pressure and low-temperature conditions, and at flow rates which bracketed flow conditions experienced in actual plant and UHI operation; 150-300 gpm/assembly for UHI tests and 1000-2000 gpm/assembly for normal plant tests.

The facility was instrumented with pitot-static tubes for measuring dynamic pressure and, in conjunction with static pressure wall taps, for measuring static pressure differentials. Several differential pressure transducers were used to convert the pressure signal to a recordable electronic signal, which was monitored by two 4-channel recorders. The instrumentation locations are shown in figure 2-5. Pitot-static tubes were placed in the following strategic locations:

- In the lower plenum baffle, approximately 12 inches below the upper core plate at both the column and guide tube locations. These locations provided a measurement of the respective assembly inlet flows.
- In the lower guide tube bottom plate and "cards", to determine the flow distribution of the lower guide tube.

The static pressure wall taps located in the upper plenum baffle provided a measurement of the static pressure differential across the upper core plate. This measurement facilitated the calculation of the core outlet unrecoverable pressure loss and the pressure loss coefficient. The static pressure wall taps located inside the column and guide tube provided measurement of the static pressure difference between each column and tube.

In addition to the instrumentation mentioned above, a Bourdon tube pressure gage and a 450-gallon water collection system were employed during some phases of the testing to determine the overall hydraulic loss coefficients of the guide tube and support column.

The results of this experimental work, as related to the upper head region calculations, can be summarized as follows:

- The overall hydraulic resistance of the guide tube and support column from the upper core plate elevation to the upper head region were determined.
- The difference between the internal pressure of the support column and the equivalent value within the guide tube was [ ]b,c,e psi at typical reactor conditions. This value is applicable in the central core locations where the upper plenum flow patterns were simulated in the test vessel.

468 083

8999-6

c,e

Figure 2-4. 17 x 17 Upflow Test Facility, Cross Section

468 084

8999-7

c,e

Figure 2-5. 17 x 17 Upflow Test Instrumentation

- The pressure in the support column was found to be equal to the total pressure of the flow at the exit of the support column, i.e., at the core plate fuel assembly interface.

2-5. 1/7-Scale UHI Upper Internals Test

The primary purpose of the 1/7-scale, UHI upper internals test was to verify the mechanical integrity of the UHI upper internals hardware (i.e., flow loadings on the critical guide tubes and support columns). In addition to the acquisition of mechanical data, hydraulic data were obtained relating to the upper core plate flow and static pressure distribution and the variation in pressure in the guide tubes.

The test apparatus consisted of a 1/7-scale simulation of the reactor vessel, lower reactor internals structures, and UHI upper reactor internals structures. The test facility provided flow rates up to 140 percent of the prototype values at fluid temperatures in the range of 170°F.

The hydraulic instrumentation in this 1/7-scale model consisted of the following:

- Static pressure taps located in the guide tubes along an imaginary line from the center of the core to the center of the vessel outlet nozzle (see figure 2-6). The static pressure taps were located in the vicinity of the top side of the upper support plate (refer to figure 2-1). This instrumentation provided data regarding the variation of pressure in the upper section of the guide tube as a function of the distance of a particular core location away from the vessel outlet nozzle.

- Static pressure taps located at various locations on the upper side of the upper core plate at the radial positions, shown in figure 2-7. This instrumentation provided data regarding the variation in static pressure at the upper core plate as a function of the distance from the vessel outlet nozzle.

- Pitot-static tubes located in the upper core plate assembly along an imaginary line from the center of the core to the center of the vessel outlet nozzle as shown in figure 2-7. The data obtained from this instrumentation provided information regarding the variation in dynamic pressure at the upper core plate as a function of distance from the vessel outlet nozzle.

Data were obtained from the above-mentioned instrumentation for flow rates ranging from 50 to 140 percent of the prototype value. The data were normalized to a value corresponding to the core outlet conditions of a plant. The normalized results are shown graphically in figures 2-8 through 2-10.

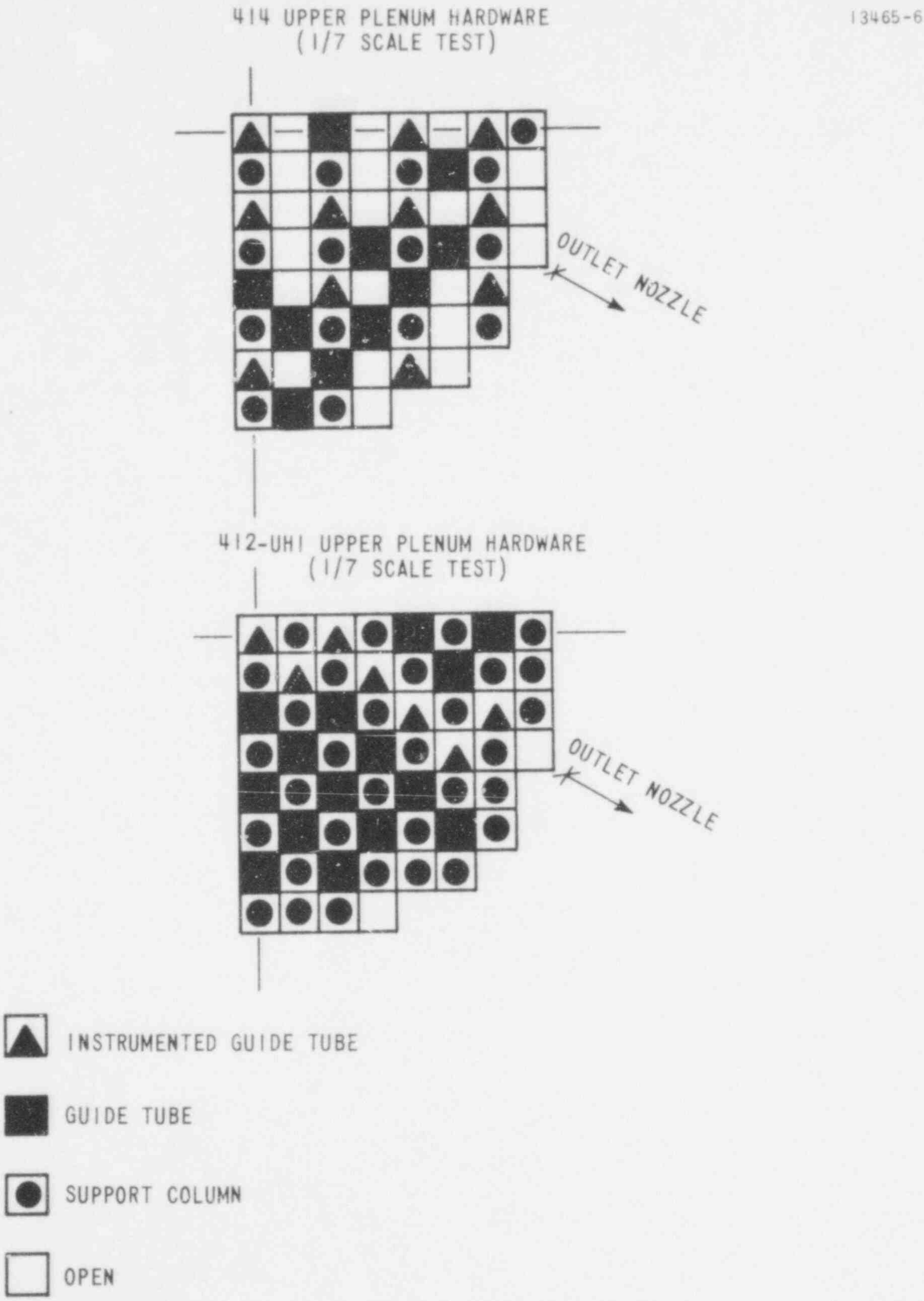

Figure 2-6. 1/7-Scale Model Guide Tube Static Pressure Taps

468 087

13465-7

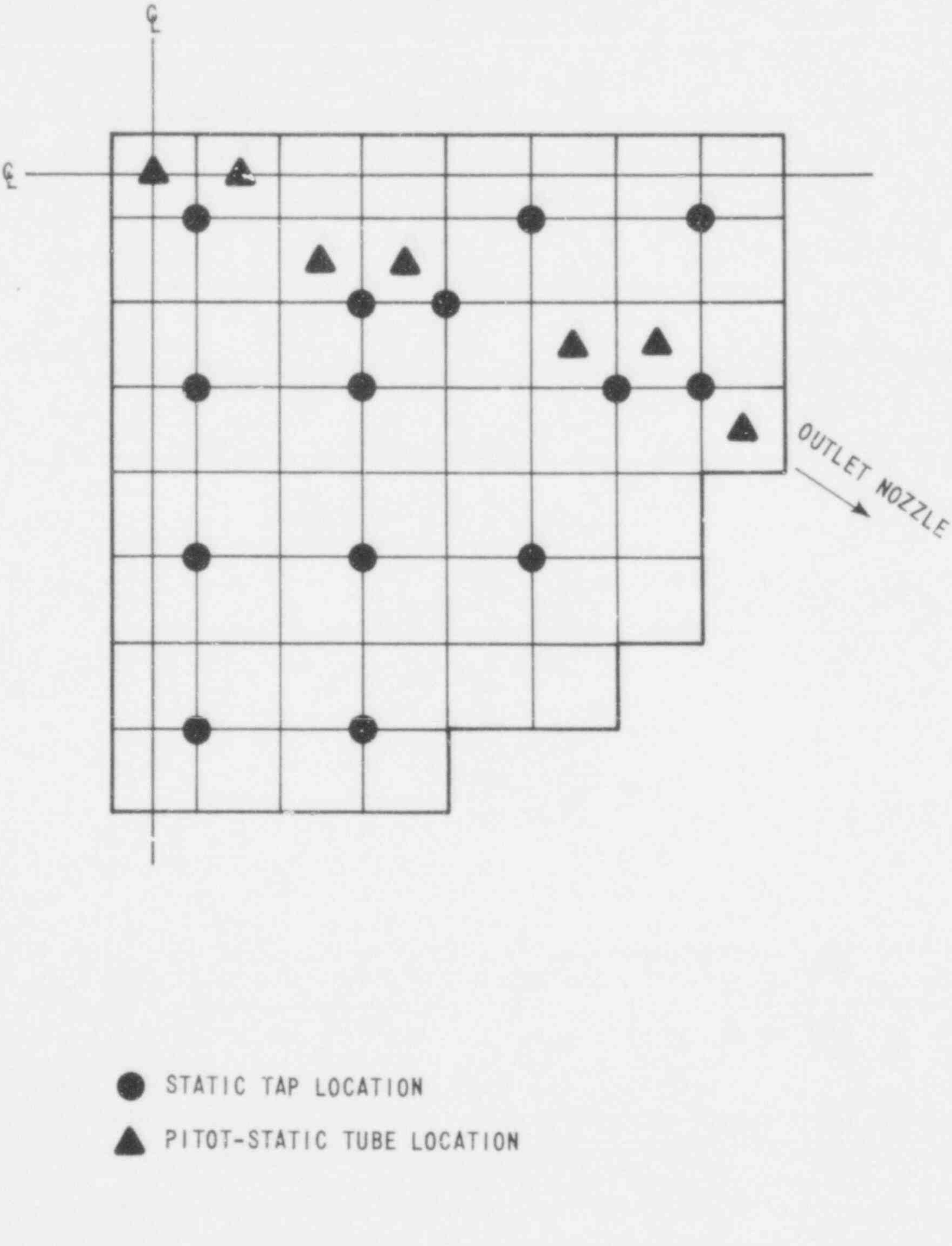

Figure 2-7. 412-UHI 1/7 Scale Model Upper Core Plate Pressure Tap Locations

468 088

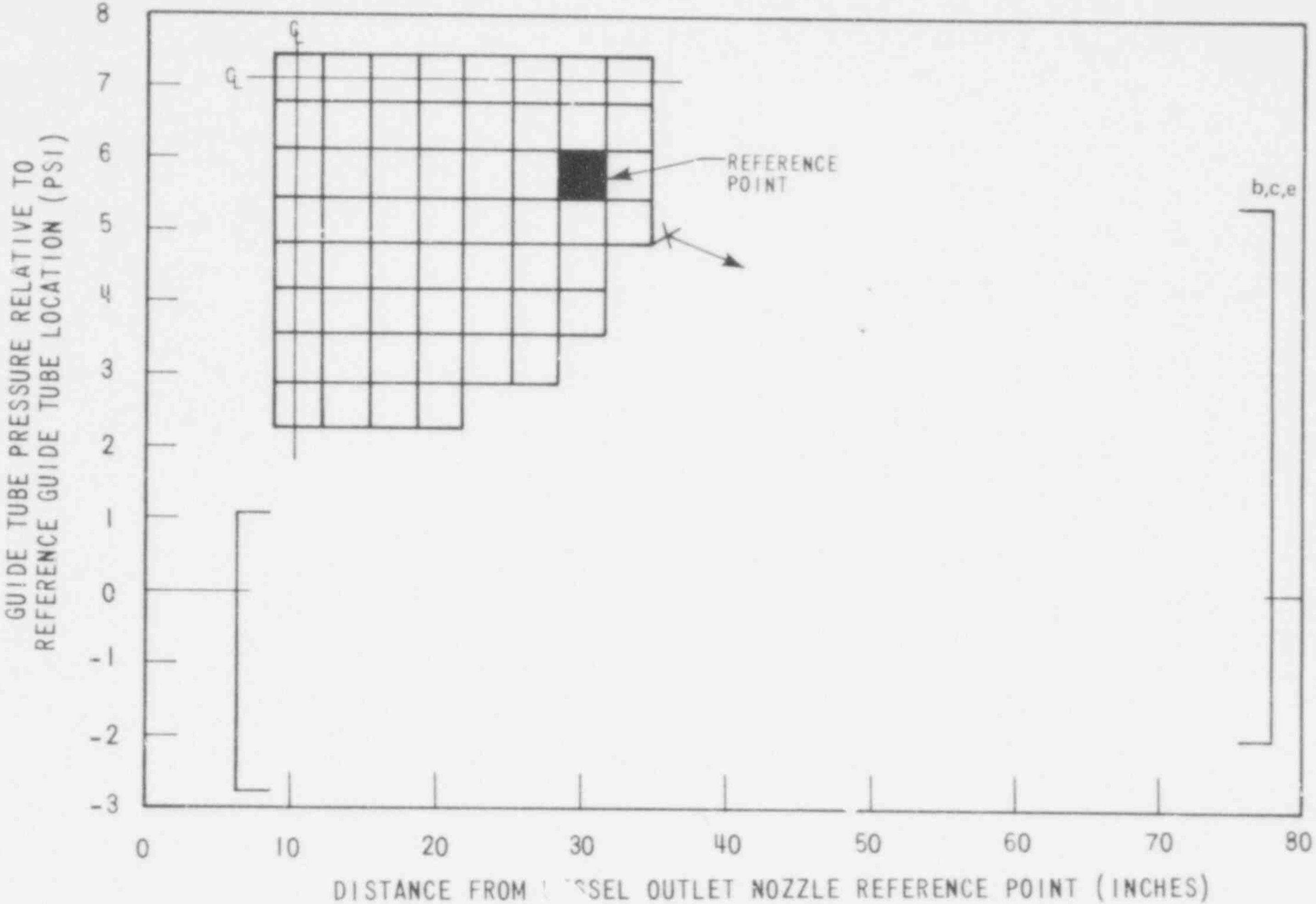

13465-8

Figure 2-8. Comparison of 414 & 412 UHI Guide Tube Pressures Relative to Peripheral Guide Tube Location (Normalized to Plant Conditions)

468 069

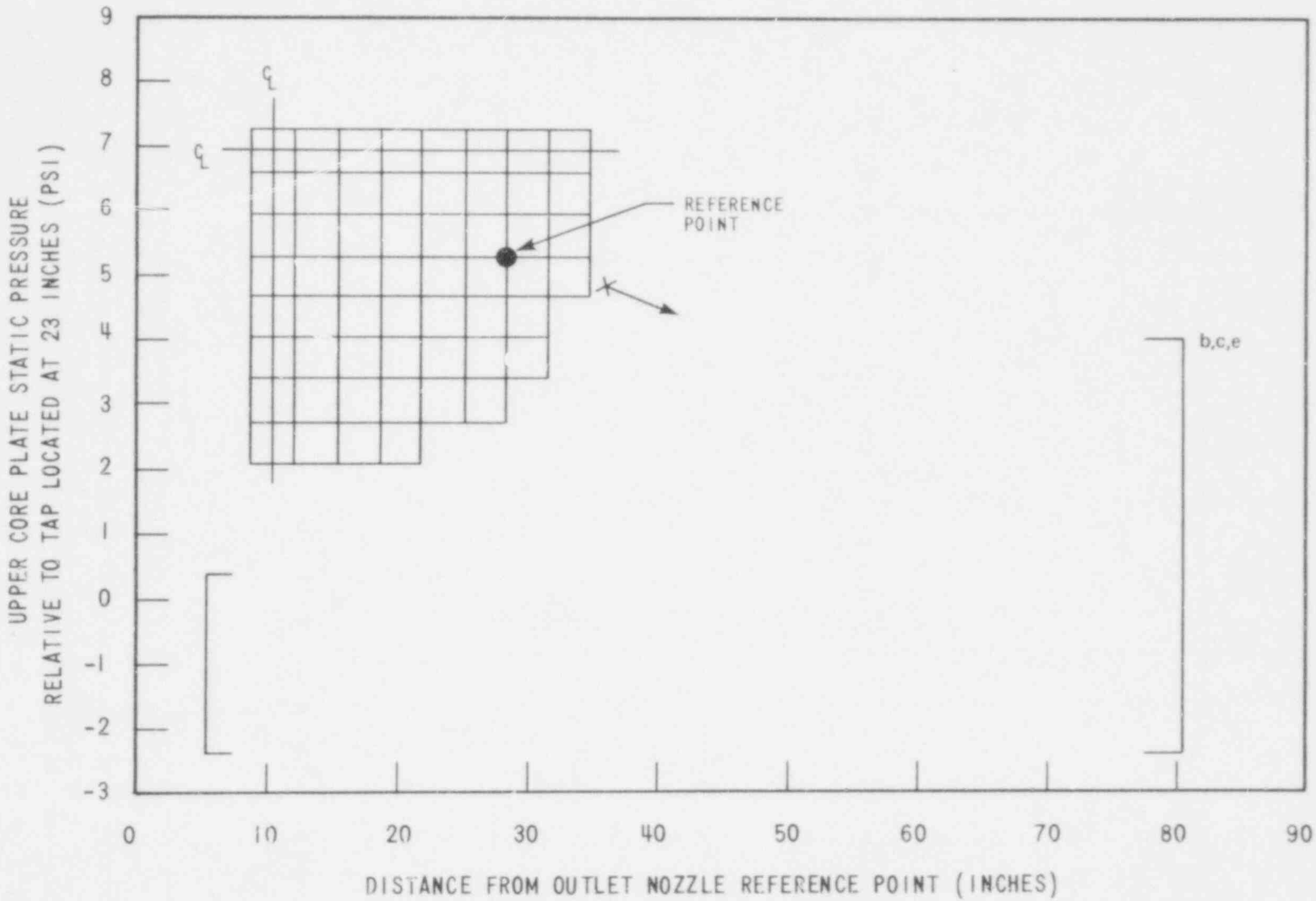

Figure 2-9. Upper Core Plate Static Pressure Distribution Measured During 412-UHI 1/7 Scale Model Test (Normalized to Plant Conditions)

468 090

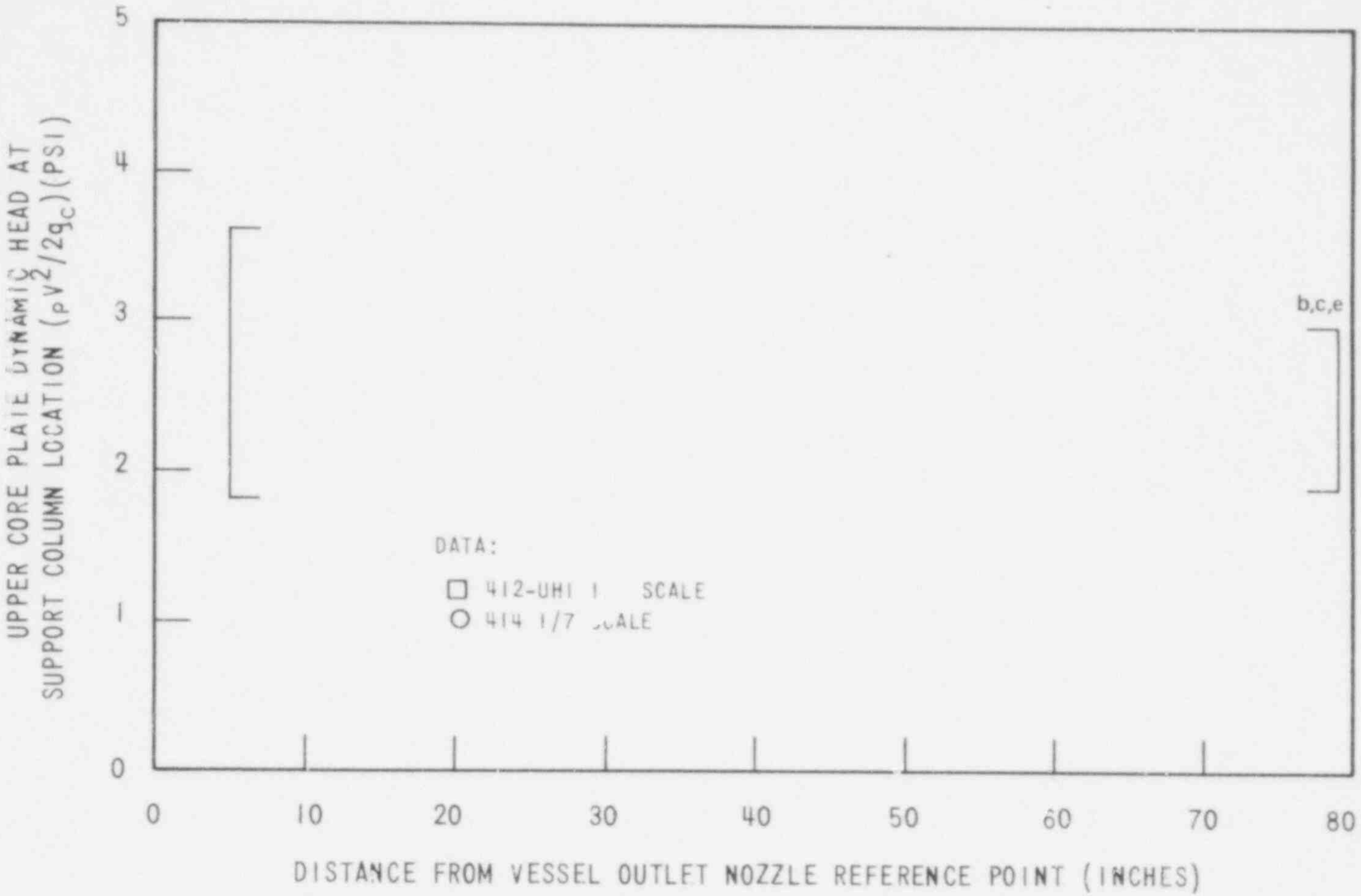

Figure 2-10. Comparison of 414 & 412 UHI Upper Core Plate Dynamic Head at Support Column Location (Normalized to Plant Conditions)

13465-10

Figure 2-8 depicts the variation in upper guide tube pressure relative to the guide tube closest to the vessel outlet nozzle. The abscissa of the figure corresponds to the prototype rather than the model and, in addition, the distance from the vessel outlet nozzle reference point corresponds to the straight-line length from the center of a particular core location to a point along the centerline of the vessel outlet nozzle at the inside diameter of the barrel.

The normalized results reflect the definite relationship between the upper guide tube pressure as a function of the distance away from the vessel outlet nozzle. This variation in upper guide tube pressure corresponds to the skew which will exist in the plant.

Figure 2-9 depicts the variation in the static pressure at the upper core plate normalized to prototype conditions. The variation in static pressure has been referenced to the tap location closest to the vessel outlet nozzle. This information reflects the relationship between the upper core plate static pressure as a function of the distance away from the vessel outlet nozzle and corresponds to the skew which will exist in the UHI plant.

Figure 2-10 depicts the variation in upper core plate dynamic head at a support column location as a function of distance from the vessel outlet nozzle. This variation corresponds to the skew in support column dynamic head which will exist in the UHI plant.

2-6. 1/7-Scale 414 Flow Test

The primary purpose of the 1/7-scale 414 flow test was to verify that the core inlet flow distribution associated with a single lower core support plate concept was as uniform as the previous lower core plate and lower support plate configuration which had been tested previously.

The test apparatus consisted of a complete 1/7-simulation of the reactor vessel, lower reactor internals structures, and a UHI-style upper reactor internals structures. The test facility provided flow rates ranging from 70 to 140 percent of the prototype values at fluid temperatures in the range of 170°F.

The hydraulic instrumentation used in this model and related to evaluation of the vessel upper head region is as follows:

- Static pressure taps located in the upper section of various guide tubes (as shown in figure 2-6) at an elevation in the upper support plate. As can be seen from the figure, the instrumented guide tubes were dispersed throughout the entire quadrant of the core to further verify the relationship between guide tube pressure and distance away from the vessel outlet nozzle. These data provided further verification of the guide tube pressure variation measured in the 1/7-scale UHI flow test.

- Flow venturi devices located at the outlet of each fuel assembly location in the instrumented quadrant. These data provided additional verification of the upper core plate dynamic head at the support column locations.

Data were obtained from the above-mentioned instrumentation for flow rates ranging from 70 to 100 percent of the prototype value. The data were normalized to a value corresponding to the core outlet conditions of a plant. The normalized results are shown graphically in figures 2-8 and 2-10. It can be seen from the figures that the 1/7-scale 414 hydraulic data agree very well with the 1/7-scale UHI hydraulic data and thus further substantiate information employed in the evaluation of the plant upper head region fluid temperature.

2-7. Test Data Correlation and Design Curves

To determine the pressures in the support columns and guide tubes for each location in a UHI plant, it was necessary to combine the information from the three tests. In this process, the data from the UHI flow distribution test were used to establish the absolute pressure difference between the two components in the center of the core. The variation in guide tube pressure and support column pressure across the core was taken from the scale model data.

The variation in guide tube internal pressure across the upper plenum was measured directly on both the 1/7-scale tests and correlates well with distance of the guide tube from the vessel outlet nozzle (figure 2-8). The pressure within the support column was not measured directly on the 1/7-scale tests. It has therefore been established from the variations of static pressure and core outlet dynamic pressure measured in these tests. This was done by combining the two pressures to obtain the total pressure at the core plate. The basis for this comes from the UHI flow distribution test in which the support column pressures were measured and found to be equal to the total pressure at the elevation of the upper core plate. Thus, the support column pressure variation across the core can be established by adding the curves in figures 2-9 and 2-10. The absolute variation between the support column pressure variation and the guide tube pressure variation was established from the UHI flow distribution test data in which a pressure differential of [ ]^{b,c,e} psi was recorded. This is applicable in flow regimes similar to those near the center of the core so that the [ ]^{b,c,e} differential may be observed on the design curves (figure 2-11) at 60 inches from the outlet nozzle.

468 093

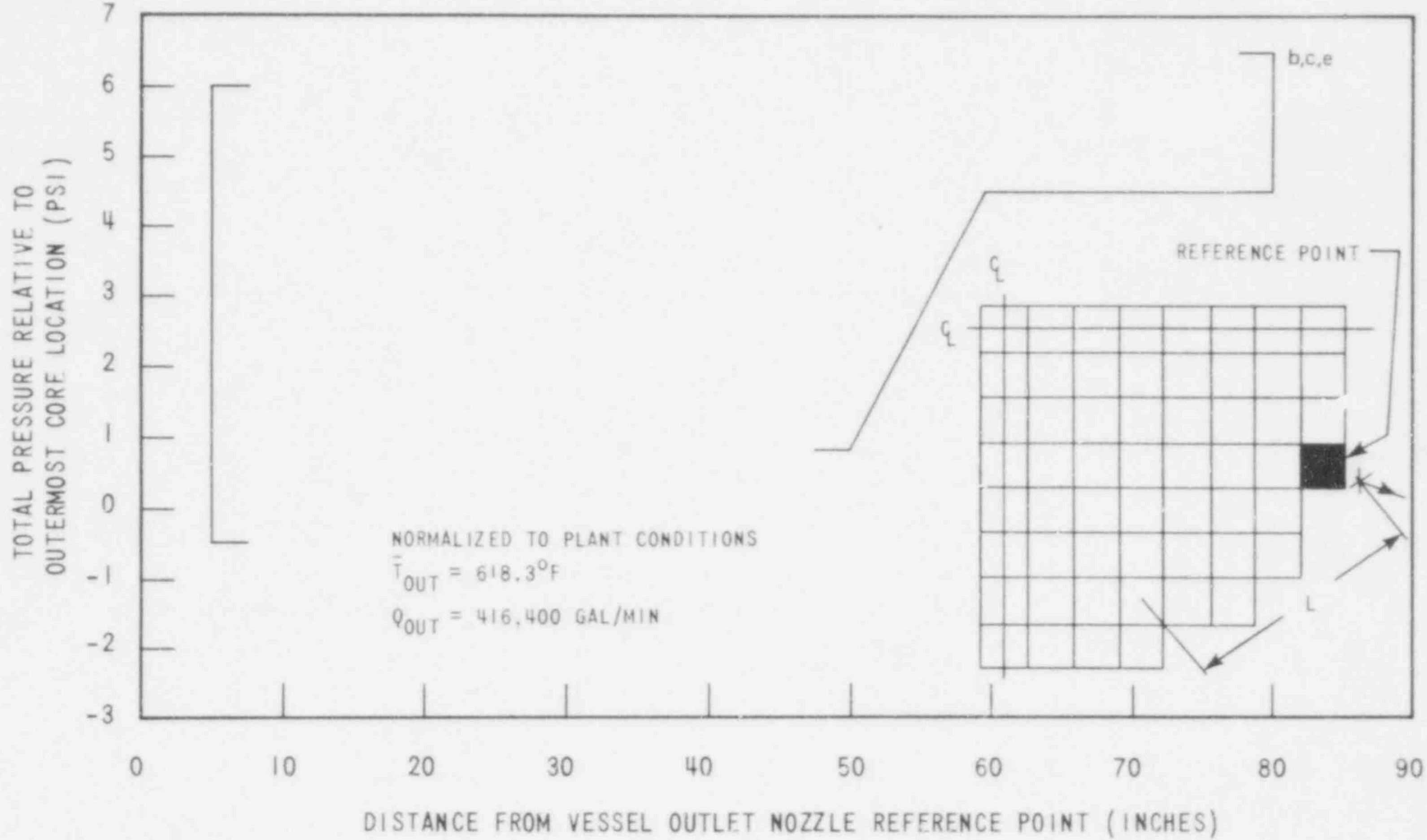

13465-11

Figure 2-11. Guide Tube & Support Column Total Pressure Distribution Employed in 412-UHI Upper Head Region Fluid Temperature Analysis

468 09A

SECTION 3
1/5-SCALE MODEL UPPER HEAD TEMPERATURE TEST

3-1. TEST OBJECTIVES

The overall objective of the test is to experimentally determine the relationship between normal operation (i.e., steady-state) temperatures in the reactor vessel upper head region and the "head cooling" flow rate. Within this general objective it is necessary to

- Determine the upper head region fluid temperature distribution in a 4-loop plant with UHI for the nominal head cooling flow rate of 0.92 percent of total vessel flow.
- Determine the upper head region fluid temperature distribution in a 4-loop plant with UHI for head cooling flows ranging from 0.92 percent of total vessel flow to the amount required to maintain the upper head region fluid temperature at the reactor vessel inlet value (i.e., T_{cold}).
- Determine the upper head region fluid temperature distribution in a 4-loop plant without UHI for head cooling flows ranging from 0.34 percent of total vessel flow to the amount required to maintain the upper head region fluid temperature at the reactor vessel inlet value (i.e., T_{cold}).

3-2. GENERAL MODEL DESCRIPTION

The 1/5-scale upper head region fluid temperature test model consisted of a half-hemisphere geometry with a diameter of approximately 36 inches (1/4.67 scale). The upper head region of the 4-loop UHI style plant was modeled with simulation of the reactor vessel head radius and the reactor internals components including the upper guide tubes, stub ends of the support columns, thermal sleeves, drive rods, UHI injection ports, and head cooling spray nozzle jets. Figures 3-1 and 3-2 present the elevation and plan views of the section modeled. The McGuire Unit 2 plant (DBP) was considered the reference plant for the 4-loop UHI design and flow via the support columns for the 4-loop plant without UHI was eliminated.

The model was designed to accommodate variable head cooling flow rates (ranging from zero to 4 percent of total vessel flow) without significant changes in head cooling spray nozzle jet velocity. The model was capable of accommodating water temperature of 140°F to allow the necessary temperature differential (~70°) for mixing measurements, and a salt solution was employed to duplicate the in-plant density gradients. The front section of the model was

468 095

13465-12

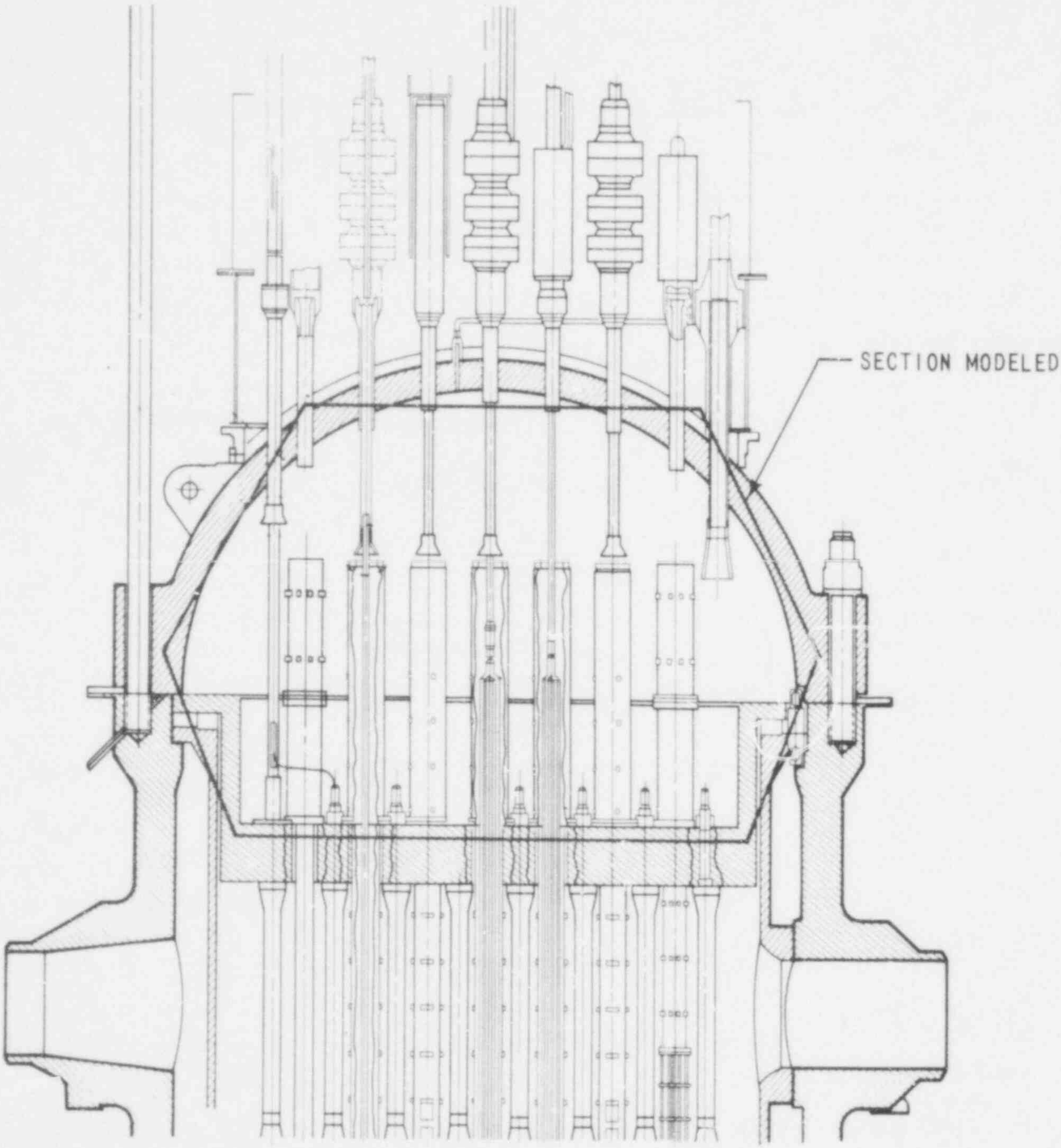

Figure 3-1. Model Description, Elevation View

468 096

13465-13

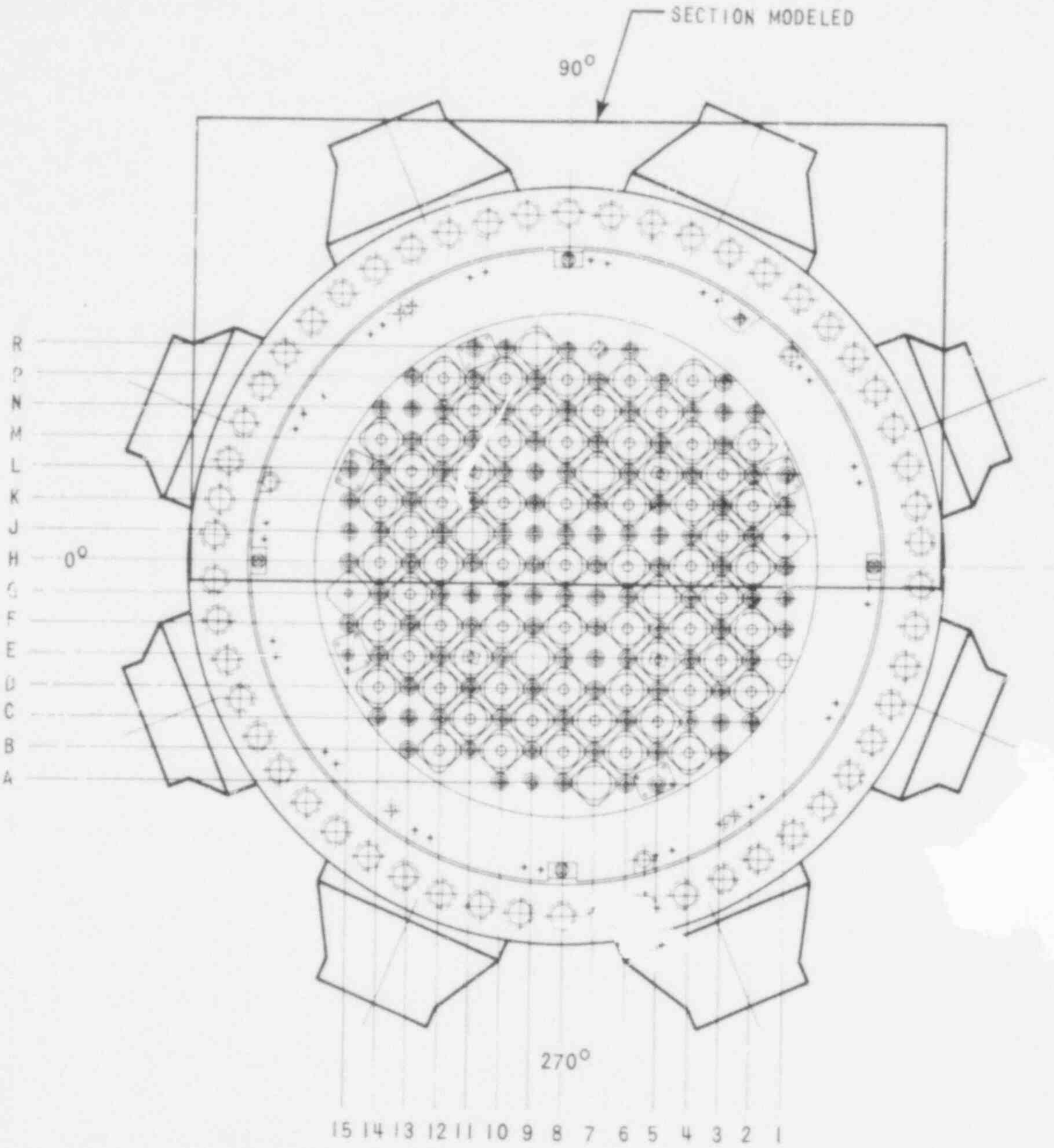

Figure 3-2. Model Description, Plan View With Head Removed

468 027

constructed of Lexan and dye injection ports were incorporated to facilitate viewing of the flow patterns.

A known flow rate was directed into the upper head region via the head cooling spray nozzles. The guide tube and support column pressure distributions were based on the results of the 414 1/7-scale model, UHI 1/7-scale model, and UHI flow distribution tests. The support column and guide tube pressure distributions were maintained by using standpipes of a specified height. Pressure measurements were obtained for each standpipe to verify the pressure distribution. In addition, the standpipes were designed to maintain a constant density over the entire length of the standpipe (i.e., prevent salt solution from entering the standpipe).

The upper head region of the model contained 60 thermocouples to monitor temperatures in the region. Additional thermocouples indicated the temperature of the head cooling spray flow and the standpipe flow prior to entering the model. The thermocouples were connected to a data acquisition system which sampled two thermocouples a second. To obtain the desired density variation it was necessary to use a salt solution. Also, to better control the salt solution and the temperature of the "hot" fluid, it was decided to inject "hot" salt water into the head cooling jets and employ "cold" pure water for the guide tubes and support columns. The resulting density gradients in the model are the same as in a plant; however, the temperatures will be exactly the opposite of those in the plant (i.e., in the model the "hottest" temperature corresponds to the "coldest" temperature in plant).

3-3. DISCUSSION OF MODELING

Modeling is discussed in the following paragraphs from the standpoint of similarity, boundary conditions, the standpipe system, and placement of thermocouples.

3-4. Model Similarity

The following is a list of parameters considered to be significant in the determination of flow and temperature patterns in the upper head region:

- Momentum and direction of flow entering and exiting the region.
- Density/buoyancy effects associated with temperature differences between flow entering the region via the head cooling nozzle and via the guide tubes/support columns.
- Viscous drag associated with hardware components in the upper head region.
- Variations in specific heat between the head cooling and guide tube/support column flow.

468 098

By considering the above parameters, it is possible to preserve thermal and hydraulic similarity between the model and the plant. The above parameters are therefore modeled accurately where feasible, and conservatively where precise scaling could not be achieved. Model/plant similarity was accomplished through use of geometric scaling, the Richardson number, the Euler number, the Reynolds number, the Peclet number, and the ratio of specific heats and densities.

The geometric similartiy of the upper head region has been preserved by use of a linear scale factor (1/4.67) on all dimensions, with particular attention to inlet and outlet flow path geometrie The numerical value of the scale factor was selected to provide a practically sized mode, and facilitate the use of a standard size hemispherical head.

The Richardson number is a ratio of gravity force/inertial force and, as shown in the following discussion, the model value will exactly simulate the plant value. The Richardson number is defined as follows:

$$N_{RI} = \frac{(-g/\rho)\ (\delta\rho/\delta L)}{(\frac{\delta V^2}{\delta L})}$$

where

g = gravitation constant 32.2 ft/sec^2.

ρ = density, lb$_m$/ft^3.

V = velocity, ft/sec

L = length, ft

The Richardson number can also be expressed as,

$$N_{RI} = \frac{-g(\Delta\rho/\Delta L)}{\rho\left(\frac{\Delta V}{\Delta L}\right)^2} = \frac{-g(\rho_1-\rho_2)\Delta L}{\rho\Delta V^2}$$

In this form it is easier to visualize the physical significance of the Richardson number. To assure similarity between the plant and the model Richardson number, the following evaluation was performed:

$$\frac{-g\ (\rho_1-\rho_2)_{plant}\ (\Delta L)_{plant}}{\rho_{plant}\ \Delta V^2_{plant}} = \frac{-g\ (\rho_1-\rho_2)_{model}\ (\Delta L)_{model}}{\rho_{model}\ \Delta V^2_{model}}$$

then

$$\Delta L_{model} = \frac{\Delta L_{plant}}{4.67}$$

and

$$\frac{(\rho_1-\rho_2)_{model}}{\rho_{model}} = \frac{(\rho_1-\rho_2)_{plant}}{\rho_{plant}}$$

Therefore, after substitution,

$$\left(\frac{\rho_{plant}}{\rho_{model}}\right)\left(\frac{1}{4.67}\right)\left(\frac{(\rho_1-\rho_2)_{model}}{(\rho_1-\rho_2)_{plant}}\right)\Delta V^2_{plant} = \Delta V^2_{model}$$

At this point, the only parameter which has not been specified is ΔV^2_{model}, which can be determined as follows:

Water in the plant at 558.1°F and 2250 psi:	ρ = 46.36 lb_m/ft^3
Water in the plant at 627.1°F and 2250 psi:	ρ = 40.58 lb_m/ft^3
22% by weight salt water in model at 140°F and 14.7 psi:	ρ = 71.24 lb_m/ft^3
Water in model at 60°F and 14.7 psi:	ρ = 62.35 lb_m/ft^3

and for the guide tube and support column flow,

$$\left(\frac{40.58}{62.35}\right)\left(\frac{1}{4.67}\right)\left(\frac{8.89}{5.78}\right)\Delta V^2_{\substack{plant\\GT/SC}} = \frac{1}{4.67}\Delta V^2_{\substack{plant\\GT/SC}} = \Delta V^2_{\substack{model\\GT/SC}}$$

Similarly, for the head cooling flow:

$$\left(\frac{46.36}{71.24}\right)\left(\frac{1}{4.67}\right)\left(\frac{8.89}{5.58}\right)\Delta V^2_{\substack{plant\\SN}} = \frac{1}{4.67}\Delta V^2_{\substack{plant\\SN}} = \Delta V^2_{\substack{model\\SN}}$$

The preceding evaluation indicates that the Richardson number of the head cooling and guide tube/support column flows can be exactly simulated by scaling such that the ΔV^2_{model} = 1/4.67 ΔV^2_{plant}. To obtain the appropriate ΔV^2 scaling in the model, the plant pressures must be scaled by a factor of 1/3.04, as per the following discussion:

$$\frac{\Delta P_{model}}{\Delta P_{plant}} = \frac{(K\rho V^2)_{model}}{(K\rho V^2)_{plant}}$$

468 100

where

ΔP = pressure differential

K = hydraulic loss coefficient

ρ = density

V = velocity

Since the hydraulic loss coefficients in the model are assumed to be the same as the plant values:

$$\frac{\Delta P_{model}}{\Delta P_{plant}} = \frac{\rho_{model} \rho V^2_{model}}{\rho_{plant} \rho V^2_{plant}}$$

For the guide tube and support column locations:

$$V^2_{\substack{model \\ GT/SC}} = \frac{1}{4.67} V^2_{\substack{plant \\ GT/SC}}$$

$$\rho_{\substack{model \\ GT/SC}} = \frac{62.35}{40.58} \rho_{\substack{plant \\ GT/SC}}$$

And by substitution:

$$\Delta P_{\substack{model \\ GT/SC}} = \Delta P_{\substack{plant \\ GT/SC}} \frac{62.35}{40.58} \frac{1}{4.67} = \frac{1}{3.04} \Delta P_{\substack{plant \\ GT/SC}}$$

In the same manner, it can be shown that:

$$\Delta P_{\substack{model \\ SN}} = \frac{1}{3.04} \Delta P_{\substack{plant \\ SN}}$$

The Euler number corresponds to one-half the hydraulic loss coefficient, as shown below, with the appropriate unit corrections, and is a ratio of pressure force/inertial force.

$$\frac{(\Delta P)\ (2g_c)\ (144)}{\rho V^2} = K = \text{hydraulic loss coefficient}$$

$$\frac{g_c(\Delta P)\ (144)}{\rho V^2} = \text{Euler number}$$

For the Euler number in the model and the plant to be the same, the following must be true:

$$\frac{\Delta P_{model}}{(\rho V^2)_{model}} = \frac{\Delta P_{plant}}{(\rho V^2)_{plant}}$$

or

$$\Delta P_{model} = \Delta P_{plant}\left(\frac{\rho_{model}}{\rho_{plant}}\right)\left(\frac{V^2_{model}}{V^2_{plant}}\right)$$

$$= \Delta P_{plant}\left(\frac{1.54_{plant}}{\rho_{plant}}\right)\left(\frac{V^2_{plant}}{4.67\ V^2_{plant}}\right) = \Delta P_{plant}\ \frac{1}{3.04}$$

By simulating the Richardson number of the plant in the model it was necessary to reduce the plant pressures by a factor of 3.04. This reduction in pressure compensates for the dynamic head (i.e., ρV^2) differences in the plant and the model. The simulation of the Richardson number was based on the plant and model hydraulic loss coefficients being identical, which implies that the Euler number in the model and plant are identical. The above algebraic manipulations merely verify that if the pressures in the model are equal to 1/3.04 of the plant value, the Euler number in the model and plant will be identical.

The Reynolds number is a ratio of inertial force/viscous force. The following calculation indicates that the Reynolds number in the model will be approximately 1/100 of the plant Reynolds number. This indicates that Reynolds number similarity between the plant and model cannot be preserved. However, with respect to the test, a lower than in-plant Reynolds number implies that the turbulence intensity in the model will be lower than in plant. Decreased turbulence levels infer a greater potential for flow stratification in the model than in the plant. If stratified flow exists, large temperature gradients could exist in the upper head region; the latter is undesirable. Since the model has greater potential for flow stratification than the plant, the model test results will be conservative relative to the plant.

The Reynolds number is a ratio of inertial forces/viscous forces and can be expressed as:

$$N_{Re} = \frac{DV\rho}{\mu}$$

where

D = hydraulic diameter, ft
V = velocity, ft/sec
ρ = density, lb_m/ft^3
μ = viscosity, lb_m/ft-sec

468 102

Now, assuming exact simulation between the plant and model Reynolds number:

$$N_{Re_{model}} = \left(\frac{DV\rho}{\mu}\right)_{model} = \left(\frac{DV\rho}{\mu}\right)_{plant} = N_{Re_{plant}}$$

or

$$N_{Re_{model}} = N_{Re_{plant}} \left(\frac{D_{model}}{D_{plant}}\right)\left(\frac{V_{model}}{V_{plant}}\right)\left(\frac{\rho_{model}}{\rho_{plant}}\right)\left(\frac{\mu_{plant}}{\mu_{model}}\right)$$

From previous discussion:

$$D_{model} = \frac{D_{plant}}{4.67} \qquad V_{model} = \frac{V_{plant}}{\sqrt{4.67}}$$

$$\rho_{model} = 62.35\ lb_m/ft^3 \qquad \mu_{model} = 2.71$$

$$\rho_{plant} = 40.58\ lb_m/ft^3 \qquad \mu_{plant} = 0.23$$

Therefore

$$N_{Re_{model}} = N_{Re_{plant}} \left(\frac{1}{4.67}\right)\left(\frac{1}{\sqrt{4.67}}\right)\left(\frac{62.35}{40.58}\right)\left(\frac{0.23}{2.71}\right) = N_{Re_{plant}} \ (1.3 \times 10^{-2})$$

It should be noted that the decreased Reynolds numbers in the model could lead to nonconservative results because variations in hydraulic loss coefficients of the model guide tubes and support columns are greater than the in-plant values. Idel'chik [1] indicates that for "low" Reynolds numbers, contraction and expansion hydraulic loss coefficients tend to increase. To determine the relationship between the model guide tube and support column hydraulic loss coefficients and the Reynolds number, a flow test was performed for flow rates ranging from 0.3 to 3.75 gpm with 65°F water. The results of the test are shown in figure 3-3. It can be seen from the figure that the loss coefficients for upflow and downflow in the guide tube and support column vary with Reynolds number. However, in the range of interest for the guide tube (i.e., $N_{Re} > 5000$) and support column (i.e. $N_{Re} > 10{,}000$) the variation is less than 10 percent, which has a small impact on the upper head region fluid temperature.

Up to this point in the discussion, all similarity comparisions have been based on hydraulic parameters. With respect to thermal similarity, the dimensionless group of interest is the Peclet number. The Peclet number is a ratio of bulk heat transfer/conductive heat transfer. As shown in the following, in both the plant and the model, bulk heat transfer completely overshadows any

---

1. I. E. Idel'chik, *Handbook of Hydraulic Resistance*, pp. 99 and 128. Israel Program for Scientific Translation, Jerusalem 1966.

468 103

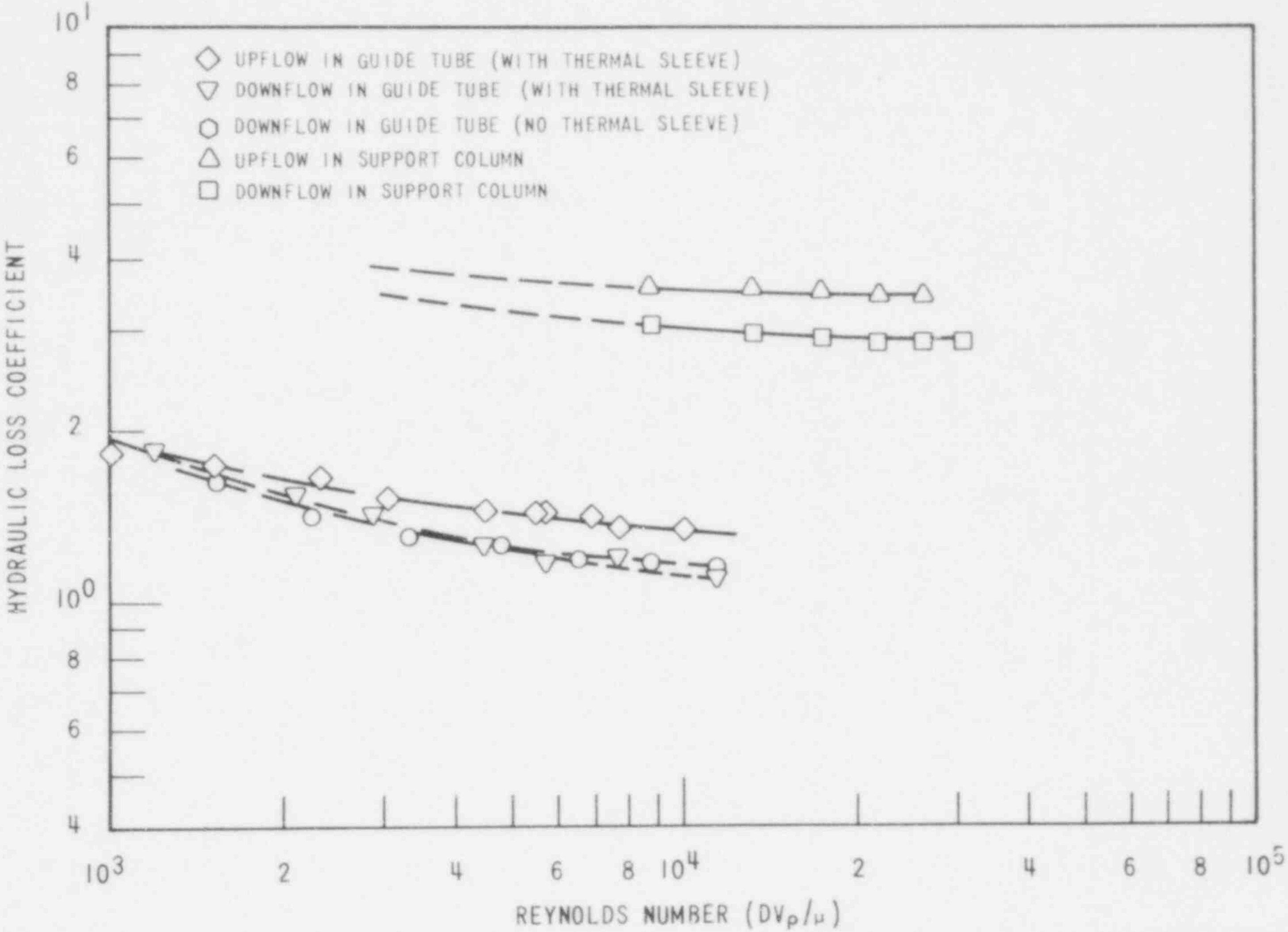

Figure 3-3. 1/5 Scale Model Test Guide Tube and Support Column Hydraulic Loss Coefficient Versus Reynolds Number

468 104

conductive heat transfer. Since this is the case, the fact that the model Peclet number is only 0.078 of the plant Peclet number is insignificant. The Peclet number is expressed as,

$$N_{Pe} = \left(\frac{LV\rho Cp}{k}\right)$$

where

L = length, ft

V = velocity, ft/sec

ρ = density, lb_m/ft^3

Cp = specific heat Btu/lb_m-°F

k = thermal conductivity Btu/hr-ft-F°

For exact simualtion:

$$\left(\frac{LV\rho Cp}{k}\right)_{model} = \left(\frac{LV\rho Cp}{k}\right)_{plant}$$

or

$$N_{Pe\,model} = N_{Pe\,plant}\left(\frac{L_{model}}{L_{plant}}\right)\left(\frac{V_{model}}{V_{plant}}\right)\left(\frac{\rho_{model}}{\rho_{plant}}\right)\left(\frac{Cp_{model}}{Cp_{plant}}\right)\left(\frac{k_{plant}}{k_{model}}\right)$$

Substituting the following values:

$$L_{model} = \frac{L_{plant}}{4.67} \qquad V_{model} = \frac{V_{plant}}{\sqrt{4.67}}$$

$$\rho_{model} = 62.35\ lb_m/ft^3 \qquad k_{model} = 0.34\ Btu/hr\text{-}ft\text{-}^\circ F$$

$$\rho_{plant} = 40.58\ lb_m/ft^3 \qquad k_{plant} = 0.28\ Btu/hr\text{-}ft\text{-}^\circ F$$

$$Cp_{model} = 1.00\ Btu/lb_m\text{-}^\circ F$$

$$Cp_{plant} = 1.61\ Btu/lb_m\text{-}^\circ F$$

With L in inches and V in ft/sec

$$N_{Pe\,plant} = 5.14 \times 10^5\ (L)\ (V) \qquad N_{Pe\,model} = 3.24 \times 10^4\ (L)\ (V)$$

and,

$$N_{Pe_{model}} = N_{Pe_{plant}} \left(\frac{1}{4.67}\right) \left(\frac{1}{\sqrt{4.67}}\right)\left(\frac{62.35}{40.58}\right)\left(\frac{1.00}{1.61}\right)\left(\frac{0.28}{0.34}\right) = N_{Pe_{plant}} \quad (7.8 \times 10^{-2})$$

Another thermal characteristic of interest is the ratio of (Cp) (ρ) of the two fluids in the plant and the model. The term (Cp) (ρ) has units of Btu/ft^3-°F and is an indication of how many Btu's would be required to make 1 ft^3 of fluid experience a 1°F temperature change.

In the plant:

$$\frac{(\rho)(Cp)\ GT/SC}{(\rho)(Cp)\ SN} = \frac{(40.58\ lb_m/ft^3)\ (1.61\ Btu/lb_m\text{-}^\circ F)}{(46.36\ lb_m/ft^3)\ (1.27\ Btu/lb_m\text{-}^\circ F)} = 1.11$$

where SN refers to spray nozzle.

And in the model assuming 22 percent by weight salt solution at 140°F:

$$\frac{(\rho)(Cp)\ GT/SC}{(\rho)(Cp)\ SN} = \frac{(62.35\ lb_m/ft^3)\ (1.00\ Btu/lb_m\text{-}^\circ F)}{(71.24\ lb_m/ft^3)\ (0.81\ Btu/lb_m\text{-}^\circ F)} = 1.07$$

The above indicates that the ratio is not the same in the plant and model. This implies that the normalized ΔT in the plant and the model will not be the same. (The normalized ΔT is $(T_{point}-T_{SN})/(T_{GT/SC}-T_{SN})$. However, the error introduced due to this variation is relatively small. Based on the assumption that the specific heat is a linear function it can be shown that:

$$\%_{plant} = \frac{A}{\frac{1}{\%_{model}} - \frac{(1-A)}{100}}$$

where,

$$\%_{plant} = \left(\frac{T - T_{SN}}{T_{GT/SC} - T_{SN}}\right)_{plant} (100)$$

$$\%_{model} = \left(\frac{T - T_{SN}}{T_{GT/SC} - T_{SN}}\right)_{model} (100)$$

$$A = \left(\frac{(Cp)_{SN}}{(Cp)_{GT/SC}}\right)_{model}\left(\frac{(Cp)_{GT/SC}}{(Cp)_{SN}}\right)_{plant}$$

468 106

The maximum error would occur if $\%_{model}$ = 50 and upon substitution,

$$A = \left(\frac{(71.24)\ (0.81)}{(62.35)\ (1.00)}\right)\left(\frac{(40.58)\ (1.61)}{(46.36)\ (1.27)}\right) = 1.039$$

$$\%_{plant} = \frac{1.039}{\frac{1}{50} - \frac{(1-1.039)}{100}} = 50.97$$

which results in an error of less than one percent between the model and the plant. Since this correction is relatively minor, it will not be applied to the measured data.

3-5. Specification of Boundary Conditions for UHI Configuration

Figure 3-4 shows the distribution of hardware in the plant for McGuire Unit 2. It should be noted that the plant has half-core symmetry. This symmetry can be seen in figure 3-4 by rotating the figure 180°. In the plant, there are six types of hardware (support column, 15 x 15 guide tube, 17 x 17 Pu recycle guide tube, removable flow column, no hardware, and 17 x 17 guide tube). Figure 3-5 shows the plant pressure distribution based on the results of the 1/7-scale model testing.

Figure 3-6 presents the distribution of hardware employed in the model. The half modeled was 0°-90°-180°. This half was chosen since this plane, 0°-180°, exhibits the largest variation in pressure (refer to figure 3-5) and therefore when employing dye injection, it provides better viewing characteristics through the Lexan boundary plate. It can be seen from figure 3-6 that only 17 x 17 guide tubes and support columns will be employed in the model. This was done to standardize hardware.

The following discussion explains how the model pressure distribution for the guide tubes and support columns was determined. Figure 3-5 presented the measured pressure distribution from the 1/7-scale models. Table 3-1 summarizes the various measured pressures. There are 49 distinct pressures in the guide tubes and support columns. If one examines the magnitude of the pressure variations it can be seen that many of the values can be lumped without significantly changing the pressure. By lumping the pressures, the number of standpipe assemblies required to establish the pressure distribution will be reduced. The average weighted pressure for a model standpipe was determined according to

$$\text{average weighted pressure} = \sum_{i=1}^{n} P_i/n$$

where

n = number of guide tubes or support columns

P_i = pressure of each guide tube or support column

468 107

b,c,e

3465-15

Figure 3-4. McGuire Unit 2 Hardware Configuration and Hydraulic Resistance

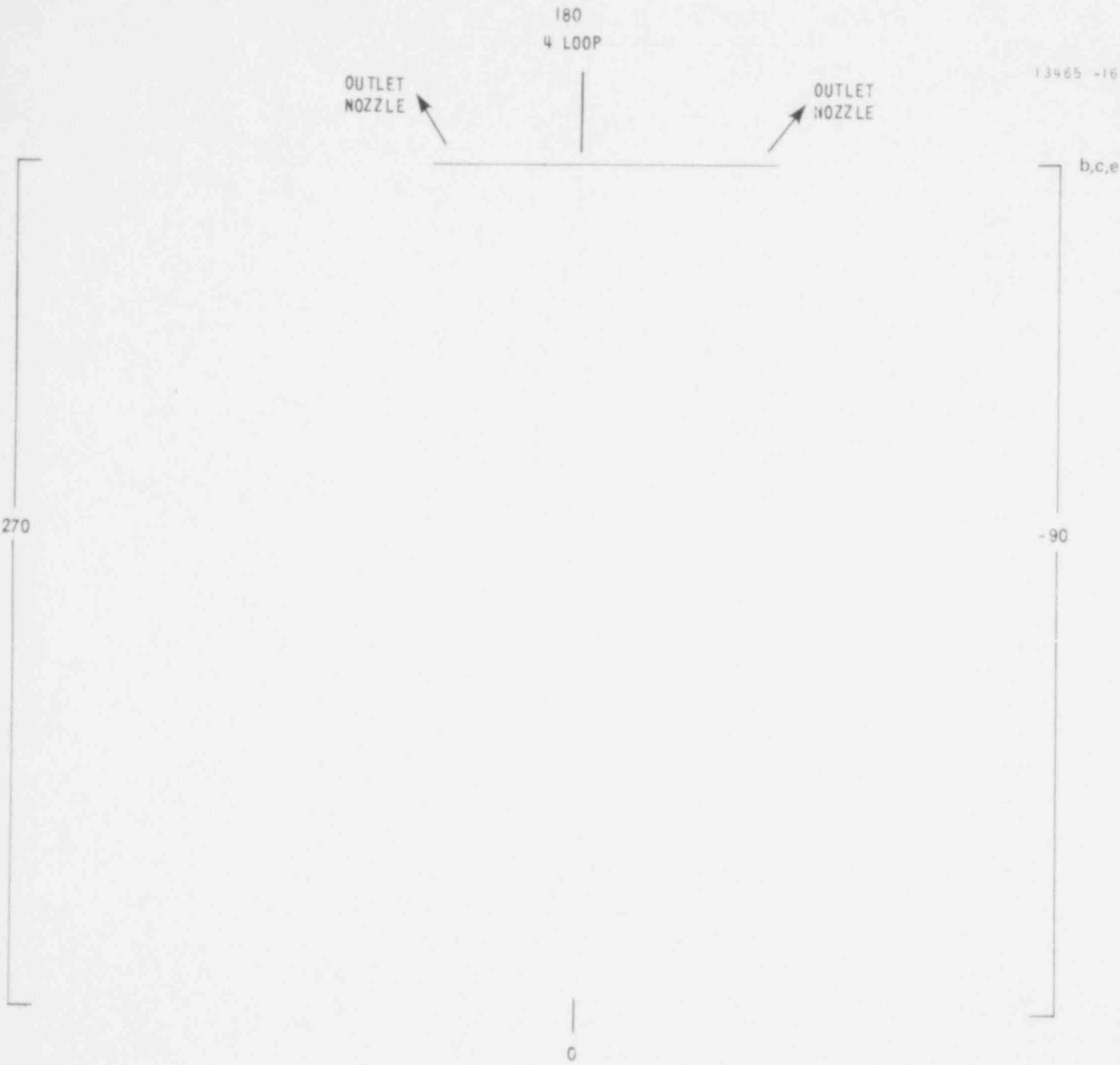

Figure 3-5. McGuire Unit 2 Pressure Distribution: (PSI)

468 109

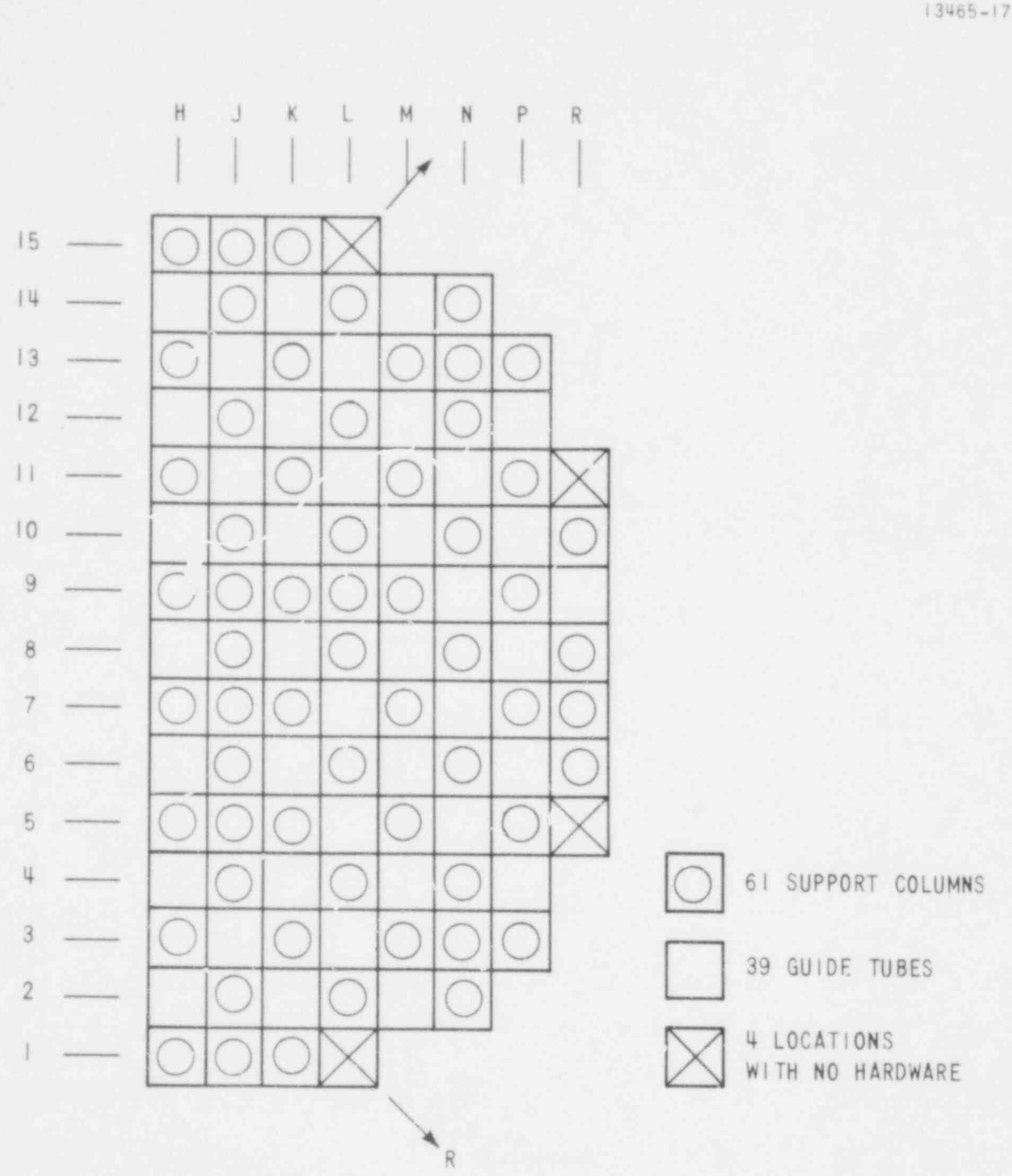

Figure 3-6. 1/5 Scale Model Test Hardware

468 110

TABLE 3-1

SUMMARY OF PLANT AND MODEL PRESSURES

Pressure (psi)	No.	Type	Average Weighed Pressure	Elevation Head Correction (psi)	Pressure Accounting for Elevation Head
b,c,e	2	S.C.[a]	b,c,e		b,c,e
	2	S.C.			
	2	S.C.		0.88	
	2	S.C.			
	2	S.C.			
	1	S.C.			
	2	S.C.			
	2	S.C.			
	2	S.C.			
	1	S.C.		0.88	
	2	S.C.			
	2	S.C.			
	2	S.C.			
	1	S.C.			
	1	S.C.			
	1	S.C.			
	1	S.C.			
	2	S.C.		0.88	
	1	S.C.			
	2	S.C.			
	10	G.T.		0.0	
	2	G.T.			
	2	S.C.		0.88	
	2	S.C.			
	2	S.C.			
	2	S.C.		0.88	
	2	S.C.			

a. Elevation Head Correction for Support Column = $\frac{(37.35)\ (40.5757)}{1728}$ = 0.88 psi

468 111

TABLE 3-1 (cont)

SUMMARY OF PLANT AND MODEL PRESSURES

Pressure (psi)	No.	Type	Average Weighed Pressure	Elevation Head Correction (psi)	Pressure Accounting for Elevation Head
[b,c,e]	2	G.T.	[b,c,e]	0.0	[b,c,e]
	2	G.T.			
	2	S.C.		0.88	
	2	S.C.		0.88	
	4	S.C.			
	2	S.C.		0.88	
	2	S.C.			
	1	G.T.		0.0	
	2	G.T.			
	2	S.C.		0.88	
	2	S.C.		0.88	
	2	G.T.		0.0	
	2	G.T.			
	2	G.T.		0.0	
	2	S.C.		0.88	
	2	G.T.		0.0	
	2	G.T.			
	2	G.T.		0.0	
	2	G.T.			
	2	G.T.		0.0	
	2	G.T.		0.0	
	2	G.T.			

By determining the standpipe pressure according to the above formula, the individual pressures are not preserved; however, the overall effect of employing the weighted pressure will be the same as if the individual pressures had been used. It should be noted that no situations exist in which guide tubes and support columns are connected to the same standpipe. This was done to avoid the potential for flow to be entering and exiting the same standpipe. By employing the above technique the number of pressures was reduced from 49 to 20 (see table 3-1).

The 1/7-scale model measured support column pressures did not account for the elevation head from the upper core plate to the beginning of the solid section of the guide tube enclosure. In the plant, the distance from the upper core plate to the beginning of the solid section of the guide tube is 37.35 inches. The density associated with the fluid is 40.5757 $1b_m/ft^3$ (P = 2250 psi, T = 627°F). The resulting elevation head correction to be applied to the support column pressures is:

$$\text{Elevation Head Correction for Support Column} = \frac{(37.35)\ (40.5757)}{1728} = 0.88 \text{ psi}$$

The result of increasing the support column pressure by 0.88 psi is shown in table 3-1. No corrections are necessary for guide tube locations.

The 1/7 scale model test data presented in figures 2-8 and 2-9 of section 2 indicate that there is approximately a 0.5 psi variation of guide tube and support column pressure about the least squares regression analysis of the measured data. This pressure uncertainty was incorporated into the 1/5-scale model test by increasing all support column pressures by 0.5 psi and decreasing all guide tube pressures by 0.5 psi. By adjusting the pressures as indicated, the amount of flow entering the upper head region via the support columns and guide tubes is maximized. Table 3-2 presents the in-plant pressures accounting for the support column elevation head correction and the pressure uncertainty.

At this point, the only correction remaining to determine the model pressure distribution is to scale the pressures such that the Richardson number is preserved. As discussed previously, to preserve the Richardson number the pressures must be reduced by a factor of 3.04. This operation was performed and the result is shown in table 3-2, which presents the model pressure to be employed at each core location.

In the plant, the best-estimate head cooling flow rate based on the thermal design flow rate is 3471.41 gpm. The corresponding head cooling flow for the model was determined according to the following:

$$\frac{3471.41 \text{ gal}}{\text{min} - \text{head}}\ \frac{1}{2}\ \text{Head}\left(\frac{\text{Nozzle Area in Plant}}{4.67^2\ \text{Nozzle Area in Plant}}\right)\left(\sqrt{\frac{1}{4.67}}\right) = 36.82 \text{ gpm} = \text{Model Head Cooling}$$

TABLE 3-2

SUMMARY OF PLANT AND MODEL PRESSURE FOR EACH CORE LOCATION IN 0°-90°-180° HALF

Pressure Measured in 1/7-Scale Model Adjusted to Reduce No. of Standpipes (psi)	Plant Pressure Accounting for Support Col. Elevation Head and 0.5 psi Uncertainty (psi)	Pressure in Model	No. of and Hardware Type	Core Locations in 0°-90°-180° Half
[ ] b,c,e	[ ] b,c,e	[ ] b,c,e	10 S.C.	H11,H5,J10,J6,L10,L6,N10,N6,P11,P5
			16 S.C.	H9,H7,J9,J7,J5,K9,K7,L9,L8,M9,M7,P9,P7,R10,R7,R6
			7 S.C.	J8,K11,K5,M11,M5,N8,R8
			4 S.C.	J12,J4,N12,N4
			6 S.C.	H13,H3,L12,L4,P13,P3
			2 S.C.	N13,N3
			6 S.C.	H15,H1,K13,K3,M13,M3
			4 S.C.	J14,J2,N14,N2
			2 S.C.	J15,J1
			2 S.C.	L14,L2
			2 S.C.	K15,K1
			12 G.T.	H10,H8,H6,K8,L7,M8,N9,N7,P10,P8,P6,R9
			4 G.T.	K10,K6,M10,M6
			3 G.T.	J11,N11,N5
			4 G.T.	H12,H4,L11,L5
			2 G.T.	P12,P4
			4 G.T.	K12,K4,M12,M4
			4 G.T.	H14,H2,J13,J3
			2 G.T.	L13,L3
			4 G.T.	K14,K2,M14,M2
No Hardware at These Locations				L15,L1,R11,R5

Head cooling flows in the test ranged from 36.8 gpm to 133.4 gpm.

The uncertainty associated with the head cooling flow is ± 7 percent. This uncertainty is based on the sqare root sum of squares of a 10 percent uncertainty on spray nozzle loss coefficient and a 10 percent uncertainty on the pressure loss. The tests were performed using 7 percent less than the best estimate head cooling flow rate and all presentations of the measured data will reflect flow 7 percent greater than the best estimate value.

3-6. Specification of Boundary Conditions for Standard Plant Configuration

The pressure boundary conditions described for the UHI plant were applied to the standard plant, with one exception. For the standard plant, the support columns are not a flow path. Therefore, flow was not permitted to enter or exit the head region via the support columns.

With respect to head cooling flow, the standard plant spray nozzle dimensions were scaled in the same manner as for the UHI nozzle (i.e., diameter model = 1/4.67 plant diameter). In the plant, the best estimate head cooling flow is 1290.73 gpm, based on the thermal design flow. The corresponding head cooling flow for the model was determined according to the following:

$$\frac{1290.73 \text{ gal}}{\text{min - head}} \; \frac{1}{2}\left(\frac{\text{Nozzle Area in Plant}}{4.67^2 \text{ Nozzle Area in Plant}}\right)\frac{1}{\sqrt{4.67}} = 13.69 \text{ gpm} = \text{Model Head Cooling}$$

Head cooling flow in the test ranged from 13.7 gpm to 59.6 gpm.

3-7. Discussion of Standpipe System

As mentioned previously, a series of standpipes were employed to establish the guide tube/support column pressure distribution. The design of the standpipe system was such that

- A constant elevation head was maintained.
- The salt solution was prevented from entering the region of the standpipe above the drain level.
- Pressure losses associated with the system were minimal.
- Pressure monitoring devices were provided to determine the pressure at the entrance to the guide tube or support column.

Figure 3-7 is an outline of the standpipe system. The standpipes were made of 4-inch ID PVC piping and 1 1/4-inch ID tubing was used to connect the guide tubes and support columns to the standpipes. Pure water was fed into the top of each standpipe. To obtain the desired guide tube/support column pressure distribution, the elevation for each standpipe must be equal to the distance from the bottom of the model guide tube or support column to the top of the inside of the head plus whatever distance is required to obtain the pressures presented in table 3-2

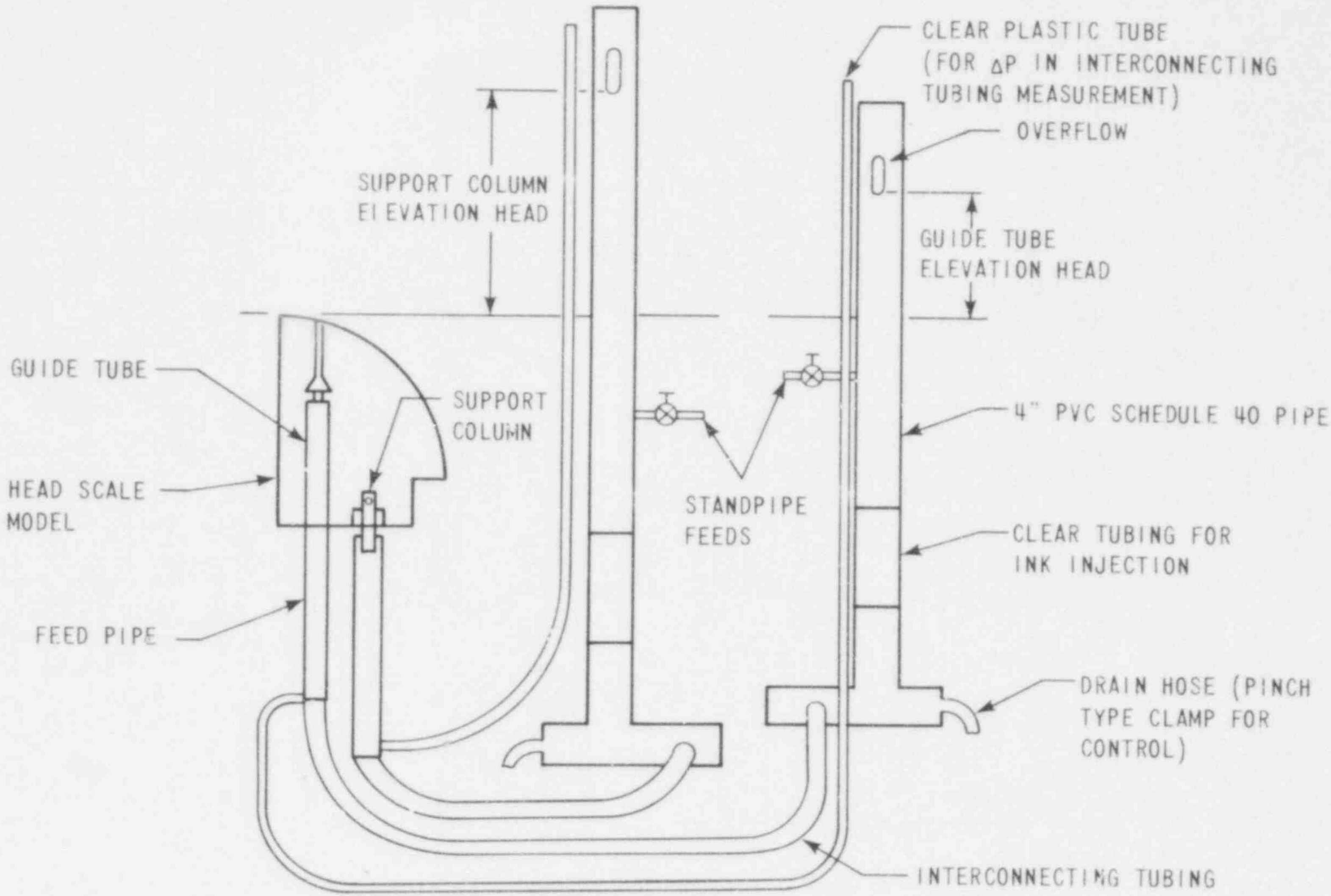

Figure 3-7. Schematic Layout of Standpipe System

468 116

[ ].[b,c,e] To assure that the elevation head for a standpipe remains constant, a constant water level was maintained by a slot at the top of the standpipe which serves as an overflow drain and no salt solution was permitted in the standpipe above the standpipe drain level.

A clear section of tubing equipped with a dye injection port was employed to indicate flow direction in the standpipe. The clear tubing section was located just above the standpipe drain. For all standpipes, the standpipe drain hose clamp was opened to a point which indicated flow was downward. By assuring that the standpipe flow was downward, the possibility of salt solution affecting the pressure distribution was eliminated. The centerline of the drain hose was located at an elevation corresponding to the bottom end of the support column, and for guide tubes at an elevation corresponding to the point where the solid section of the guide tube enclosure begins. By locating the hose clamp at these locations, the elevation head variation in the model, accounting for scaling, will be the same as in a plant. If this variation in the model had not been maintained, the effect of elevation head on the pressure distribution would not be properly modeled.

The 1 1/4-inch ID tubing employed to connect the guide tubes and support columns was chosen to minimize pressure losses between the standpipes and the model. By employing the 1 1/4-inch ID tubing, the hydraulic resistance associated with the connecting tubing was in the range of 8.2 in.$^{-4}$ compared with hydraulic resistances (K/A^2) of approximately 200 in.$^{-4}$ for a guide tube and 479.7 in.$^{-4}$ for the support column. Based on the above, the line losses associated with the connecting tubing are relatively small. To assure uniformity in line losses for each location attached to a given standpipe, the length of tubing to make the connection will be the same.

To monitor the pressure distribution at the entrance to the guide tubes and support columns, at least one individual tube per standpipe was monitored for pressure. The pressure-monitoring device consisted of a tube running from the model hardware (at an elevation corresponding to the centerline of the standpipe drain hose) and was attached to the side of the standpipe. The pressure-sensing tube protruded approximately 2 feet above the standpipe weir to accommodate conditions where the guide tube or support column pressure was greater than the standpipe pressure. This tube sensed the static pressure into the guide tube or support column. Due to the small dynamic heads anticipated in the guide tubes and support columns at the sensing point (i.e., ~ 0.003 psi), the pressure indicated will be considered as the total pressure. These pressure sensors provided: a. an estimate of line losses between the standpipe and model; b. an indication of elevation head variations on the pressure distribution: and c. an indication of flow direction (i.e., if the elevation in the sensing tube is lower than the standpipe weir flow entering the model, or vice versa.

As was the case with the standpipe, it was essential that only pure water be in the sensing tube. This was assured by providing a sufficiently long (~ 5 ft) run of tubing horizontally before running vertically on the standpipe. It should be noted that before testing, the entire system was purged with pure water.

3-8. Placement of Thermocouples

There were 60 thermocouples dispersed throughout the 1/5-scale upper head model. In addition to the thermocouples in the model, the temperatures of the hot brine solution (head cooling flow) and guide tube/support column flow were measured.

The thermocouples in the upper head model were positioned using the UHI configuration as a base, such that regions of significantly different temperatures would be detected, if they exist. Three possible types of upper head flow patterns were postulated, as shown in figure 3-8.

If the assumption is made that the upper head flow pattern is controlled by density gradients, one would anticipate the temperature distribution depicted as Type A of figure 3-8.

If this flow pattern exists in the plant the majority of low density core exit flow will enter the upper head via the support columns at a location just above the support plate and a "chimney" of relatively unmixed core exit flow will be created. This will result in the presence of a region with a temperature substantially greater than the mixed mean temperature. Since the density gradient is assumed to control the flow pattern, the relatively dense head cooling flow will enter the region and will gradually alter direction from vertically upward to downward. In addition, the initial momentum of the head cooling flow will create a vortex as it entrains the surrounding fluid. The fluid in this region would have a temperature significantly lower than the average. For this type of flow pattern, the maximum in-plant temperature would exist just above the upper support plate between the two cold leg nozzles.

Based on the assumption that the upper head flow pattern is controlled by form/viscous drag, the temperature distribution depicted as Type B of figure 3-8 would exist. The majority of low-density core exit flow will enter the upper head region via the support columns at a location just above the support plate. The presence of guide tubes and support columns in the lower portion of the upper head creates form/viscous drag. The density gradient and kinetic energy of the support column flow is not sufficient to overcome the form/viscous drag. Therefore, the majority of core exit flow will remain in the lower cylindrical portion of the upper head region. The head cooling flow entering the upper head region will establish a vortex in the upper section of the region. The upper section fluid will contain essentially all the head cooling flow and therefore will have a temperature substantially lower than the mixed mean temperature. The maximum in-plant temperature for this flow pattern would be found just above the support plate between the two cold leg nozzles.

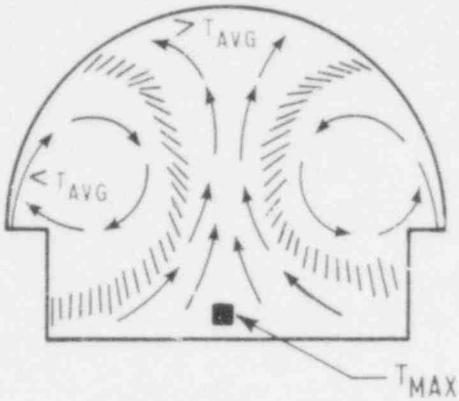

TYPE A. DENSITY GRADIENT CONTROLLED

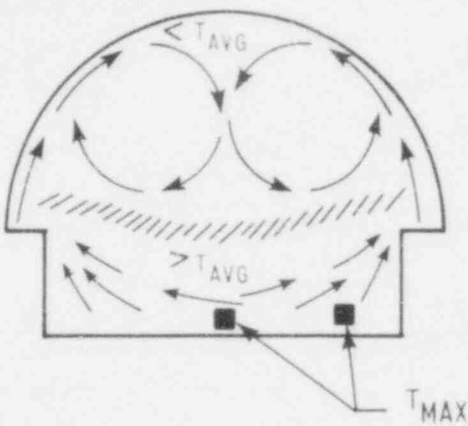

TYPE B. FORM/VISCOUS DRAG CONTROLLED

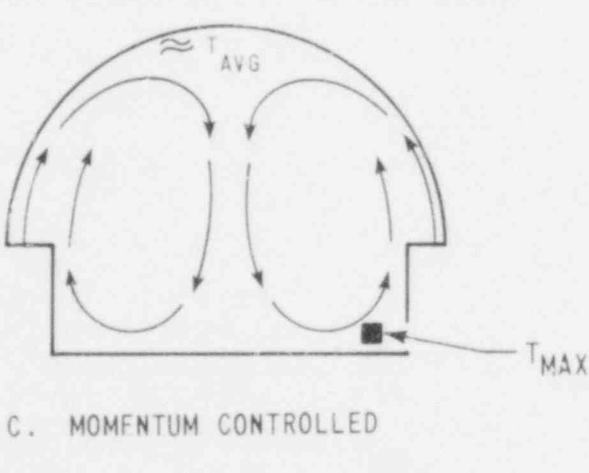

TYPE C. MOMENTUM CONTROLLED

Figure 3-8. UHI Upper Head Region Limiting Flow Patterns

468 119

The most probable upper head region flow pattern is presented as Type C of figure 3-8. This flow pattern is based on the assumption that the momentum of the head cooling flow is sufficient to create a toroidal vortex in the entire region. For this particular flow pattern, the upper head region will have a relatively uniform temperature. When the majority of the core exit fluid enters the region via the support column, the maximum in-plant temperature for this flow pattern exists just above the support plate between the two cold leg nozzles.

The axial and radial placement of the 60 thermocouples in the upper head region is presented in figures 3-9 through 3-20. From the figures it can be seen that 13 of the 60 thermocouples located in the model represent positions at which in-plant measurements might be obtained. These 13 locations are not considered when determining the mean upper head region temperature of the model, but could be employed to relate in-plant measurement to the model measurements.

Based on the postulated flow patterns, if a "hot" region existed it would be in the area between the upper support plate and upper support plate flange. Approximately 25 percent of the vessel upper head region fluid volume is in the above region. Twenty-six of the 47 model thermocouples are located in this region (i.e., thermocouple levels 1 and 2). Therefore, each thermocouple measurement represents approximately one percent of the volume. At the remaining levels of instrumentation each of the 21 thermocouples represents approximately 3.5 percent of the vessel upper head region volume.

3-9. TEST FACILITY

Figures 3-21, 3-22, and 3-23 are pictorial views of the test facility which was primarily designed, built, and operated by Westinghouse Research and Development Center personnel. The primary components of the system are labeled to aid the reader in understanding the system. The principal elements are described in the following paragraphs.

3-10. Reactor Head Scale Model

Closeup views of the 0.214-to-1 upper head scale model prior to instrumentation are shown in figures 3-24, 3-25, and 3-26. Figures 3-27, 3-28, and 3-29 are closeup views of the model after the addition of 60 thermocouples. The selected model scale was based on the availability of a 35.8-inch ID hemispherical spinning and judgment as to the necessary supply of hot brine for a reasonable test duration. The hemisphere was cut near the center to include all the guide tubes and support columns in one half plus the center row. The open face of the model was closed with a transparent 0.5-inch-thick Lexan plate.

Regions where water either entered or exited the upper head were modeled in detail. These included the head cooling holes or spray nozzles shown in figure 3-29, the region around the holes in the support columns (figure 3-27, and the region around the top of the guide tubes including the orifice, RCC drive rod, and thermal sleeve (figure 3-24).

468 120

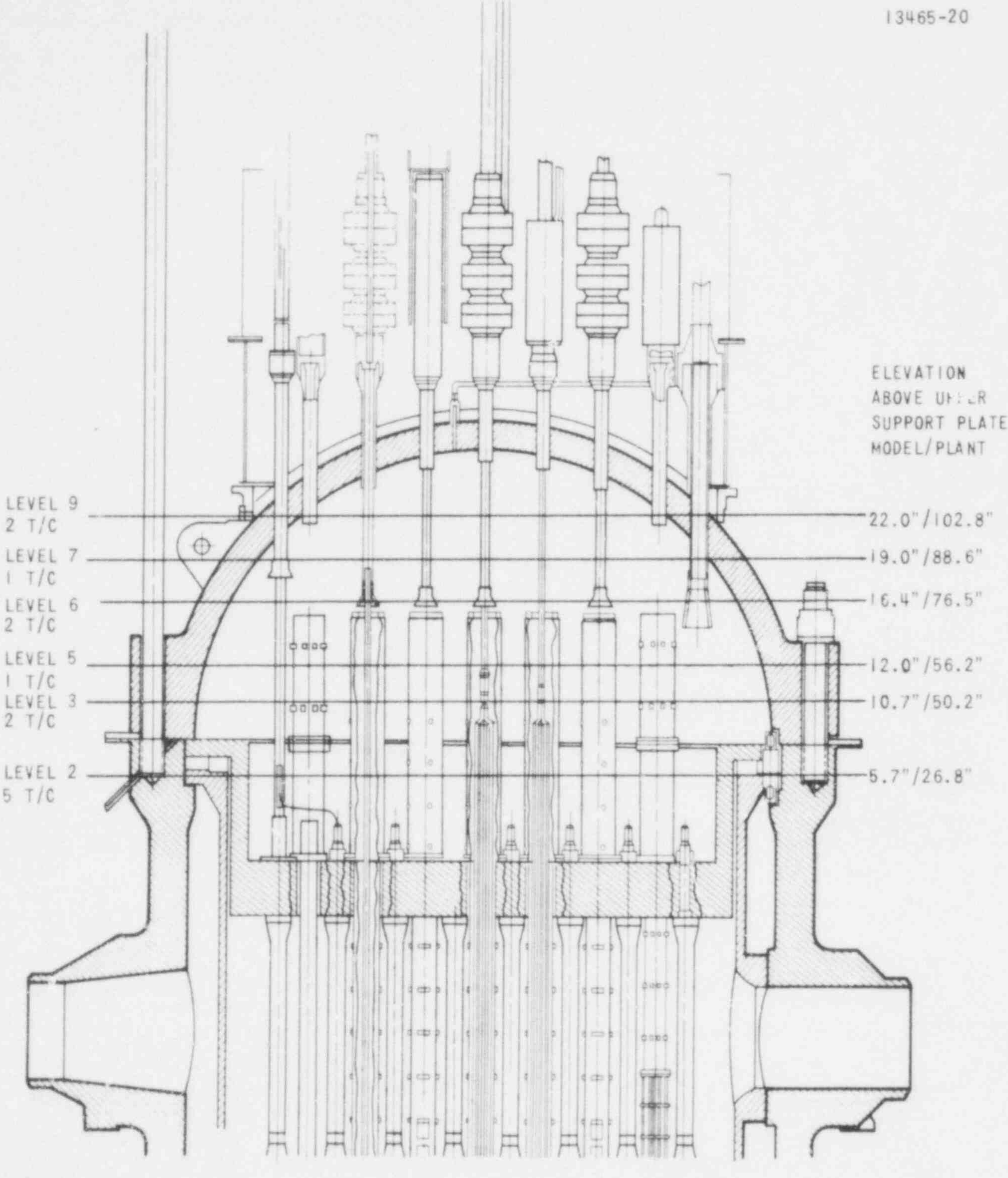

Figure 3-9. Number of Thermocouples in 1/5 Scale UHI Upper Head Region Model at Levels 2, 5, 6, 7, and 9 (T/C's in Both Plant and Model)

468 121

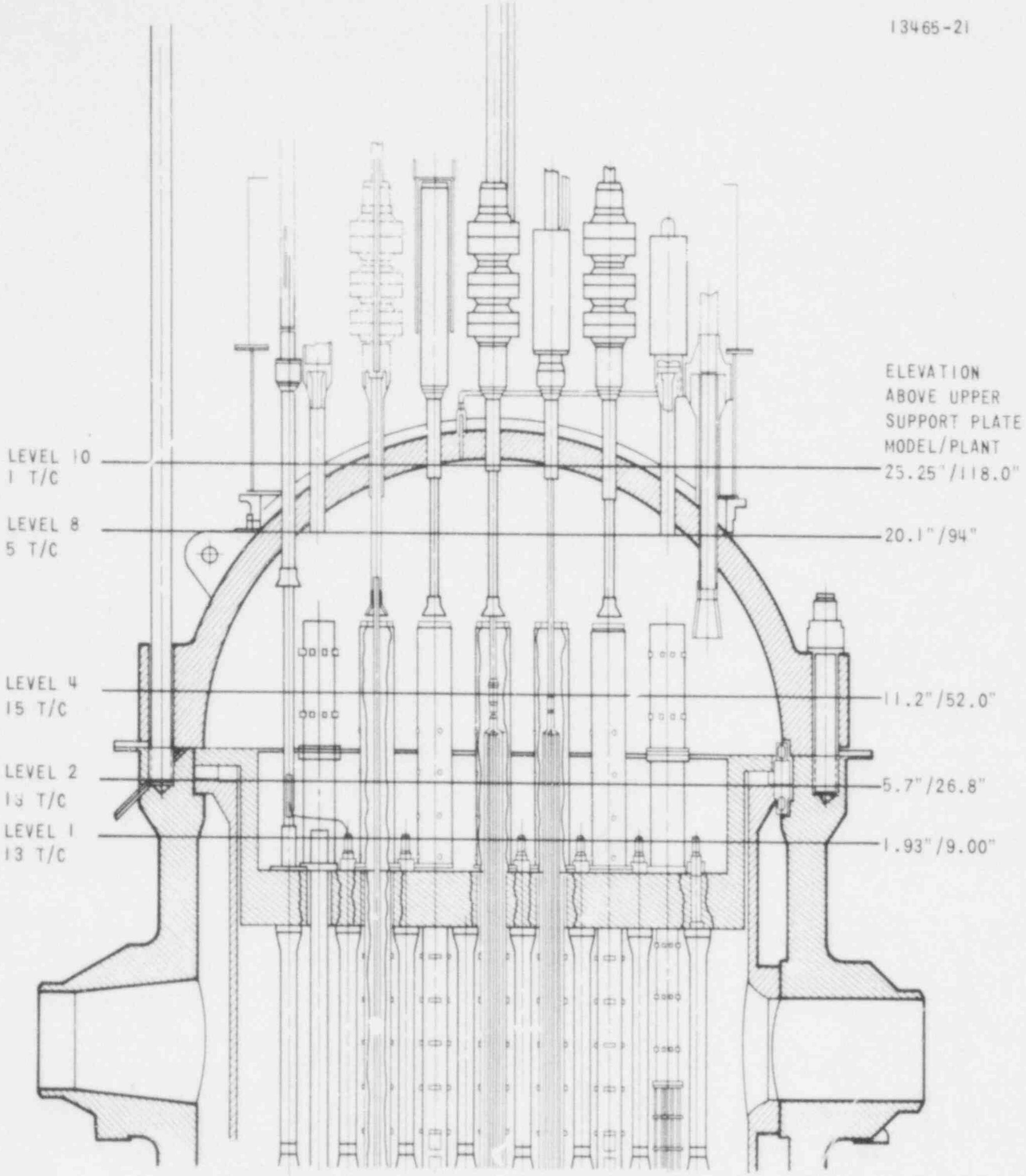

Figure 3-10. Number of Thermocouples in 1/5 Scale UHI Upper Head Region Model at Levels 1, 2, 4, 8, and 10 (T/C's in Model)

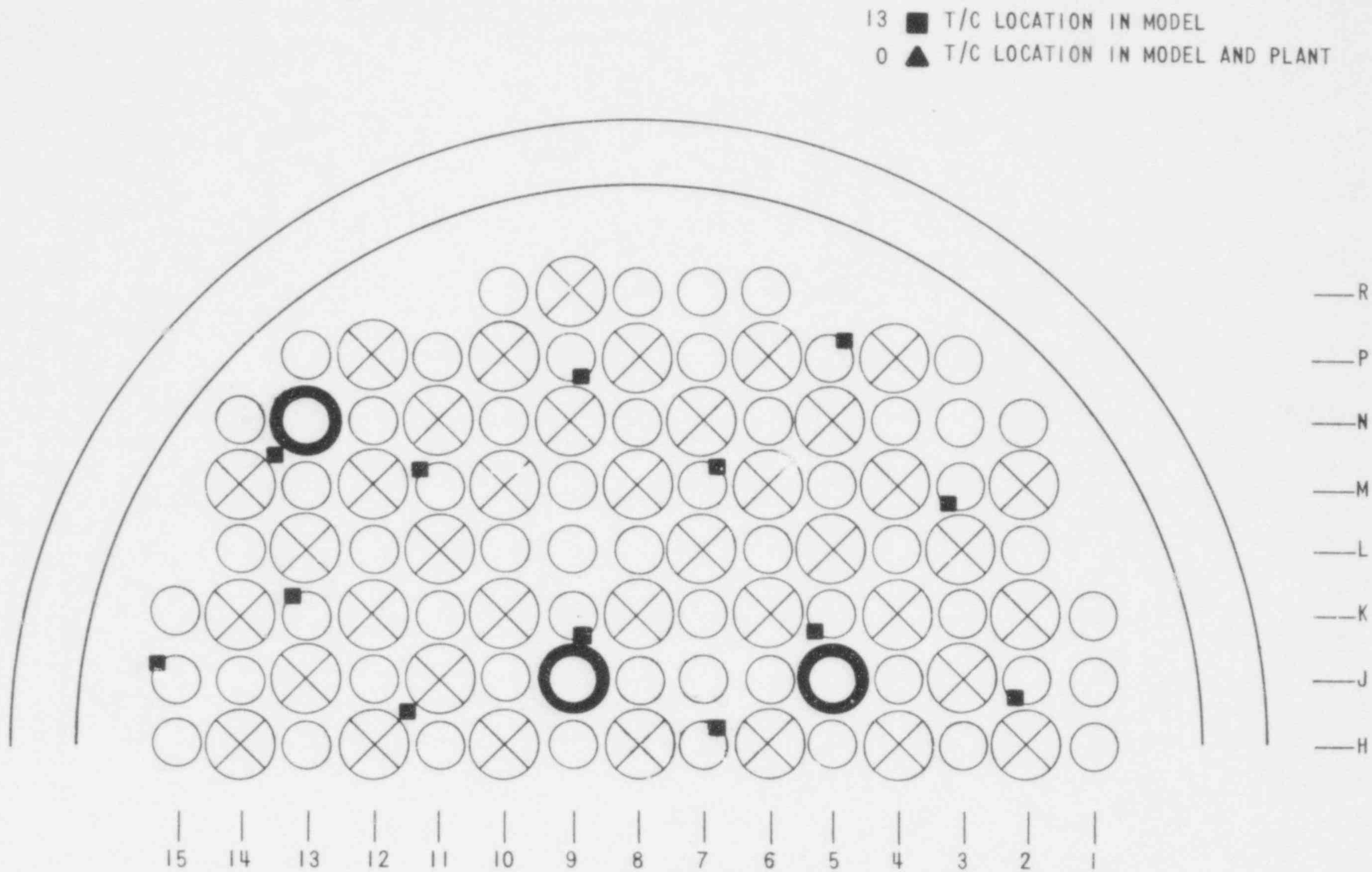

Figure 3-11. Location of Thermocouples in 1/5 Scale Upper Head Region Model at Level 1

468 123

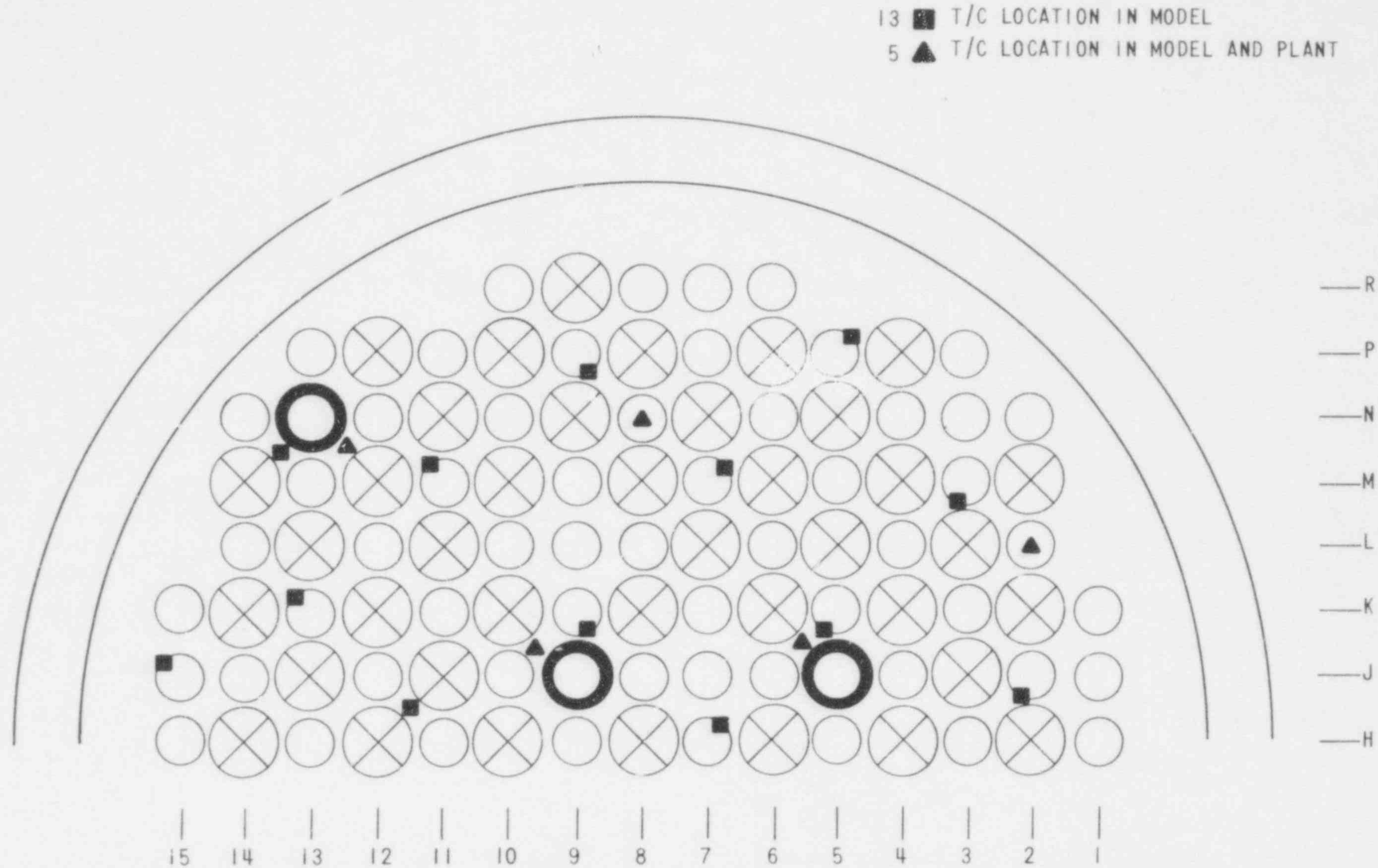

Figure 3-12. Location of Thermocouples in 1/5 Scale Upper Head Region Model at Level 2

468 124

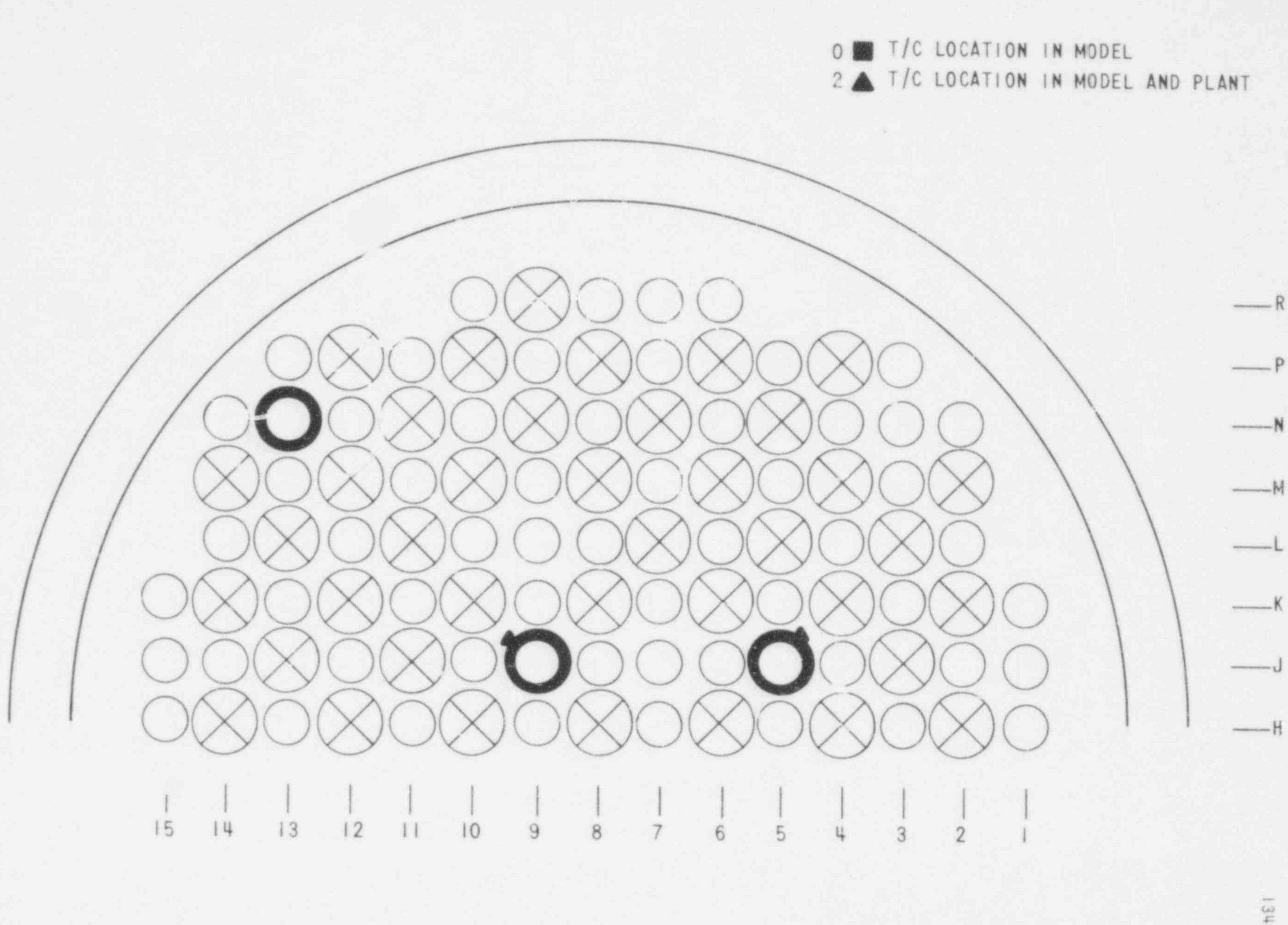

Figure 3-13. Location of Thermocouples in 1/5 Scale Upper Head Region Model at Level 3

468 125

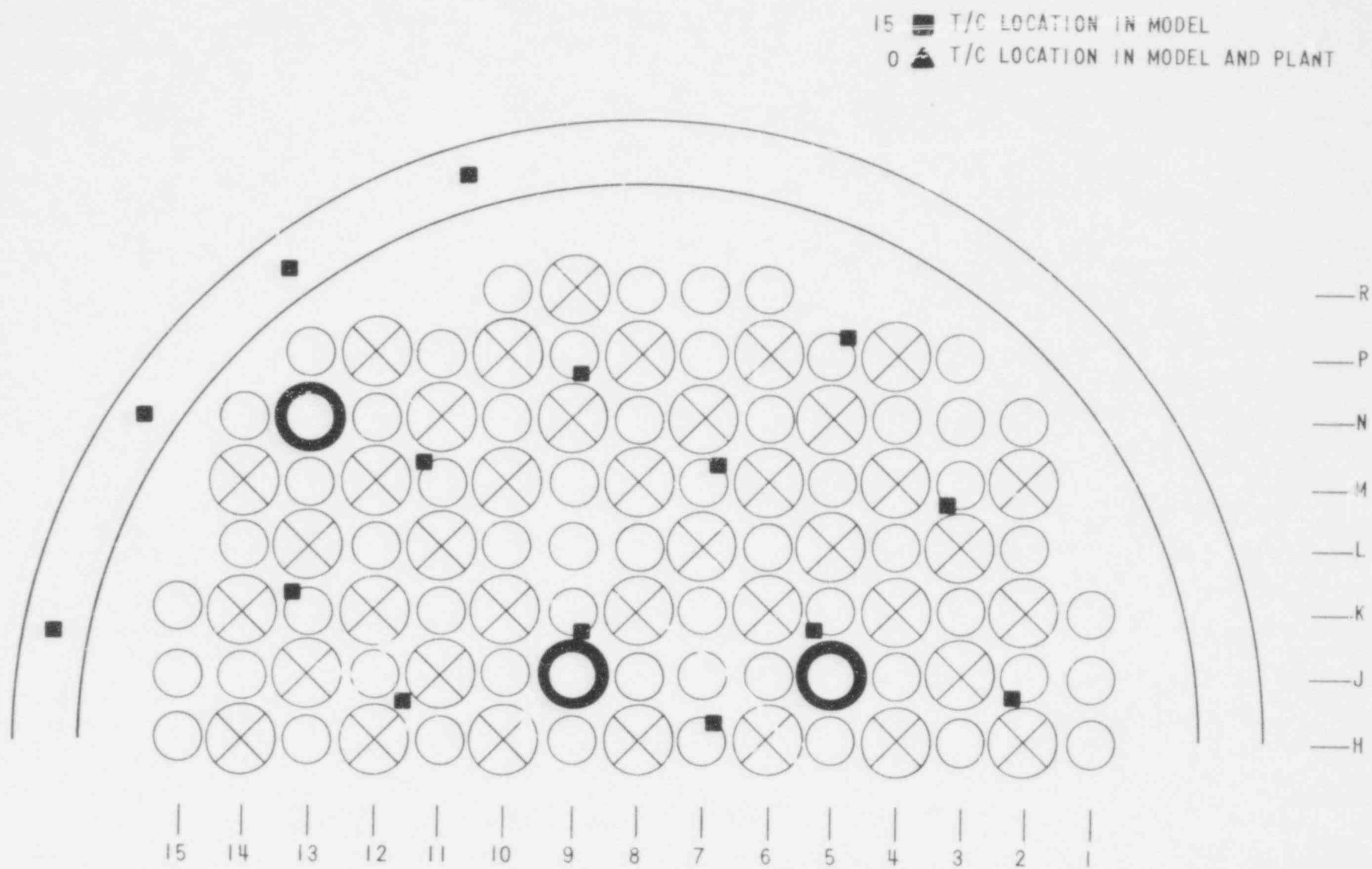

Figure 3-14. Location of Thermocouples in 1/5 Scale Upper Head Region Model at Level 4

468 126

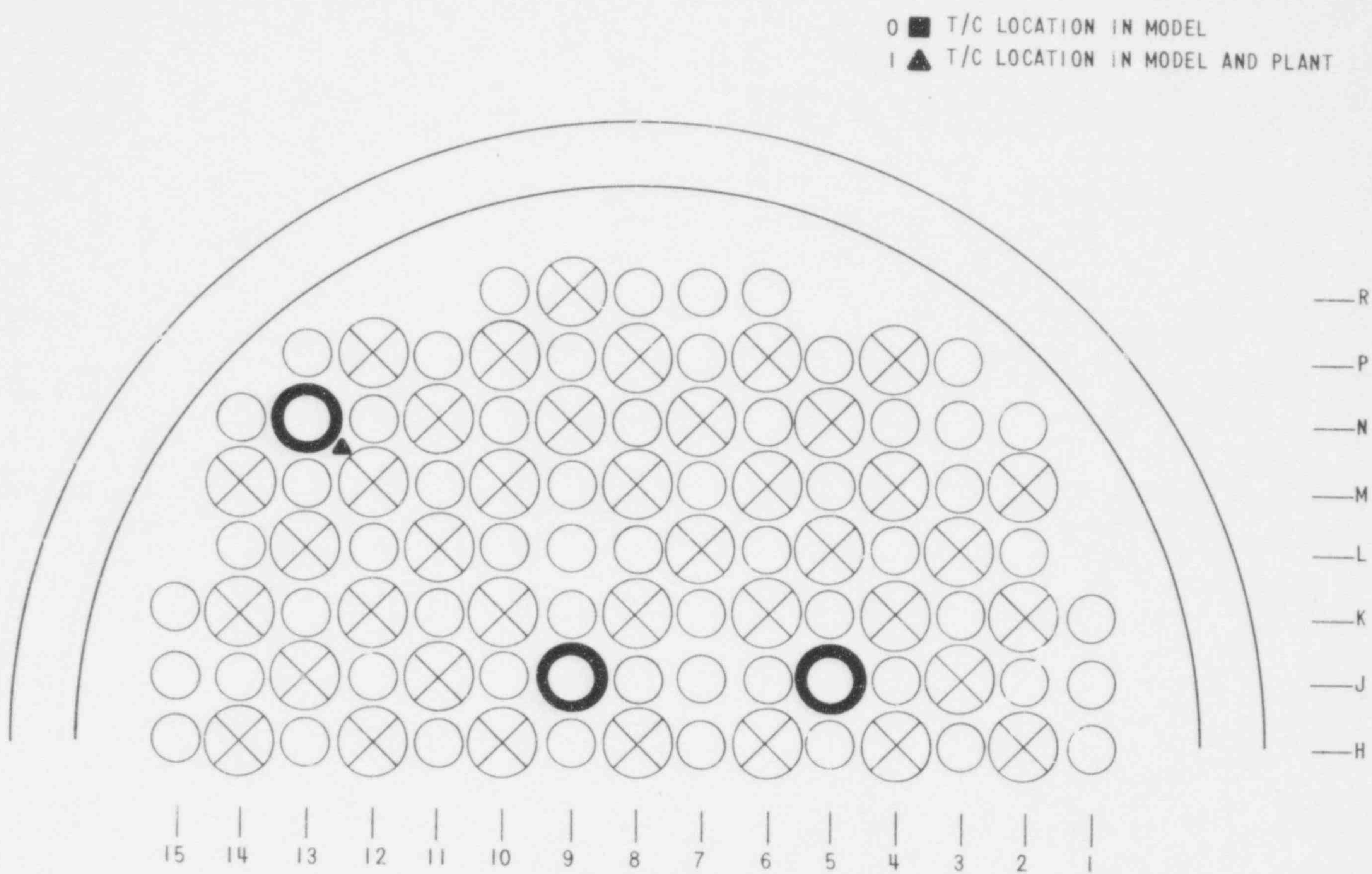

Figure 3-15. Location of Thermocouples in 1/5 Scale Upper Head Region Model at Level 5

468 127

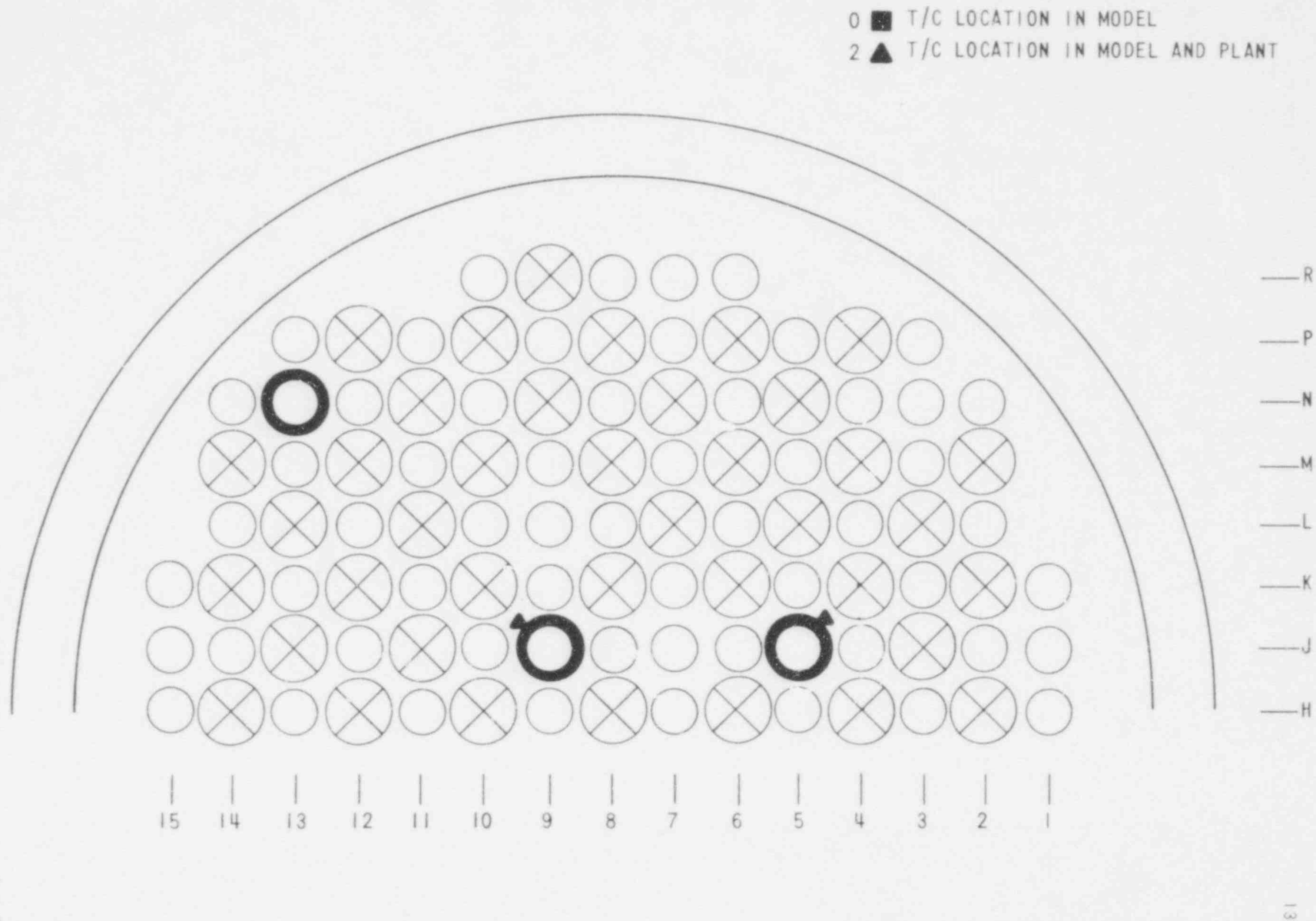

Figure 3-16. Location of Thermocouples in 1/5 Scale Upper Head Region Model at Level 6

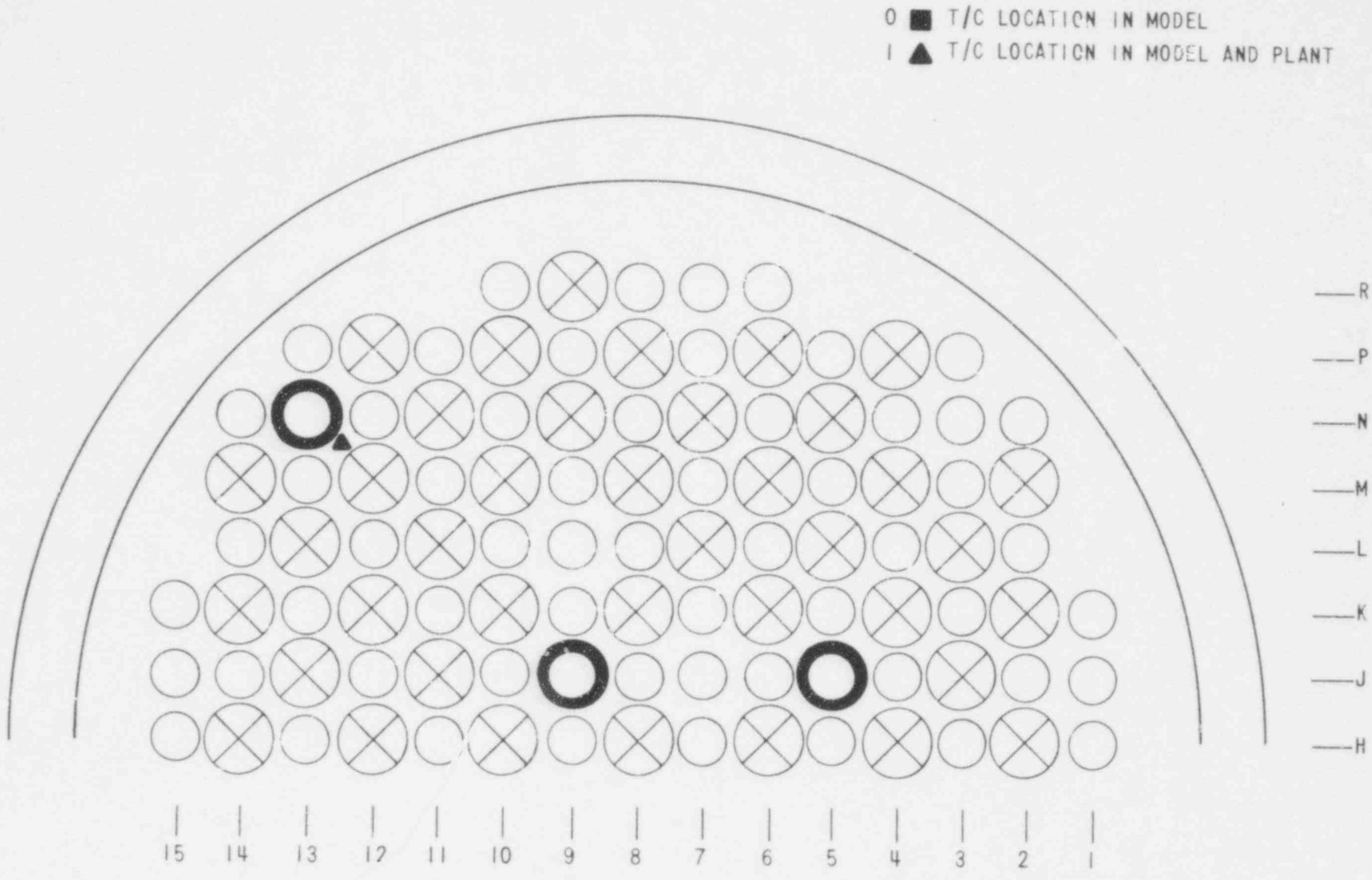

Figure 3-17. Location of Thermocouples in 1/5 Scale Upper Head Region Model at Level 7

468 129

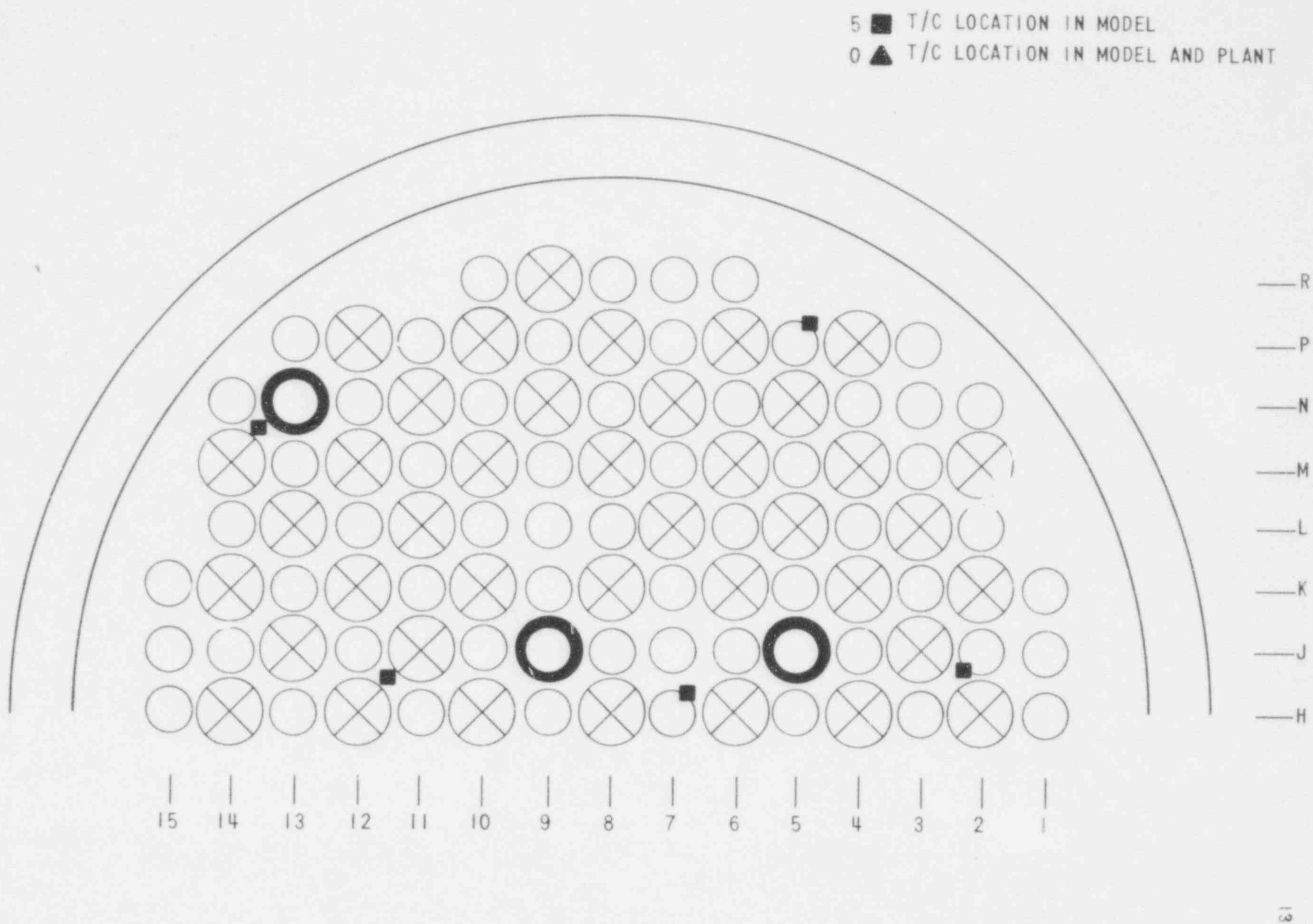

Figure 3-18. Location of Thermocouples in 1/5 Scale Upper Head Region Model at Level 8

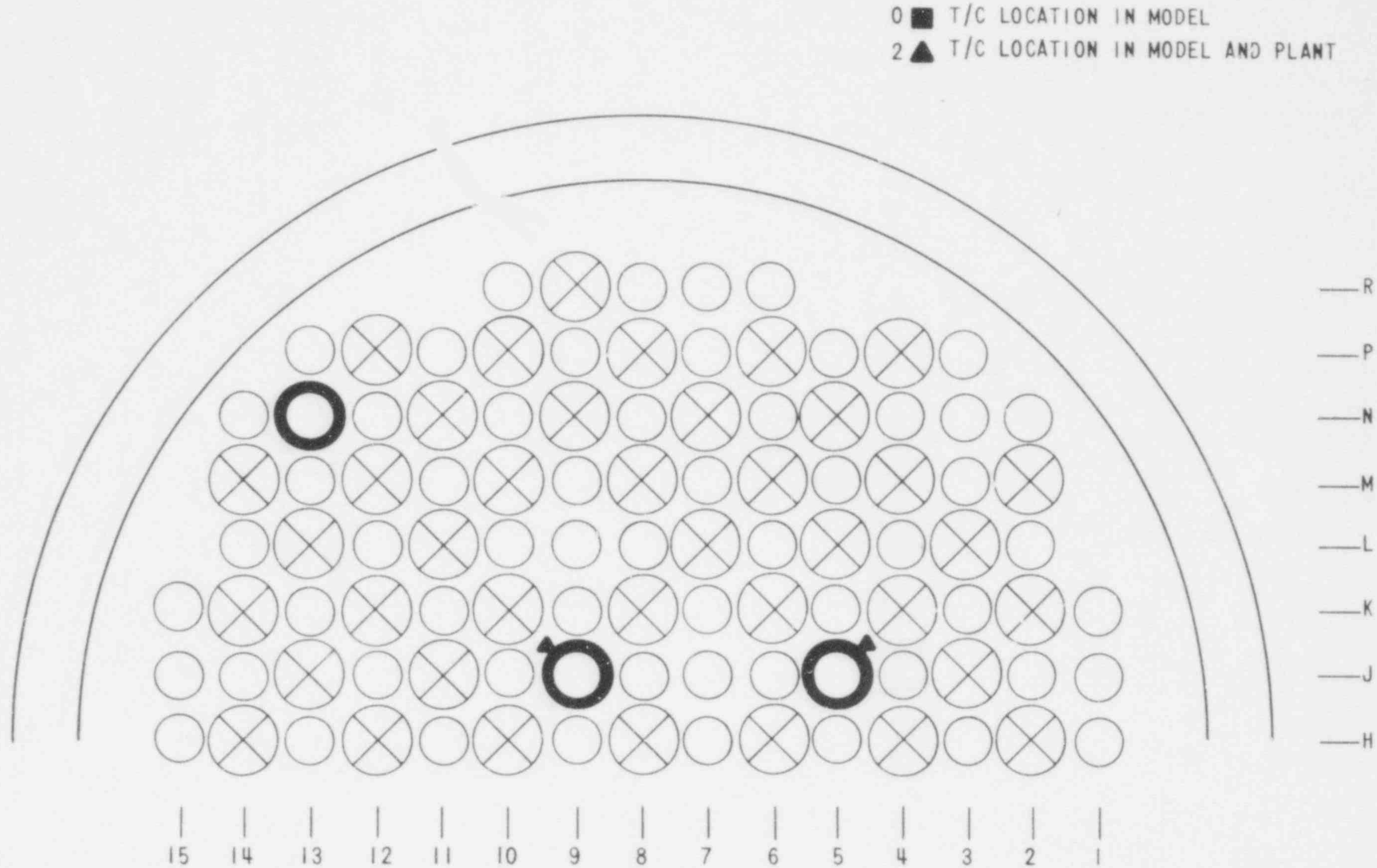

Figure 3-19. Location of Thermocouples in 1/5 Scale Upper Head Region Model at Level 9

468 131

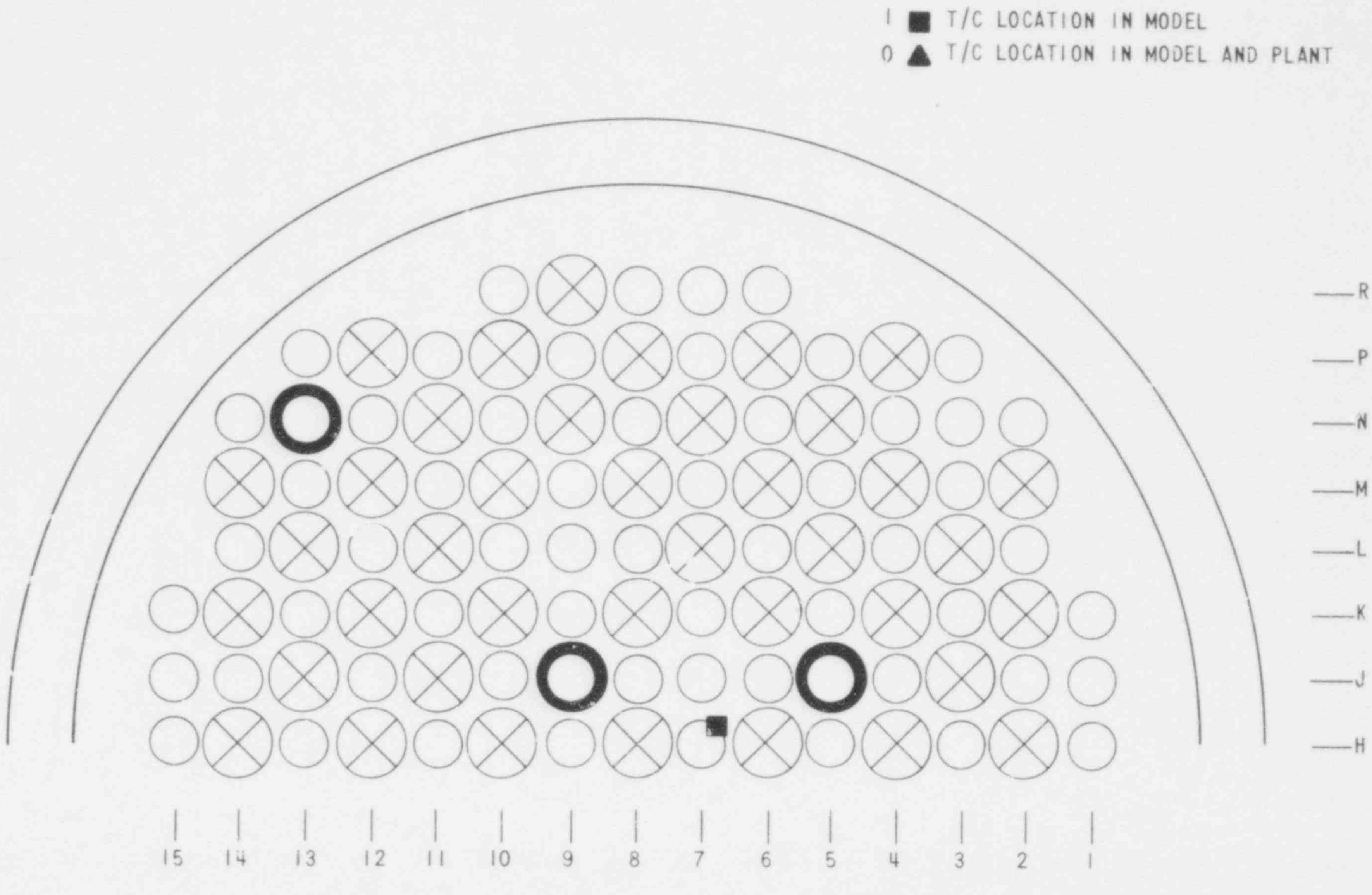

Figure 3-20. Location of Thermocouples in 1/5 Scale Upper Head Region Model at Level 10

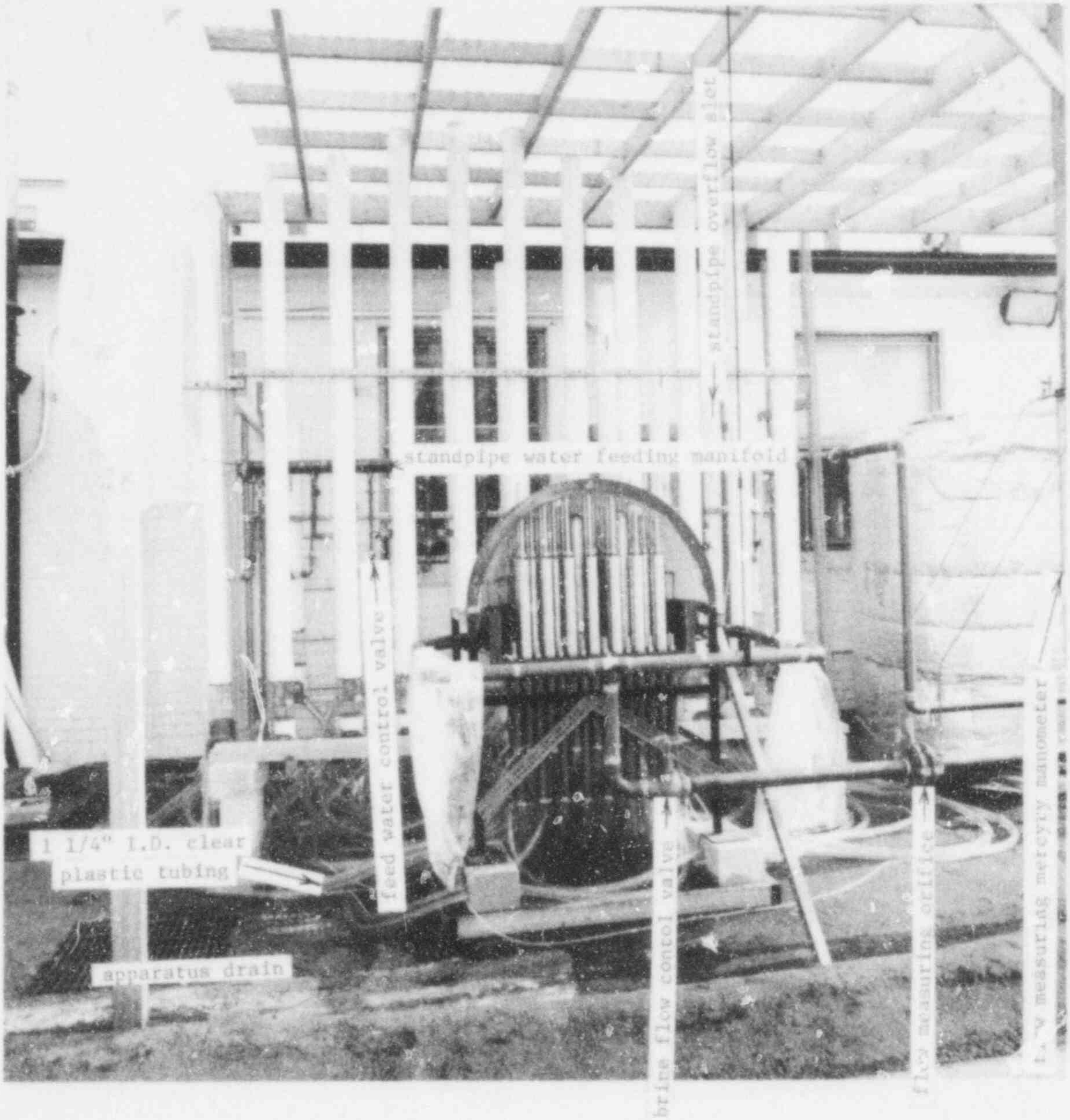

Figure 3-21. Front View of Test Cell

468 133

Figure 3-22. Side View of Test Cell

468 134

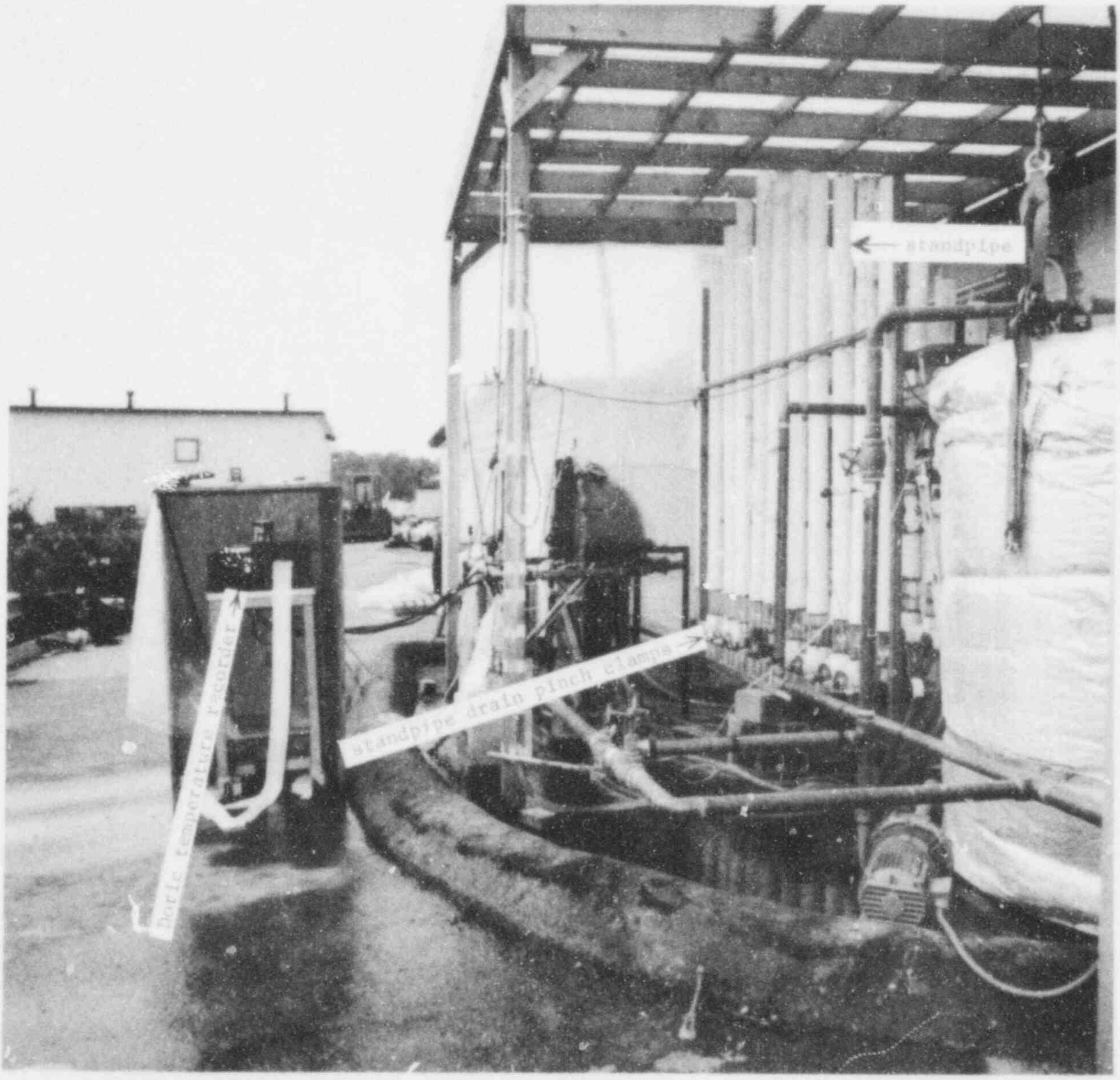

Figure 3-23. Side View of Test Cell

13465-25a

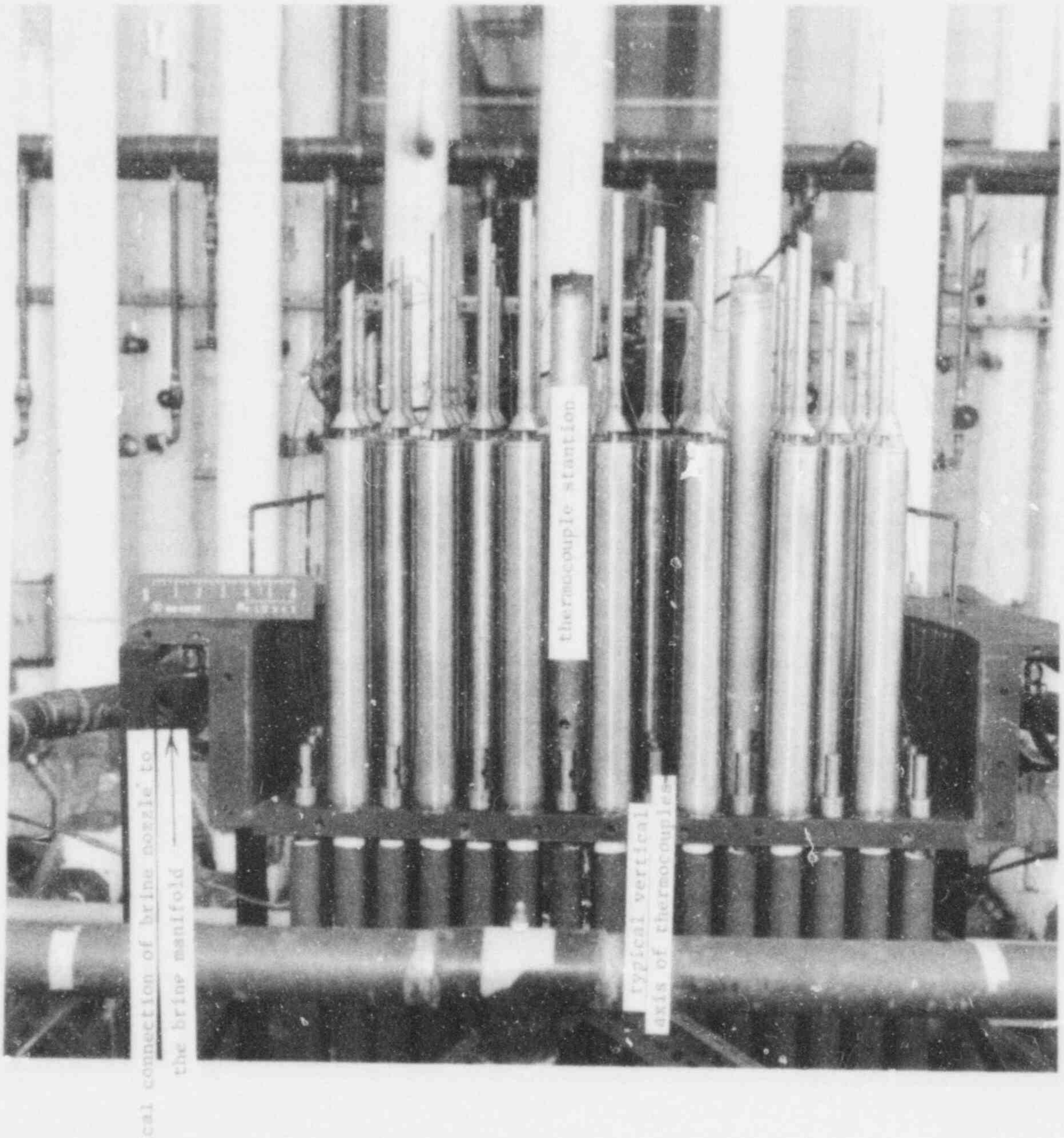

Figure 3-24. Front View of Head Model

468 136

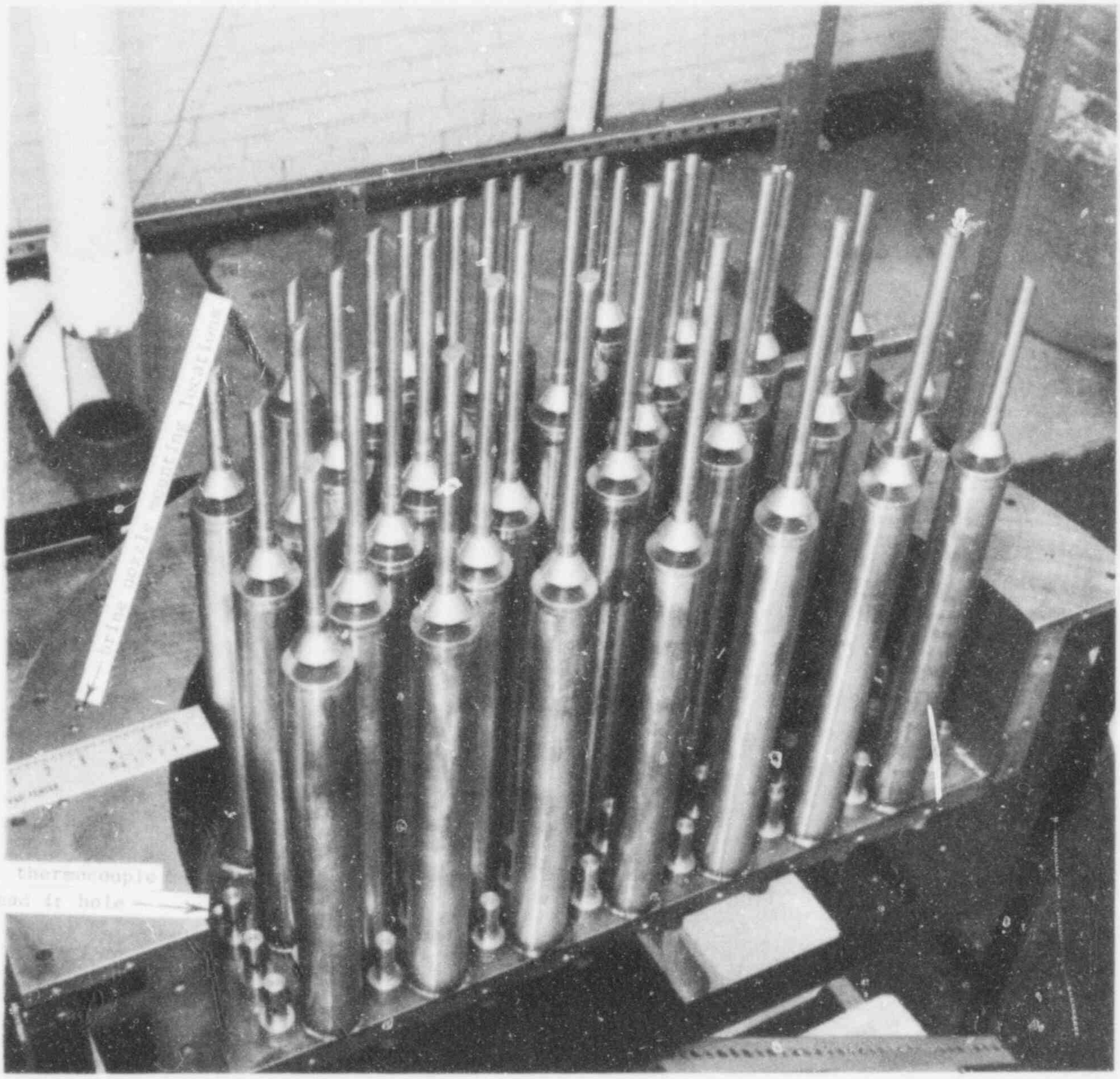

Figure 3-25. Angle View of Head Model

468 137

13465-34a

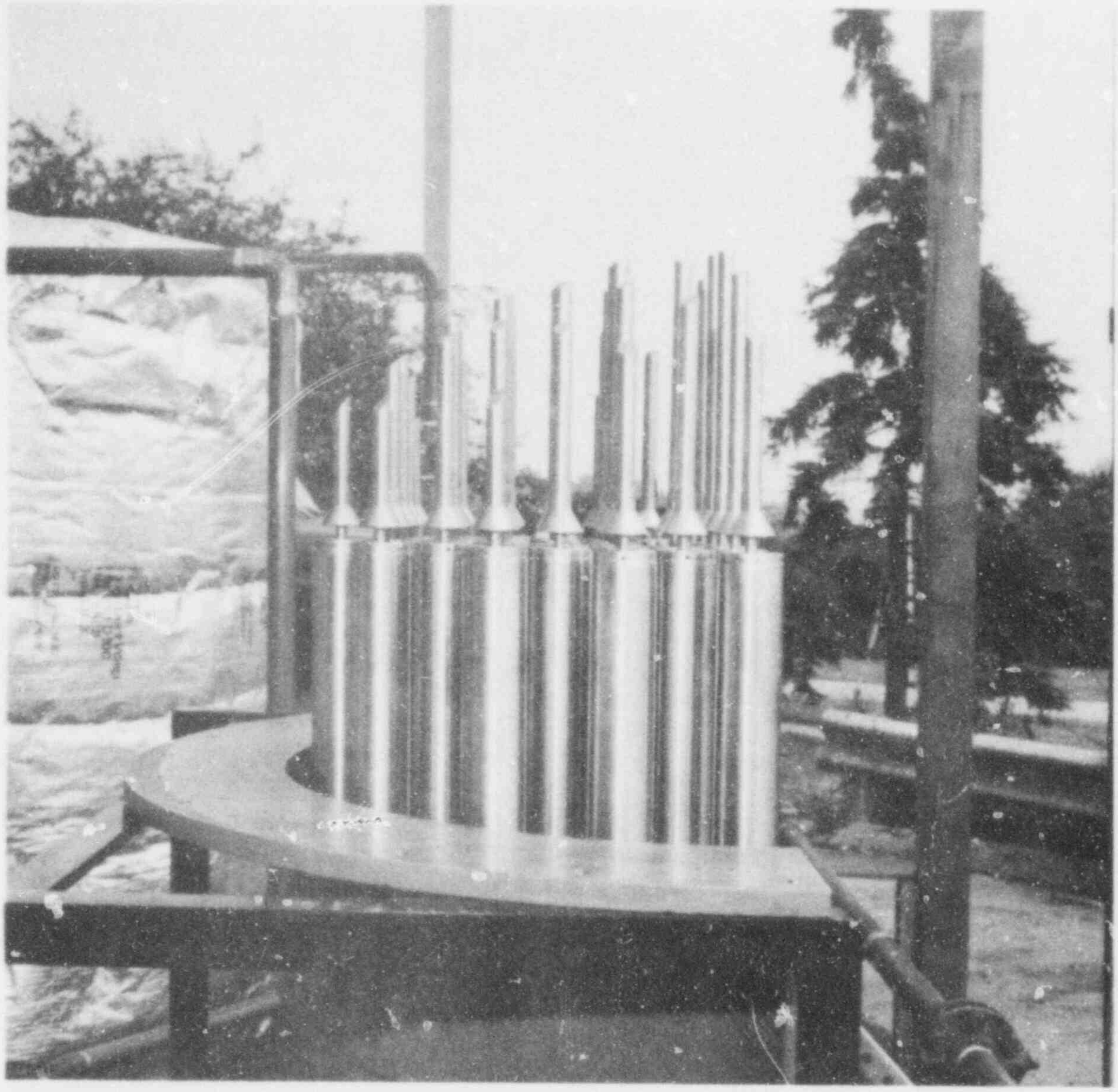

Figure 3-26. Side View of Head Model

468 138

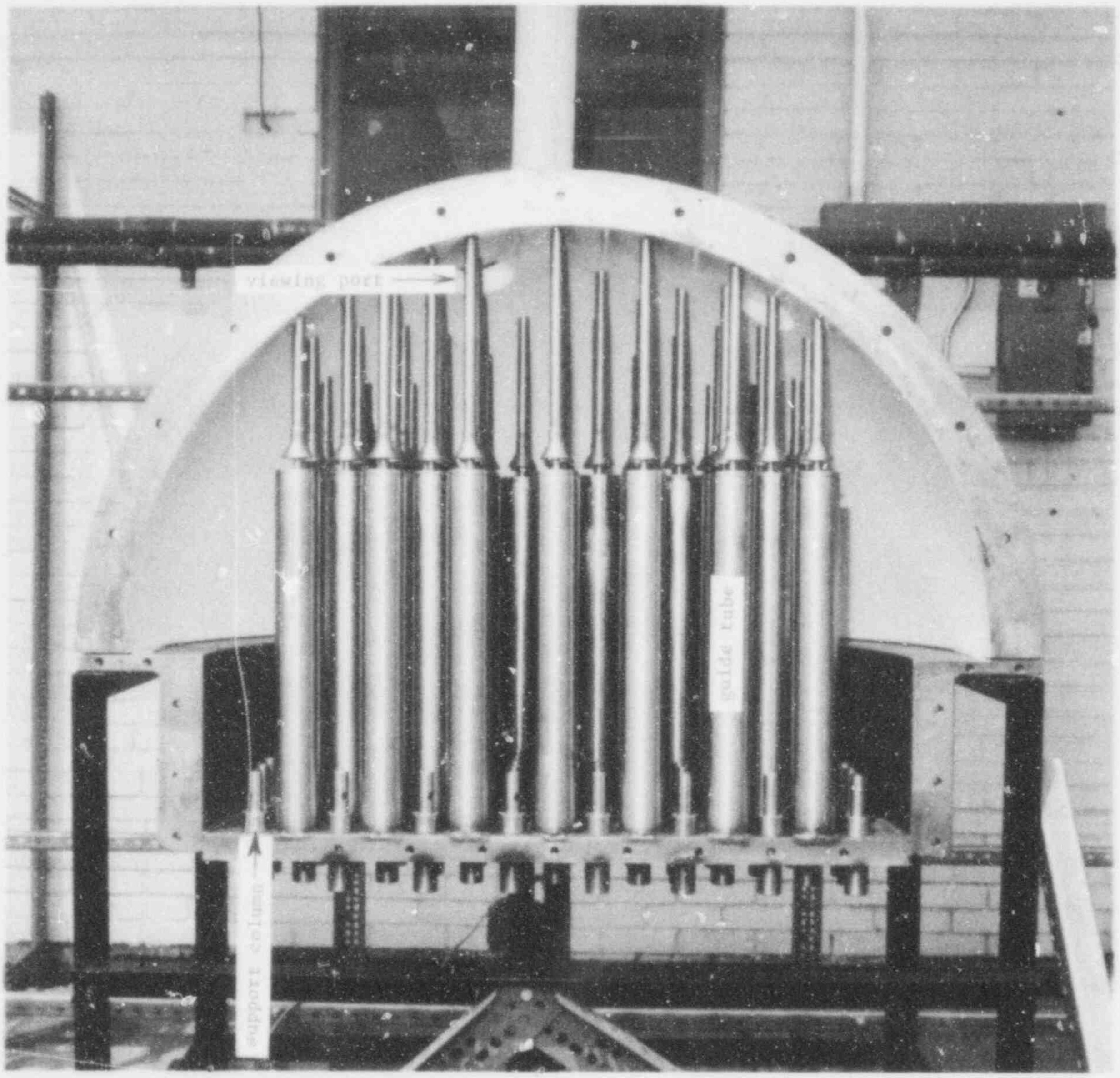

Figure 3-27. Front View of Instrumented Head Model

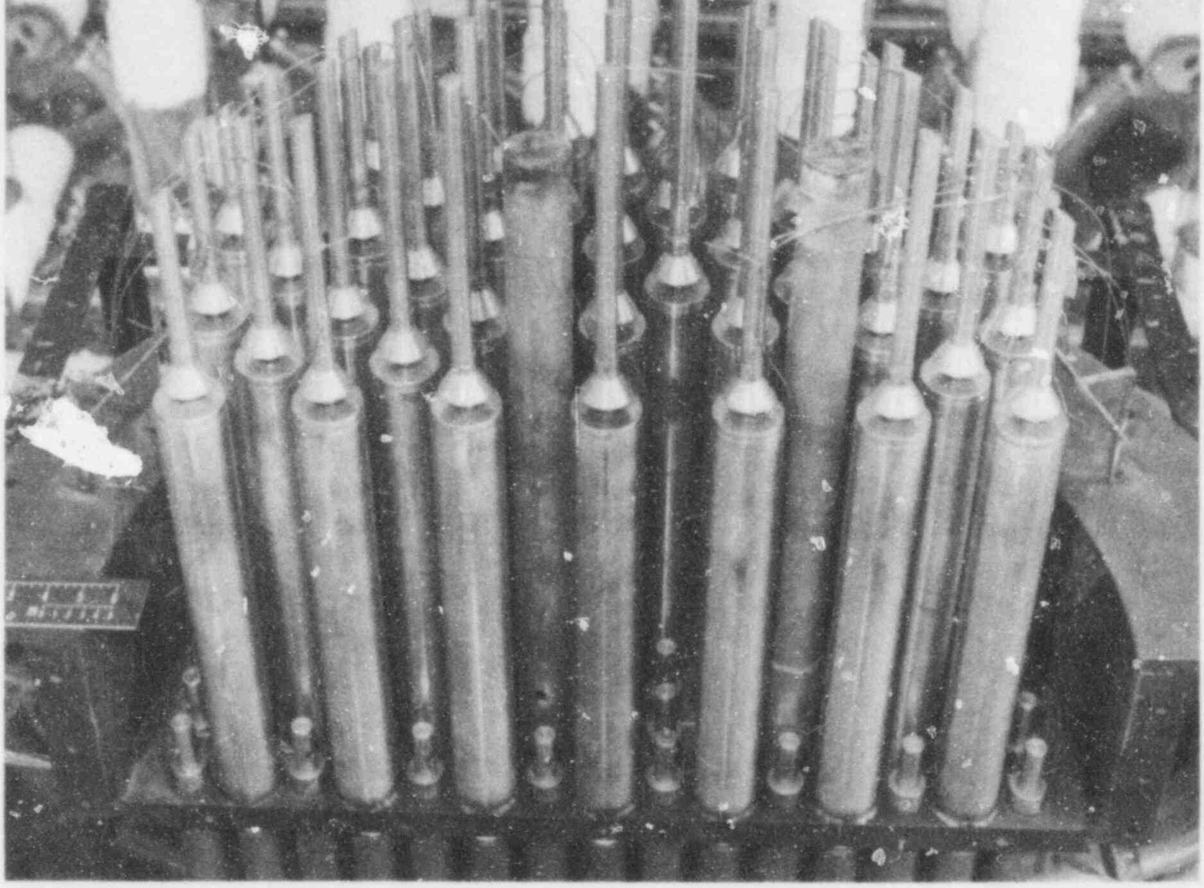

Figure 3-28. Angle View of Instrumented Head Model

468 140

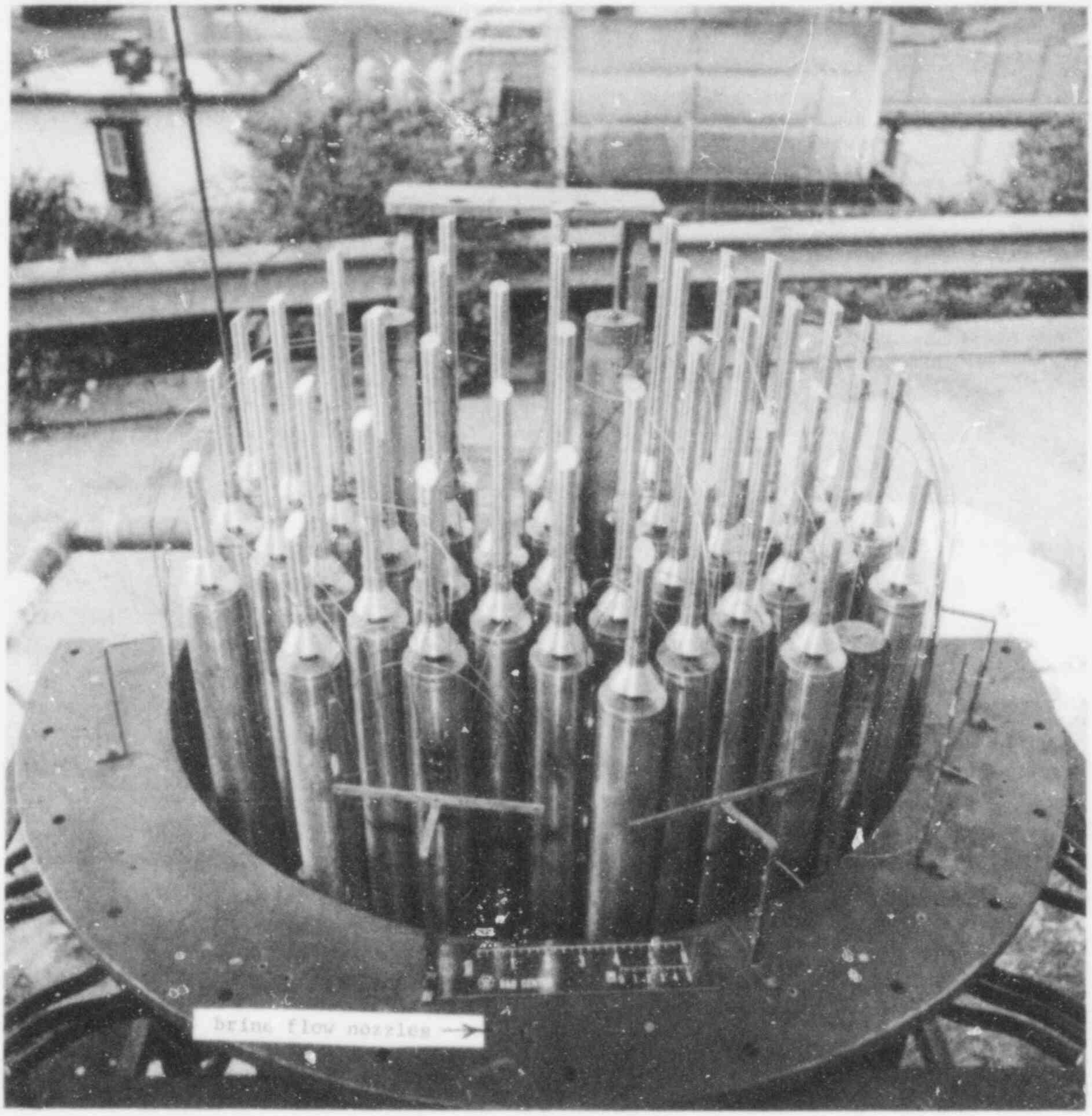

Figure 3-29. Back Top View of Instrumented Head Model

468 141

To model the hydraulic resistance of the entire support column, a 0.290-inch ID, 0.5-inch-long orifice with chamfered ends was installed at the bottom of the truncated support columns (used in the model). A straight piece of rigid plastic one-inch pipe was attached to the bottom of each guide tube and support column. The orifices at the inlet of each support column were held in a bored-out area at the top of these extension pipes. As discussed previously, these assemblies were tested prior to installation to insure proper hydraulic modeling of the actual reactor flow hardware.

The head model was instrumented with 60 stainless-steel-sheathed, ungrounded 0.040-inch OD copper-constantan (Type T) thermocouples located in 10 vertical planes in locations discussed previously. These were read and recorded on a paper tape at the rate of two thermocouples per second with a Doric Digitrend 210 which printed out the temperature with ± 0.1°F resolution.

In addition to the viewing window provided by the Lexan plate closing the front of the model, two dome view ports were provided to allow additional observation points or to provide locations for artificially illuminating the interior of the head.

3-11. Guide Tube and Support Column Standpipes

The pressure distribution to be employed has been discussed previously. The pressure distribution was represented using 11 standpipes for the support columns and 9 for the guide tubes. The overflows in these 20 standpipes were positioned to provide the elevation heads shown in table 3-3.

Figure 3-30 shows a schematic side view of the standpipe system for a typical guide tube and a support column. The 11 front standpipes (figure 3-23) fed the support columns only. Individual 1.25-inch ID, clear plastic tubes connected the several guide tubes and support columns with the appropriate standpipe. The diameter of these tubes was selected to make the flow pressure drops across the tubes very small. A small-diameter, clear plastic tube was connected to a tap in the side of one of the rigid plastic extension tubes beneath the model connection to each standpipe. The upper end of the small diameter tubing was attached adjacent to its respective standpipe overflow and acted as a sight glass. The elevation difference between the overflow and the tube water level indicated the flow pressure drop in the standpipe and connecting tubing. Each standpipe was supplied with city water at a point remote from both its top and bottom.

A short length of clear plastic was included near the bottom of each four-inch-diameter standpipe so that ink or dye injected into the standpipe at that elevation would clearly indicate whether the standpipe flow was up or down. A downward flow of city water was maintained in all standpipes so that only city water (not salt water) of a known density was in the standpipes. The downward flow in each standpipe was maintained by a soft plastic tubular drain at its base with flow restricted by the use of a modified C-clamp.

468 142

TABLE 3-3
STANDPIPE ELEVATION HEIGHTS

Support Column Standpipe	Elevation of Overflow Slot Above Head Model Top (in.)	Guide Tube Standpipe	Elevation of Overflow Slot Above Head Model Top (in.)
S-1	[b,c,e]	G-1	[b,c,e]
S-2		G-2	
S-3		G-3	
S-4		G-4	
S-5		G-5	
S-6		G-6	
S-7		G-7	
S-8		G-8	
S-9		G-9	
S-10			
S-11			

468 143

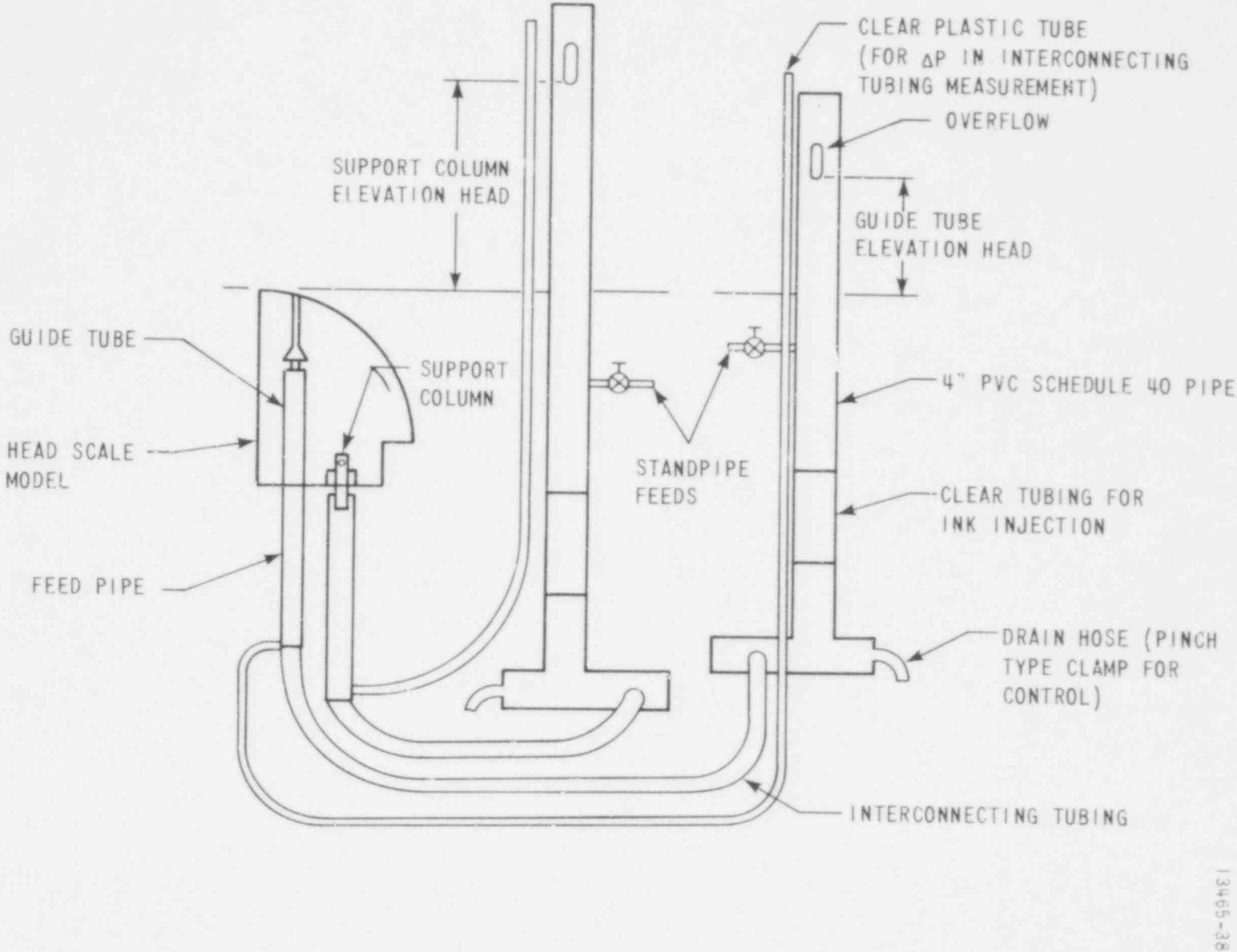

Figure 3-30. Schematic Layout of Standpipe System

468 144

3-12. Hot Brine Storage and Circulating System

A view of this portion of the apparatus is shown pictorially in figure 3-22. It consists of an insulated 1,000-gallon tank, a 15-kw immersion heater, a centrifugal pump, a flow-measuring orifice, and suitable brass or copper tubing, fittings and valves. The system was constructed so that it can circulate water in the tank and/or deliver a measured flow of salt water to the model spray nozzles. The pump draws suction from a fitting on the side near the bottom of the tank. The valved recirculation line enters the top of the tank and delivers water at a 45° angle about 10 inches above the bottom near the side. This establishes a vortex in the tank which aids in dissolving the salt in the water when the brine solution is being made up.

The pump was capable of 150 gpm at a 70-foot head. The inside of the 1,000-gallon steel tank and the manhole in the top were coated with a 0.004- to 0.006-inch-thick coating of Bisonite 957 to prevent rusting. Unfortunately, this coating chipped off in several places on the bottom of the tank and some rusting did occur.

When performing a test, the recirculating flow was reduced and the majority of the pump flow directed through a sharp-edged orifice with two-inch flange taps to the flow control valve and thence to the spray nozzles. Depending on the flow rate selected for any given test, either a 0.9558- or a 1.394-inch ID orifice was used. The orifice pressure drop was indicated by a U-tube mercury manometer. The orifice meter was used over the flow rate range of 30 to 150 gpm. For lower flows, a stop watch and the tank water level change were used. The tank water level was indicated by a clear plastic tube connected to the tank. This tube or height gauge can be seen taped to the roof support on the left edge of figure 3-22.

3-13. City Water Supply

The city water supply was drawn from a low pressure hydrant (18 psi) and led to the test apparatus through 150 feet of 2 1/2-inch fire hose. The end of this hose can be seen in figure 3-22 connected to the inlet gate valve. City water was supplied to the two standpipe supply manifolds during test, the brine manifolds for pretest flow adjustment, and also used to fill the 1,000-gallon tank before the test.

For one test requiring large flows of city water, a fire truck was connected into the supply line to raise the supply pressure.

3-14. Brine Manifolds and Nozzles

The metered brine flow passed through a control valve and into two parallel manifolds, each of which supplied up to 12 nozzles through a high presssure flexible tube connection. The actual nozzles used and their diameters are shown in figure 3-31. A special fitting in one of the flexible nozzle supply lines on either side of the model permitted the injection of dye into the brine

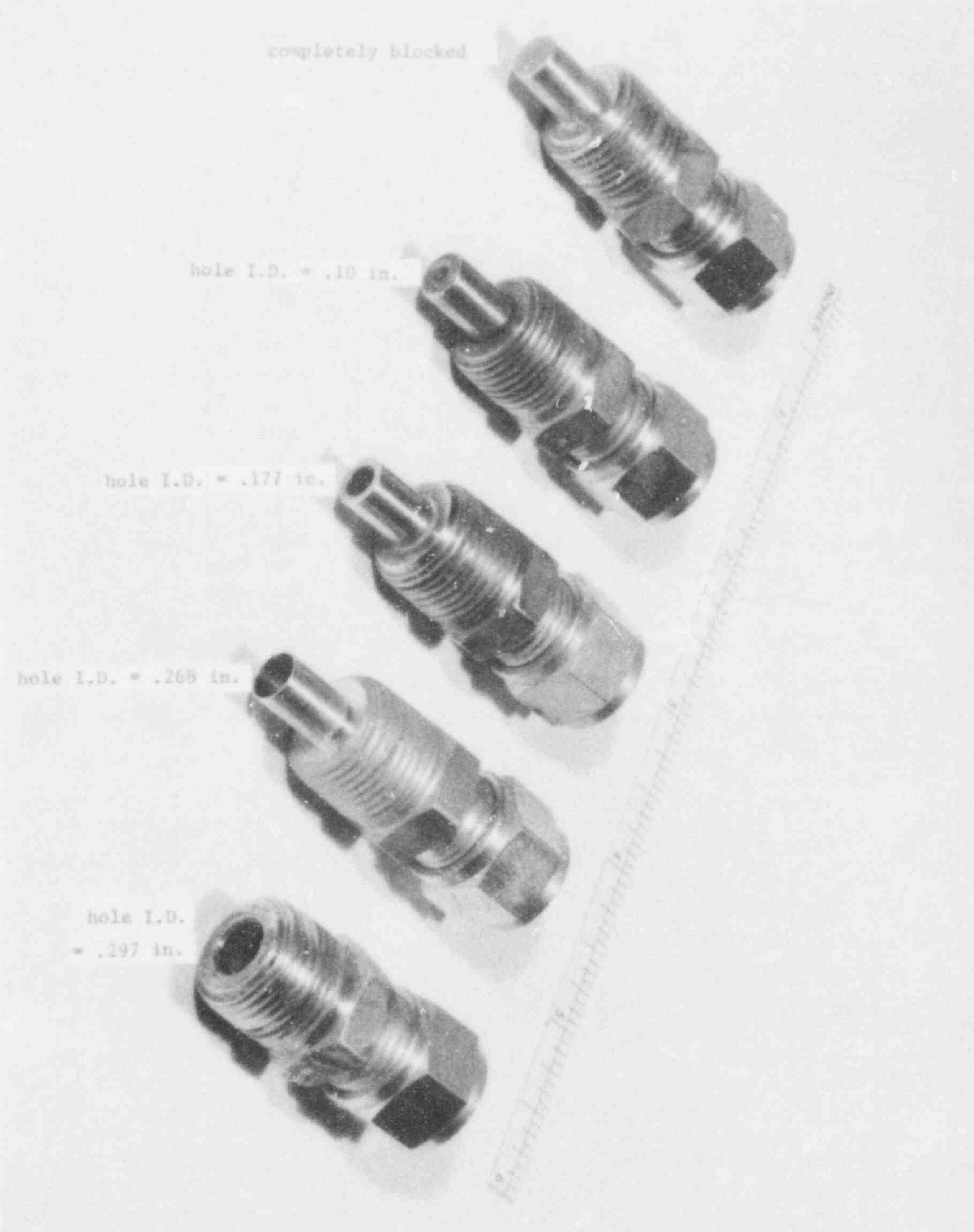

Figure 3-31. Brine Nozzles Used in Tests of Head Model

flowing through the hose so that the mixing of the dyed fluid from that nozzle with the clear water in the head could be observed visually.

3-15. EXPERIMENTAL PROCEDURE

Each test was initiated by filling the head model with fresh water. This was accomplished by successively opening the standpipe feeds on the shortest support column standpipes. Then, the same procedure was followed with the guide tube standpipes. While this was done, the air vent on the top of the head model was kept open.

Before each test a 22 percent salt solution was prepared and heated to about 140°F or roughly 70°F above the inlet water temperature. The 1,000-gallon tank was filled to a given depth with city water. The pump was then used to circulate the water. As it was being circulated about 26 80-pound bags of salt (NaCl) were poured through the manhole in the top of the tank and the heater was energized. The specific gravity of a sample of the brine was measured with a hydrometer at a relatively low temperature and near test temperature just before a run and the values were recorded. When all of the tubes had been purged of air, fresh water was admitted through a three-way valve into the brine feed nozzles at a rate near that of the desired brine flow rate.

The supply valve and drain restriction on each standpipe was then adjusted to insure that it was both overflowing and draining a moderate amount of city water. Ink was injected into the clear section of each standpipe with a hypodermic syringe to make certain the bulk water flow in the standpipe was downward.

Finally, when the temperature recorder had been turned on and a constant temperature scan of all thermocouples made, the 3-way valve was turned and the salt water solution admitted to the brine nozzles. The standpipe flows were readjusted as quickly as possible. The brine control valve was adjusted to attain the desired flow at the same time and the temperature of the mixture in the head monitored. Usually a steady state was achieved before half of the brine solution was used up. Before the brine solution ran out, the liquid level in each of the 20 small plastic tubes was marked on their respective standpipe walls. Any other special measurements or flow visualization dye injections were also made during steady-state operation of the system. A tube connected to the model vent valve was used as a manometer to determine the model mean pressure. This line was valved off and the height of fluid measured after the completion of the run.

When the brine flow ceased, the three-way valve was returned to its initial position and the model and connecting tubing flushed with city water for about 30 minutes.

3-16. FLOW VISUALIZATION

Following several attempts at flow visualization using ink, wool tufts, and neutrally buoyant spheres, a water coloring material (often employed by plumbers for tracing leaks) was tested. This material is a fluoroscein sodium salt called uranine which, when dissolved in water, yields a deep green color. Concentrated solutions of this uranine dye were injected into the hoses feeding two of the brine nozzles and permitted visual observation of the diffusion of the brine jets into the volume of water inside the head model. On several occasions, high-speed movies were taken during the dye injection.

3-17. TEST DATA

The common data recorded for each test were the following:

- The specific gravity of the hot brine solution.
- The 63 thermocouple termperature measurements in the head model and in the two water supply systems.
- The 20 small plastic tube elevations measured relative to the overflow elevations.
- The pressure in the top of the head model as measured with a vertical tube filled with fresh water.
- The pressure drop across the orifice plate in inches of mercury
- The flow direction in the interconnecting tubing between the model and each standpipe. (The brine was slightly cloudy, the city water clear. At high flows, dye injections into the model were used.)
- The locations and size of the brine nozzles.

For the extremely low flow tests, the rate of descent of the water in the 1,000-gallon tank was measured to determine the average flow rate of the brine supply. During one test, water was extracted from the model at several elevations and its specific gravity measured to correlate its salinity with temperature measurements recorded.

Thermocouple calibrations were made on two different occasions using various water temperatures between 70 and 140°F. These confirmed that all the thermocouples were reading in the range of accuracy (± 2°F) as specified by their manufactureres.

In all, 11 tests (applicable to the UHI and standard 4-loop plant), using the brine solution, were conducted consuming about 25,000 pounds of granulated salt. The initial test was run on August 19, 1977, and the final one on September 30, 1977. Table 3-4 briefly summarizes the brine flows and nozzle deployments for the 11 tests.

468 148

TABLE 3-4
TEST SCHEDULE FOR 1/5 SCALE MODEL TESTS

Test No.	Brine Flow Rate (gal/min)	Brine Nozzle Arrangement		Notes
		No. Blocked	No. & Size Open	
1	36.8	8	16-.177 in. I.D.	Shakedown run
2	36.8	8	16-.177 in. I.D.	With dye injection
3	99.2	8	16-.295 in. I.D.	
4	112.5	4	20-.295 in. I.D.	
5	66.7	8	8-.295 in. I.D. 8-.177 in. I.D.	
6	133.4	0	24-.295 in. I.D.	
7	99.2	8	16-.295 in. I.D.	Spray nozzle pattern different from Test 3
9	12.7	8	16-.10 in. I.D.	
11	29.4	8	12-.10 in. I.D. 4-.268 in. I.D.	
12	39.7	16	8-.268 in. I.D.	
13	59.6	12	12-.268 in. I.D.	

468 149

3-18. DATA REDUCTION TECHNIQUES AND PREDICTIONS

Data from the temperature-measuring tests were mathematically manipulated into a form which could be related directly to the actual plant. This was accomplished by converting each of the temperature measurements to a value corresponding to the percent of the difference between the spray nozzle flow fluid temperature, T_{SN}, and the guide tube and support column flow fluid temperature, $T_{GT/SC}$, as expressed below algebraically.

$$\% \text{ of difference} = \frac{(T - T_{SN})}{(T_{GT/SC} - T_{SN})}$$

The above calculation was performed for each thermocouple in the upper head region for at least ten sets of thermocouple measurements per test. For each thermocouple the maximum, minimum, and mean percentage of the difference between T_{SN} and $T_{GT/SC}$ were noted to ascertain the variation of the temperature with respect to time. For example, of the ten measurements recorded for a given thermocouple during a test, a maximum, minimum, and mean percent of the difference between T_{SN} and $T_{GT/SC}$ might be 53, 49, and 51, respectively. This would indicate that with respect to time, the measurements fluctuate by ± 2% around the mean value.

The spatial variation in temperature was indicated by determining a volume-weighted mean upper head region fluid temperature. The volume-weighted mean was determined by associating a given volume of the upper head region to each thermocouple (the 13 in-plant thermocouples are not used in this calculation). A total of 25 percent of the upper head fluid volume was located between the upper support plate and upper support plate flange. Twenty-six thermocouples were located in the above region. Therefore, each of the 26 represented approximately one percent of the upper head volume. Each of the remaining 21 thermocouples represented approximately 3.6 percent of the upper head volume.

Also reduced to the indicated form for use in predicting the mean upper head region fluid temperature, were the following measured parameters:

- Orifice pressure differential converted to flow in gpm.
- Specific gravity of brine solution converted to weight fraction of NaCl.
- Guide tube and support column pressure tube elevations converted to psi.

The TORCH computer code, which is presented in Appendix A, was developed to predict the mean upper head region fluid temperature for the 1/5-scale model. Equations were incorporated into the code regarding the guide tube and support column hydraulic loss coefficients and the physical properties of a brine solution. The brine properties are presented in Appendix B.

3-19. TEST RESULTS

The results of the testing can be divided into a section related to UHI plants and a second section pertaining to the standard plant. As mentioned in a previous discussion, the uncertainty in head cooling flows will be conservatively addressed in presenting the data as applied to the plant design. Specifically, the testing was performed with a flow rate which is 93 percent of the best estimate value and the measurements are reported for a flow rate which is 107 percent of the best estimate value. This represents as much as a 14 percent conservatism with respect to flow between the model results and the plant. In addition to accounting for the head cooling flow uncertainty, the possibility of fluid with temperatures in excess of the vesssel hot leg value entering the upper head region has been addressed. Based on design radial power distributions, it is conceivable that the temperature of the fluid entering the upper head region via the guide tubes and support columns (at certain locations) could be approximately 6°F greater than the vessel hot leg temperature. This effect was accounted for in the plant design data by increasing the measured percentage of the difference between T_{SN} and $T_{GT/SC}$ by 1.15, which corresponds to a value approximately 9°F above the vessel hot leg temperature. Based on in-plant measurements, the temperature of the fluid entering the upper head via the guide tubes and support columns is approximately 3°F greater than the vessel hot leg value.

A summary of the measured results of both configurations is presented in table 3-5. It can be seen from the table that as the head cooling spray flow rate is increased the mean upper head region fluid temperature decreases. This table also presents a comparison of the measured to predicted mean. As indicated in the table, the difference between the measured and predicted mean is less than 6 percent of the difference between T_{SN} and $T_{GT/SC}$. The results presented in table 3-5 represent the measured data and, as such, do not reflect the uncertainties associated with the head cooling flow rate and temperature of the fluid entering the upper head via the guide tubes and support columns.

Table 3-6 presents a summary of the design results of the 1/5 scale upper head temperature test. Tests 1 through 7 represent the UHI configuration testing and Tests 9 through 13 represent the standard plant configuration testing. The data presented in table 3-6 are based on the measured data (table 3-5) with the appropriate factors applied to account for uncertainties. Test numbers 2 and 9 represent the current UHI and standard plant configurations, respectively.

3-20. UHI Configuration Results and Conclusions

Figure 3-32 graphically presents the relationships between the maximum, minimum, and mean temperatures based on the test results along with the predicted mean temperature, all as a function of the head cooling flow rate for the UHI configuration.

468 151

TABLE 3-5
SUMMARY OF MEASURED RESULTS OF 1/5-SCALE UPPER HEAD TEMPERATURE TEST

	Head Cooling Flow (% of Total)	Head Cooling Flow (gpm)	Measured % of Difference Between T_{SN} & $T_{GT/SN}$			Predicted Average % of Difference Between T_{SN} & $T_{GT/SC}$	Measured Avg. (%) Minus Predicted Avg. (%)
			max.	min.	avg.		
UHI configuration							
1	0.92	36.8	78.5	45.1	53.9	53.1	0.8
2	0.92	36.8	81.3	50.6	59.3	54.2	5.1
3	2.48	99.2	38.0	13.9	19.1	14.1	5.0
[illegible]	2.81	112.5	21.5	5.2	10.6	8.4	2.2
5	1.67	142.0	62.1	27.2	35.2	31.8	3.4
6	3.55	66.7	0.0	0.0	0.0	2.4	-2.4
7	2.48	99.2	38.5	12.0	19.4	15.0	4.4
Standard plant							
9	0.32	12.7	63.6	47.8	57.3	62.8	-5.5
11	0.734	29.4	37.0	18.8	28.4	26.9	1.5
12	0.99	39.7	23.5	10.3	16.6	18.3	-1.7
13	1.49	59.6	0.0	0.0	0.0	1.9	-1.9

TABLE 3-6

SUMMARY OF DESIGN RESULTS OF 1/5-SCALE UPPER HEAD TEMPERATURE TEST

	Head Cooling Flow (gpm)	Design[a] Plant Head Cooling Flow (% of Total)	Measured Design[a] % of Difference Between T_{cold} & T_{hot}			Predicted Design[a] Average % of Difference Between T_{cold} & T_{hot}	Difference Between Measured and Predicted Average
			max.	min.	avg.		
UHI configuration							
1	36.8	1.05	90.3	51.9	62.0	61.1	0.9
2	36.8	1.05	93.5	58.2	68.2	62.3	5.9
3	99.2	2.84	43.7	16.0	22.0	16.2	5.8
4	112.5	3.22	24.7	6.0	12.2	9.7	2.5
5	66.7	1.91	71.4	31.3	40.5	36.6	3.9
6	133.4	3.82	0.0	0.0	0.0	2.8	-2.8
7	99.2	2.84	44.3	13.8	22.3	17.3	5.0
Standard plant							
9	12.7	0.36	73.1	55.0	65.9	72.2	-6.3
11	29.4	0.84	42.6	21.6	32.7	30.9	1.8
12	39.7	1.13	27.0	11.8	19.1	21.0	-1.9
13	59.6	1.70	0.0	0.0	0.0	2.2	-2.2

a. With respect to head cooling flow design, values are equal to 1.07 times the best estimate value. With respect to % of the difference between T_{cold} and T_{hot} design, values are 1.15 times the measured value.

468 153

13465-40

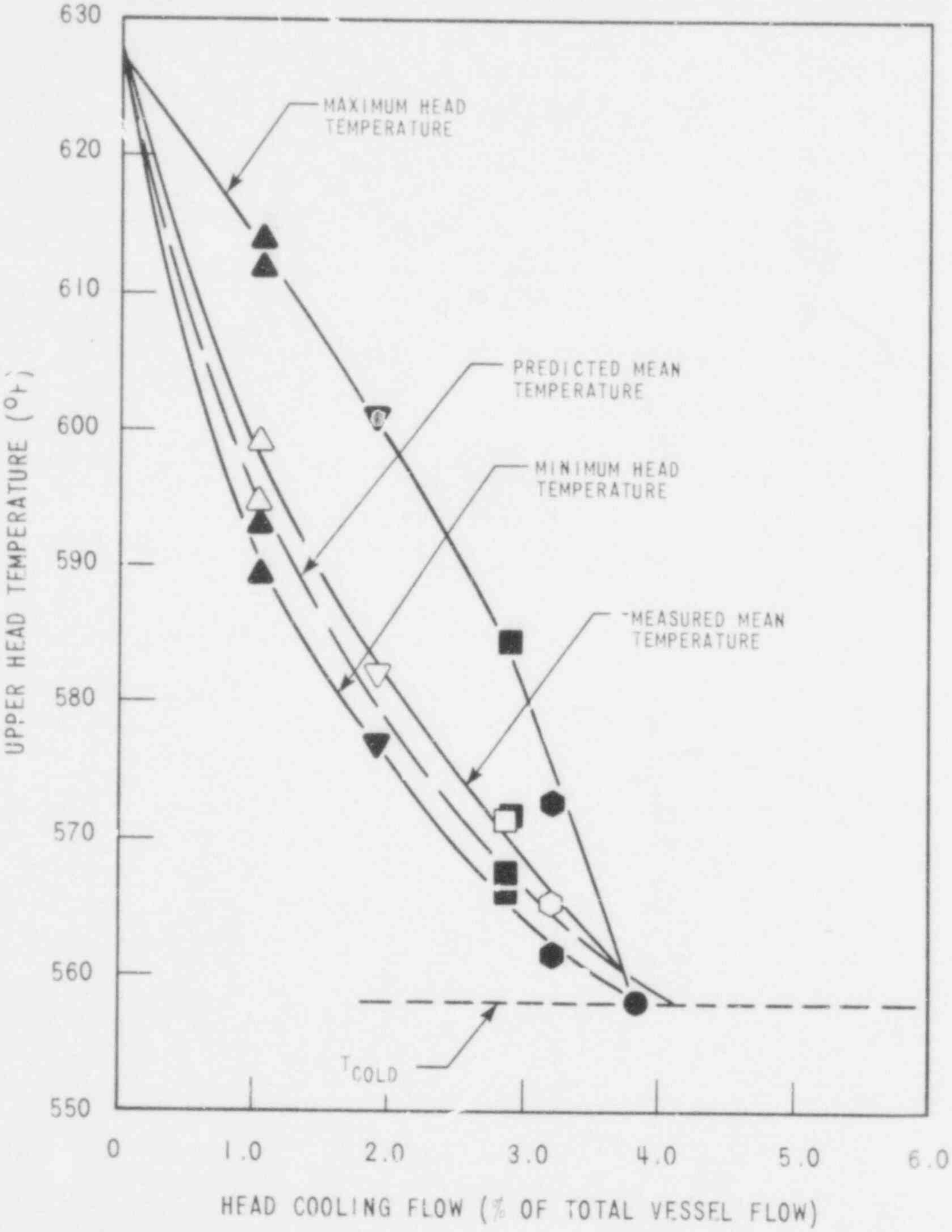

Figure 3-32. Results of 1/5 Scale UHI 4-Loop Plant Upper Head Temperature Test

468 154

Flow stratification in the upper head region was initially expressed as a concern. Although the possibility of stratified flow was believed to be extremely small, no basis for refuting its presence was available prior to completion of this test. It can be seen from figure 3-32 that definite relationships exist between the maximum, minimum, and mean upper head region temperatures. For example, for a head cooling flow rate of 0.92 percent of total vessel flow, the maximum, minimum, and average fluid temperature would be 615°F, 593.5°F, and 601°F, respectively. Considering the fact that the maximum temperature is 14°F greater than the mean, and the minimum temperature is 7.5°F less than the mean, implies that only a small portion of the upper head region volume can attain a temperature significantly greater than the mean value. Figure 3-33 presents histograms indicating what percentage of the upper head volume falls within each five percent increment between T_{cold} and T_{hot}. From the histograms the following can be determined:

- The temperatures in the region between the upper support plate and upper support plate flange are slightly greater than in the portion of the head above the support plate flange.
- Only a small portion of the fluid volume between the support plate and support plate flange possesses a fluid temperature significantly above the overall mean. (The maximum temperature is located in this region at a position between the cold leg nozzles as originally postulated.)
- As the head cooling flow is increased, the mean temperature and temperature variation tends to decrease.
- Since only a small portion of the fluid volume possesses a temperature significantly above the mean and no large temperature variations are present in the region above the upper support plate, the flow field is momentum-controlled and no appreciable flow stratification exists.

Based on figures 3-32 and 3-33, and the preceding discussion, the following conclusions are apparent regarding the UHI configuration testing:

- The predicted mean temperature is within 3.5°F of the mean based on the test results.
- A head cooling flow rate corresponding to four percent of the total vessel flow rate will result in an upper head temperature corresponding to T_{cold}.
- A maximum temperature variation in the upper head region of 28°F would exist at a head cooling flow rate of 1.91 percent of total vessel flow.
- The flow field is momentum-controlled and no appreciable flow stratification exists.

13465-41

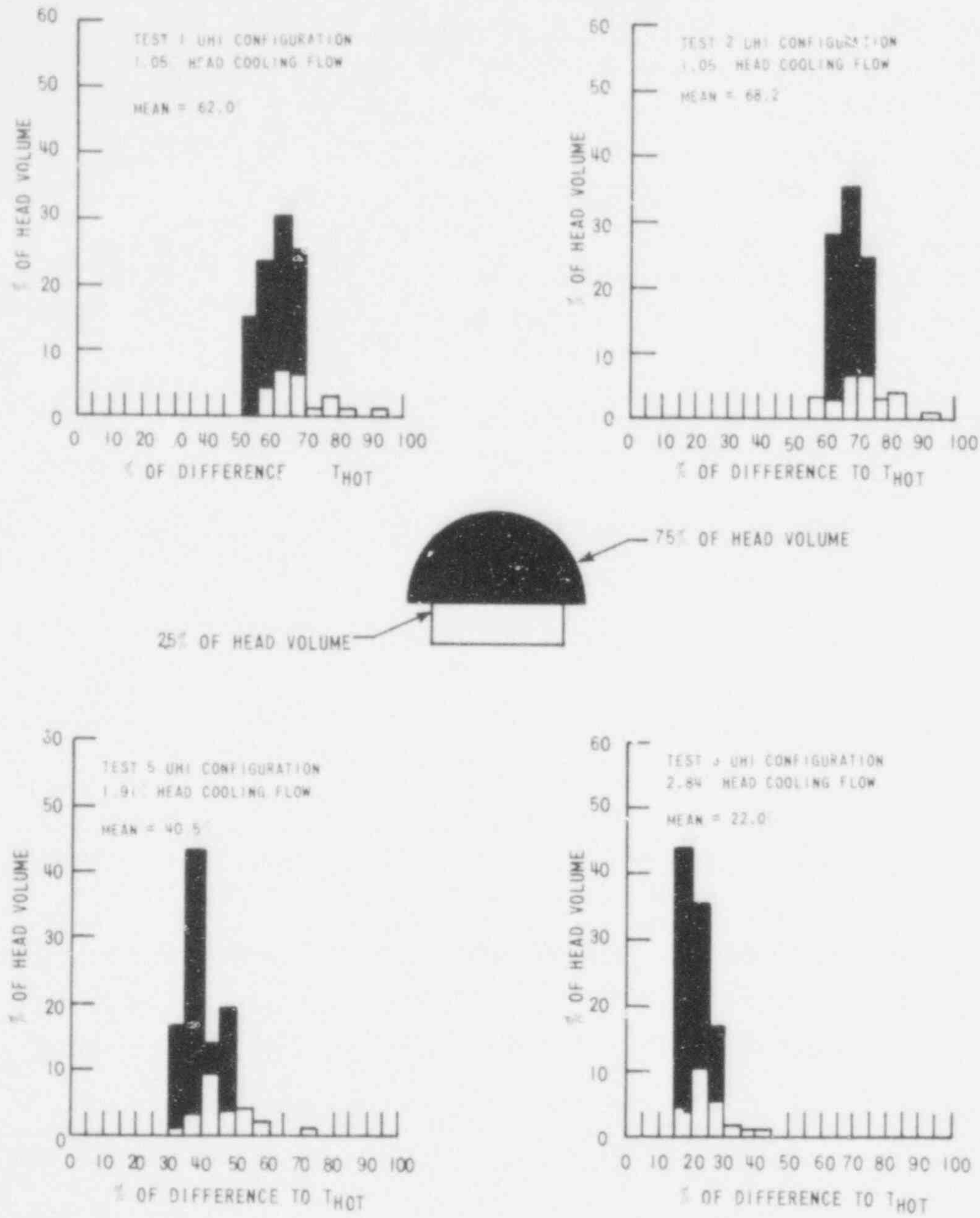

Figure 3-33. Histograms of UHI Configuration Data (Sheet 1 of 2)

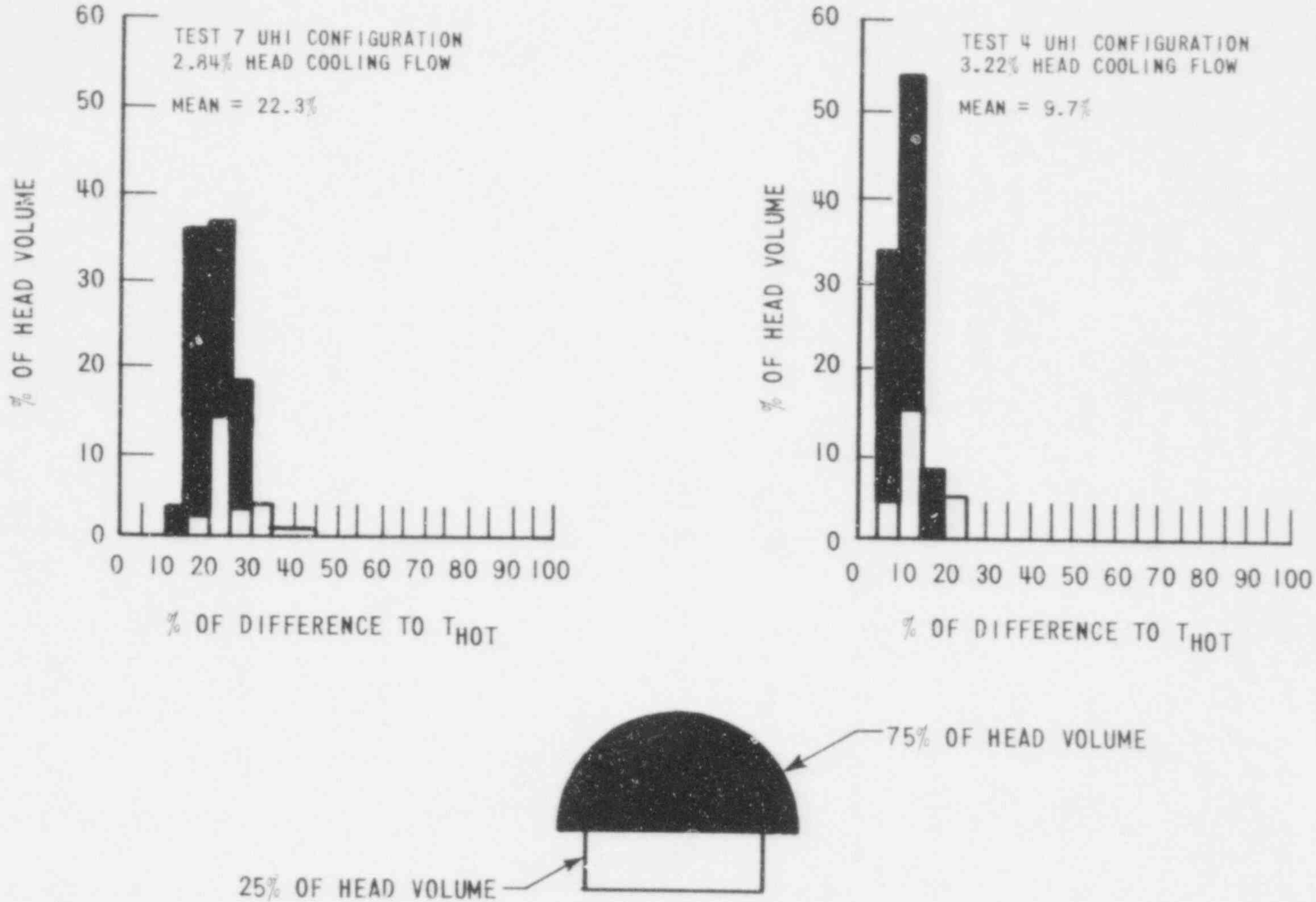

Figure 3-33. Histograms of UHI Configuration Data (Sheet 2 of 2)

13465-42

468 157

3-21. Standard Plant Results and Conclusions

Figure 3-34 graphically presents the relationships between the maximum, minimum, and mean temperatures based on the test results along with the predicted mean temperature all as a function of the head cooling flow rate for the standard plant configuration. As was the case for the UHI configuration, the possibility of the presence of stratified flow was a concern. It can be seen from figure 3-34 that for the current standard plant design head cooling flow rate of 0.36 percent of total vessel flow, there is a temperature variation of 11°F between the maximum and minimum upper head region fluid temperature with the mean temperature being approximately 5.5°F between the maximum and minimum. Figure 3-35 presents histograms indicating what percentage of the upper head volume falls within each five percent increment between T_{cold} and T_{hot}. From the histograms, the following can be determined:

- A large (approximately 60 to 70 percent) portion of the upper head volume is at essentially the same temperature. In addition, the temperature of the remaining volume is relatively "close" to the mean value.

- As the head cooling flow rate is increased, the mean temperature tends to decrease.

- The flow field is momentum-controlled and no appreciable flow stratification exists.

Based on the preceding discussion and figures 3-34 and 3-35, the following conclusions regarding the standard plant configuration can be drawn:

- The predicted mean temperature is within 4°F of the mean based on the test results.

- A head cooling flow rate corresponding to 1.7 percent of the total vessel flow rate will result in an upper head temperature corresponding to T_{cold}.

- A maximum temperature variation in the upper head region of 13°F would exist at a head cooling flow rate of 0.84 percent of total vessel flow.

- The flow field is momentum-controlled and no appreciable flow stratification exists.

13465-43

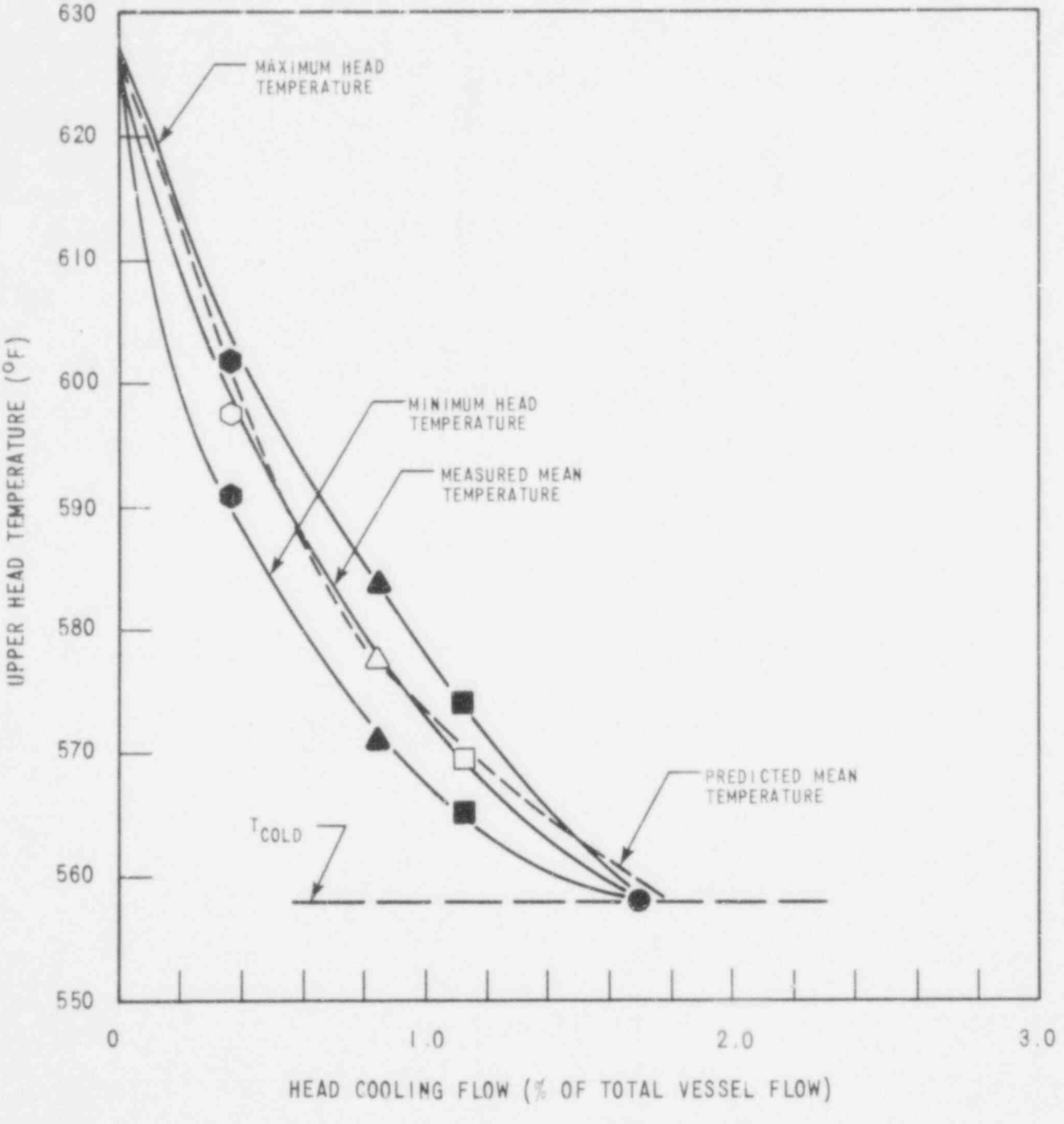

Figure 3-34. Results of 1/5 Scale Standard 4-Loop Plant Upper Head Temperature Test

468 159

13465-44

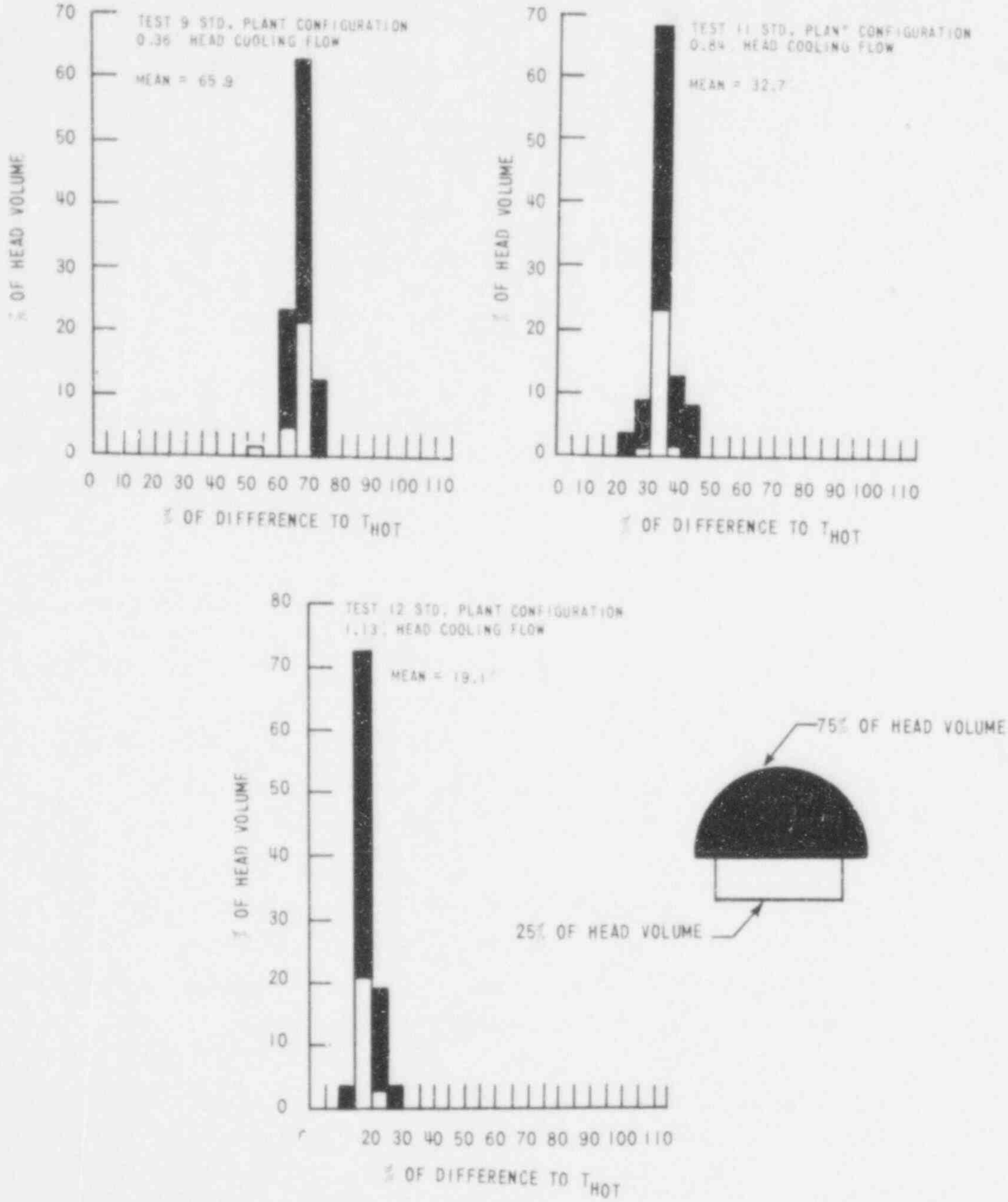

Figure 3-35. Histograms of Standard Plant Configuration Data

SECTION 4
IN-PLANT HEAD FLUID TEMPERATURE MEASUREMENT PROGRAM

4-1. INTRODUCTION

An in-plant vessel upper head region fluid temperature measurement program was developed to accomplish the following objectives:

- Determine the mean vessel upper head region fluid temperature in operating plants which verify or identify the conservatism in the Westinghouse analytical model for calculating head region fluid temperatures.
- Demonstrate that the fluid in the vessel head region is essentially at a uniform temperature, by mapping head temperatures throughout the head region.
- Demonstrate that in domestic UHI plants the upper head region fluid temperature is T_{cold}.

The objectives should lead to a basis for reducing the penalty currently imposed on LOCA analysis (i.e., the head region fluid is assumed to be at T_{hot}) and also improve the confidence that the head region fluid could be returned to the reactor inlet temperature with the flow rates calculated by the Westinghouse analytical model.

The program included plans for measurements in three 15x15 3-loop plants (H. B. Robinson Unit 2, Turkey Point Unit 4, and Surry Unit 1), one 17x17 3-loop plant (Joseph Farley Unit 1), one 15x15 4-loop plant (Zion Unit 2), two 17x17-UHI plants (McGuire Unit 1 and Sequoyah Unit 1), and one 14x14 2-loop plant (R. E. Ginna).

Table 4-1 presents a summary of the plants which have been instrumented, along with the number of thermocouples employed on each plant.

4-2. PROGRAM DESCRIPTION

The in-plant vessel upper head region fluid temperature measurement program can be divided into two categories on the basis of plant operating status (i.e., operational or under construction at initiation of the program).

TABLE 4-1

SUMMARY OF WESTINGHOUSE IN-PLANT HEAD TEMPERATURE MEASUREMENT PROGRAM

Plant	Number of Vessel Upper Head Region Thermocouples	Number of Loops
H. B. Robinson #2	1	3-Loop
Surry #1	3	3-Loop
J. M. Farley #1	13	3-Loop
Zion #2	3	4-Loop
R. E. Ginna	3	2-Loop
Turkey Point #4	3	3-Loop
Sequoyah #1	5	4-Loop UHI
McGuire #1	5	4-Loop UHI

4-3. Operating Plant Program

For plants which had achieved operating status, Westinghouse and some of its customers agreed to a program that provided measurement of the vessel upper head region fluid temperature at various radial locations in the head. Acquisition of these data did not require significant modifications to existing hardware. The program consisted of removing a few of the existing core temperature monitoring thermocouples (see table 4-1) and the reinstallation of new thermocouples in the core thermocouple conduit tubes. However, the new thermocouples terminated in the conduit tubes at a point in the vessel upper head region rather than at the core outlet. The thermocouples in the upper head region were located such that they monitored the head fluid temperature in the regions least likely to be affected by flow jetting into the head via the head cooling spray nozzles and the guide tubes. The data obtained from the thermocouples located in the upper head were intended to indicate the mean temperature of the head region. Typical locations of T/C's for plants in this category are contained in figures 4-1, 4-2, 4-3, and 4-4.

4-4. Program for Plants Under Construction

Instrumentation for Joseph Farley Unit 1, a 17x17 3-loop plant which was still in the construction phase at the initiation of the program, was designed with customer concurrence to address both radial and axial variations in the upper head region fluid temperature. The

13465-45

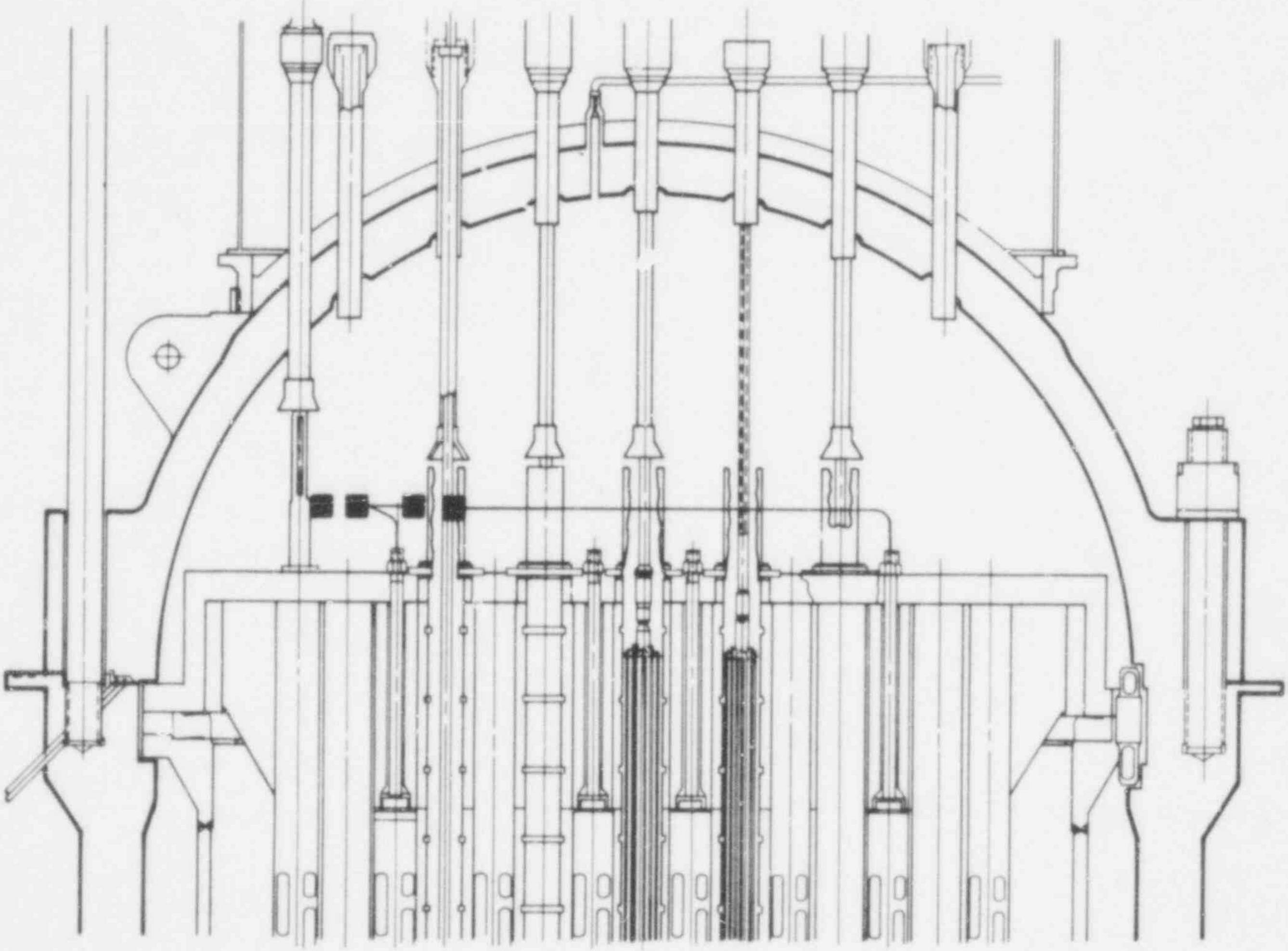

Figure 4-1. Zion Unit 2 4-Loop Upper Head Thermocouple Schematic, Elevation View

468 163

13465-46

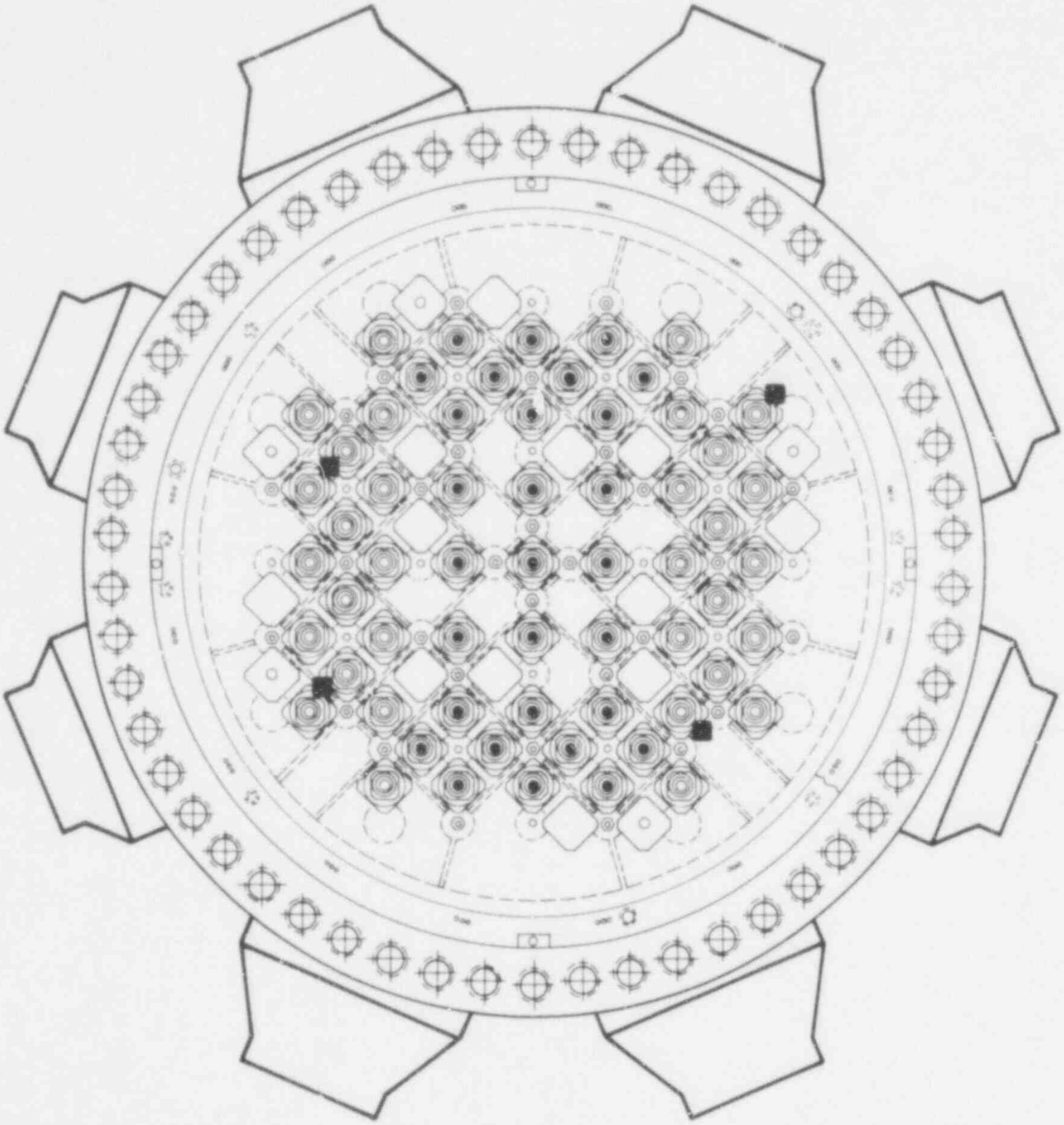

■ T/C LOCATIONS

● FLOW ENTERS HEAD REGION VIA THIS LOCATION

Figure 4-2. Zion Unit 2 4-Loop Upper Head Thermocouple Schematic, Plan View

468 164

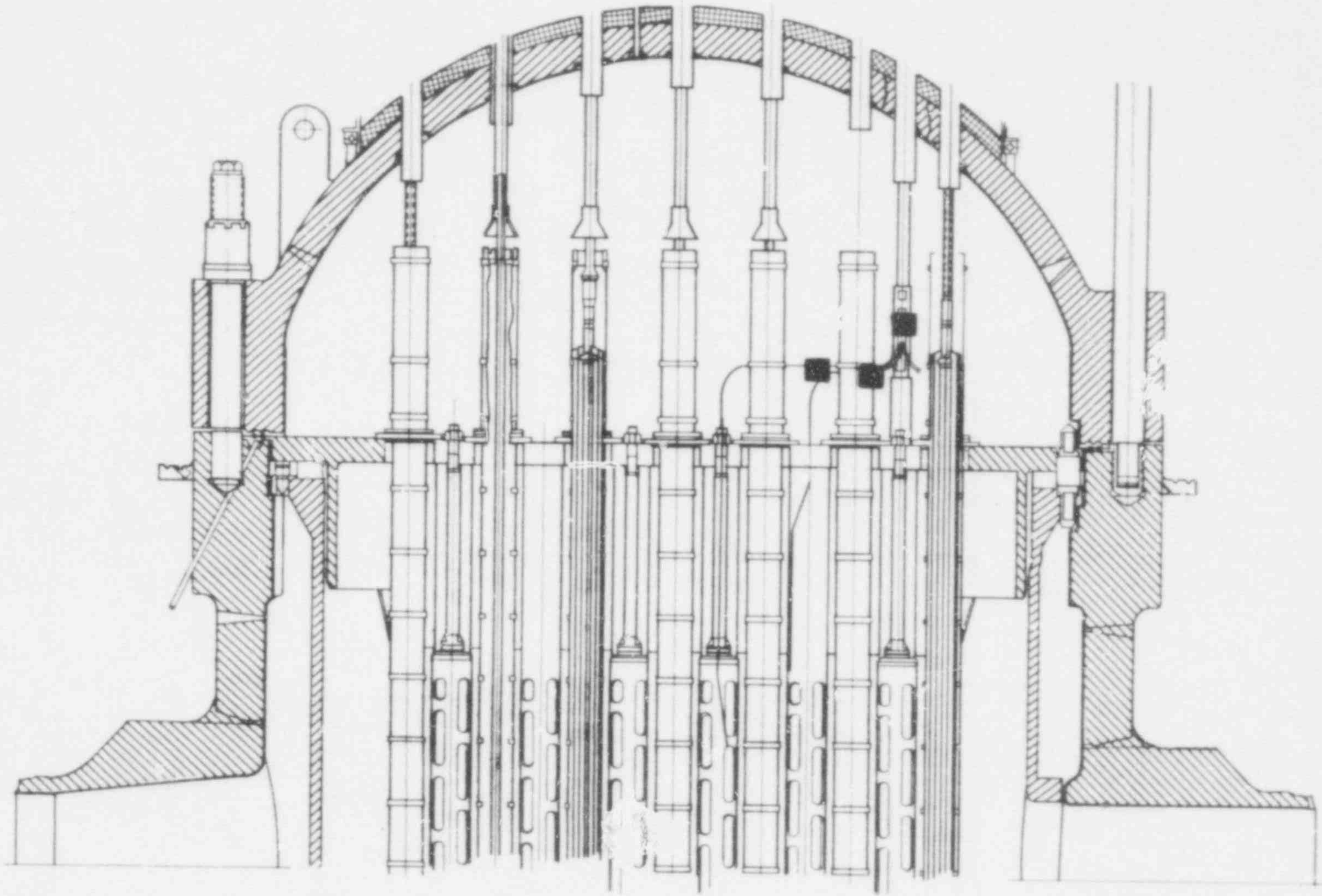

Figure 4-3. Surry, Unit 1 3-Loop Upper Head Thermocouple, Elevation View

468 165

13465-48

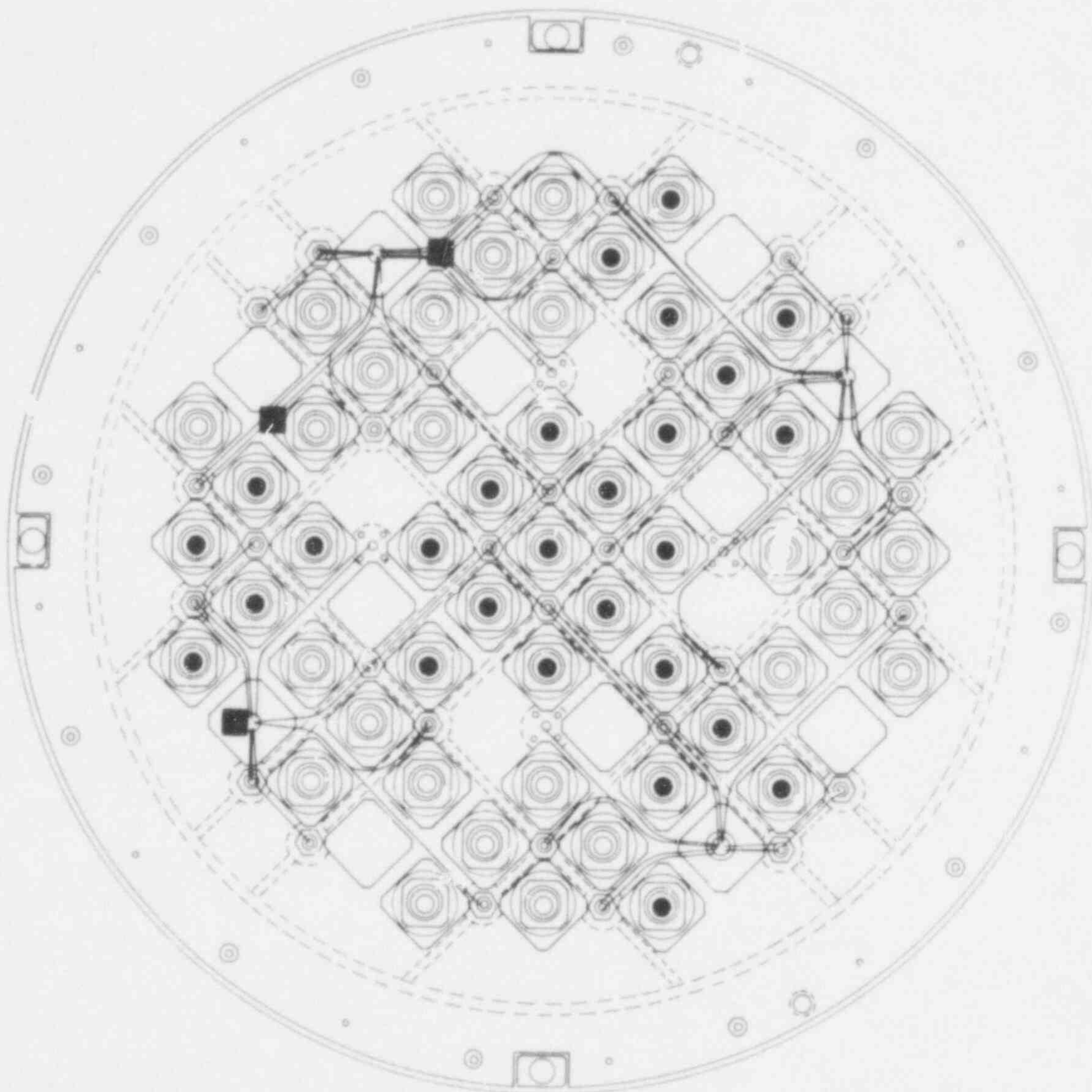

■ T/C LOCATIONS

● FLOW ENTERS HEAD REGION VIA THIS LOCATION

Figure 4-4. Surry Unit 1 3-Loop Upper Head Thermocouple Schematic, Plan View

468 166

variation in upper head region fluid temperature, between the minimum and the maximum values would be judged uniform if less than 10°F. A 10°F variation implied approximately a 100 psi change in saturation pressure. A 100 psi variation of saturation pressure results in a relatively minor effect on the time at which the vessel upper head region begins to flash.

As shown in figures 4-5, 4-6 and 4-7, 12 core monitoring thermocouples were removed and replaced by 12 thermocouples to monitor fluid temperature in the reactor vessel head. At three positions (P-7, G-6, and K-8), a shorter thermocouple was installed, terminating inside the conduit in the upper head region. At two locations, supports were erected and four thermocouple conduits each were run to those supports to measure the vertical temperature distribution in the vessel head. At the location marked E-14, a thermocouple was mounted to measure temperature at the periphery. At the thermocouple column at N-11, a thermocouple was mounted within the column at this spare thermocouple location. Therefore, 13 thermocouples were installed in the vessel head region.

The 12 thermocouples were removed from their core monitoring positions and the runs (several from each thermocouple port column) were modified to terminate in various locations in the vessel head region. Sufficient in-core thermocouples remain to preserve the ability to measure major and minor core tilts.

Although the Digital Rod Position Indicator System eliminates the need for thermocouple monitoring of the control rods out of position, this ability is still preserved with the resultant in-core thermocouple pattern.

The resultant thermocouple pattern also locates a thermocouple within king's move[1] of each fuel assembly position to aid in-core performance analysis.

In the placement of the T/C's in the Farley plant, two basic criteria were:

- The T/C's must be located such that regions of significantly different temperatures will be detected, if they exist.
- The T/C's must be located in spots which are not in the direct path of inlet flow to the head, i.e., head cooling jets and guide tube exit flow paths.

In selecting specific locations, two assumed flow fields were considered, based upon alternate flow directions of the guide tube exit flows. The first flow field assumed that a toroidal vortex is established in the head as depicted in figure 4-8, and that the guide tube exit flow is swept downward toward the support plate. In this momentum-controlled flow pattern, the T/C's in region 1 (E-7, E-12, K-5, and G-2) would record temperatures several degrees lower

1. Each fuel assembly has at least one adjacent or diagonal location which is monitored by a thermocouple.

468 167

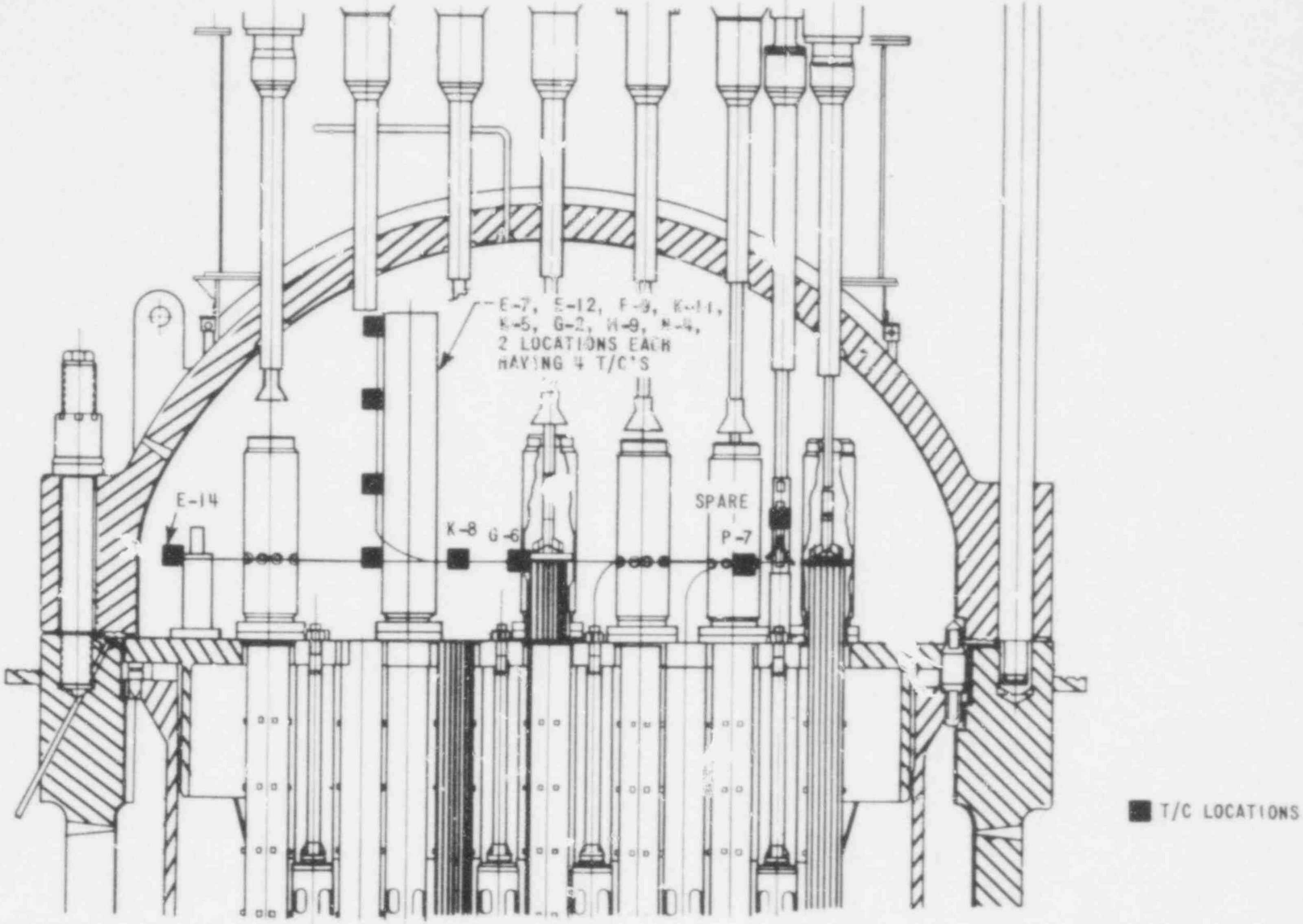

Figure 4-5. Farley Unit 1 3-Loop Upper Head Thermocouple Schematic, Elevation View

13465-49

468 168

13465-60

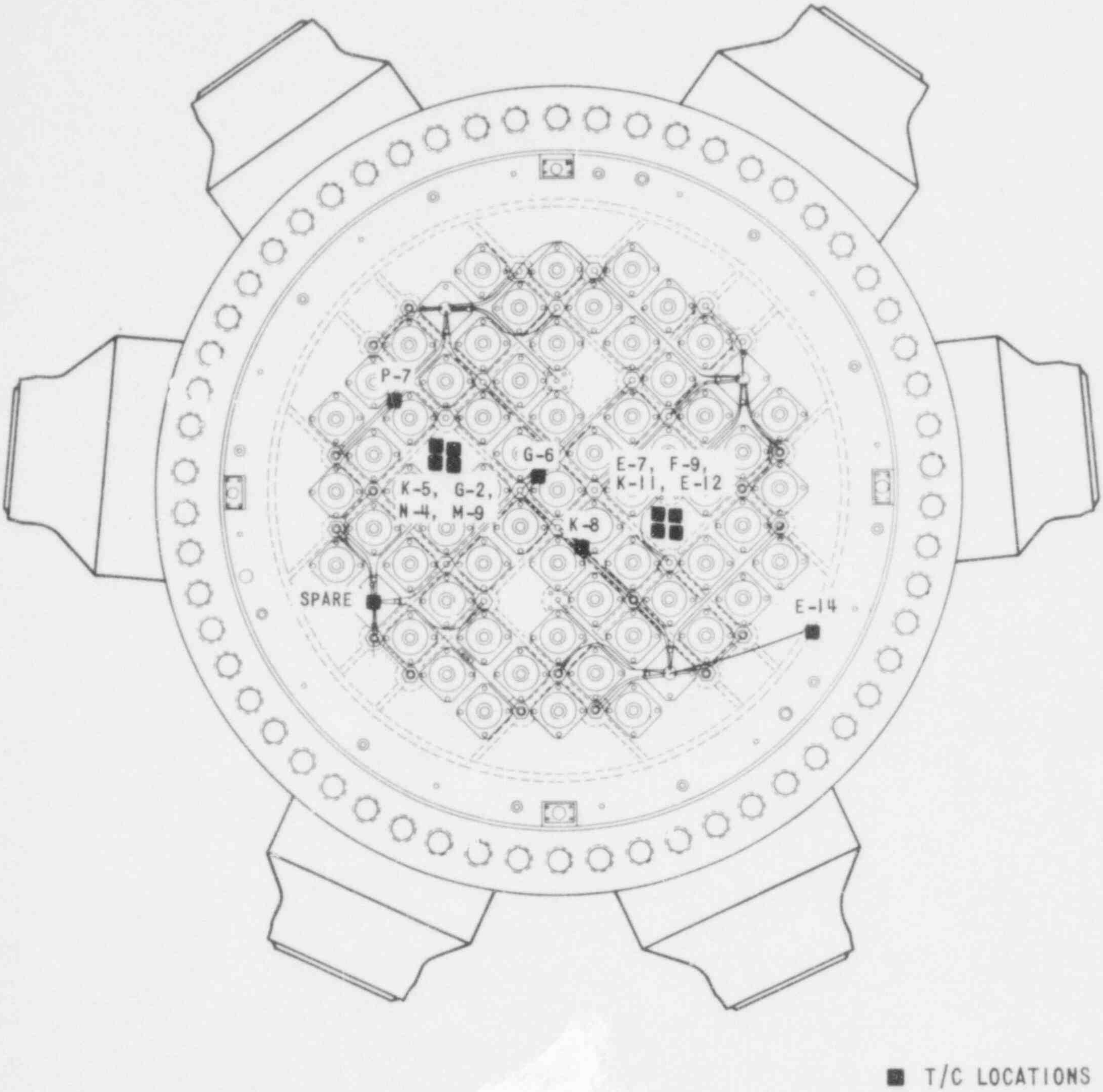

Figure 4-6. Farley Unit 1 3-Loop Upper Head Thermocouple Schematic, Plan View

468 169

13465-51

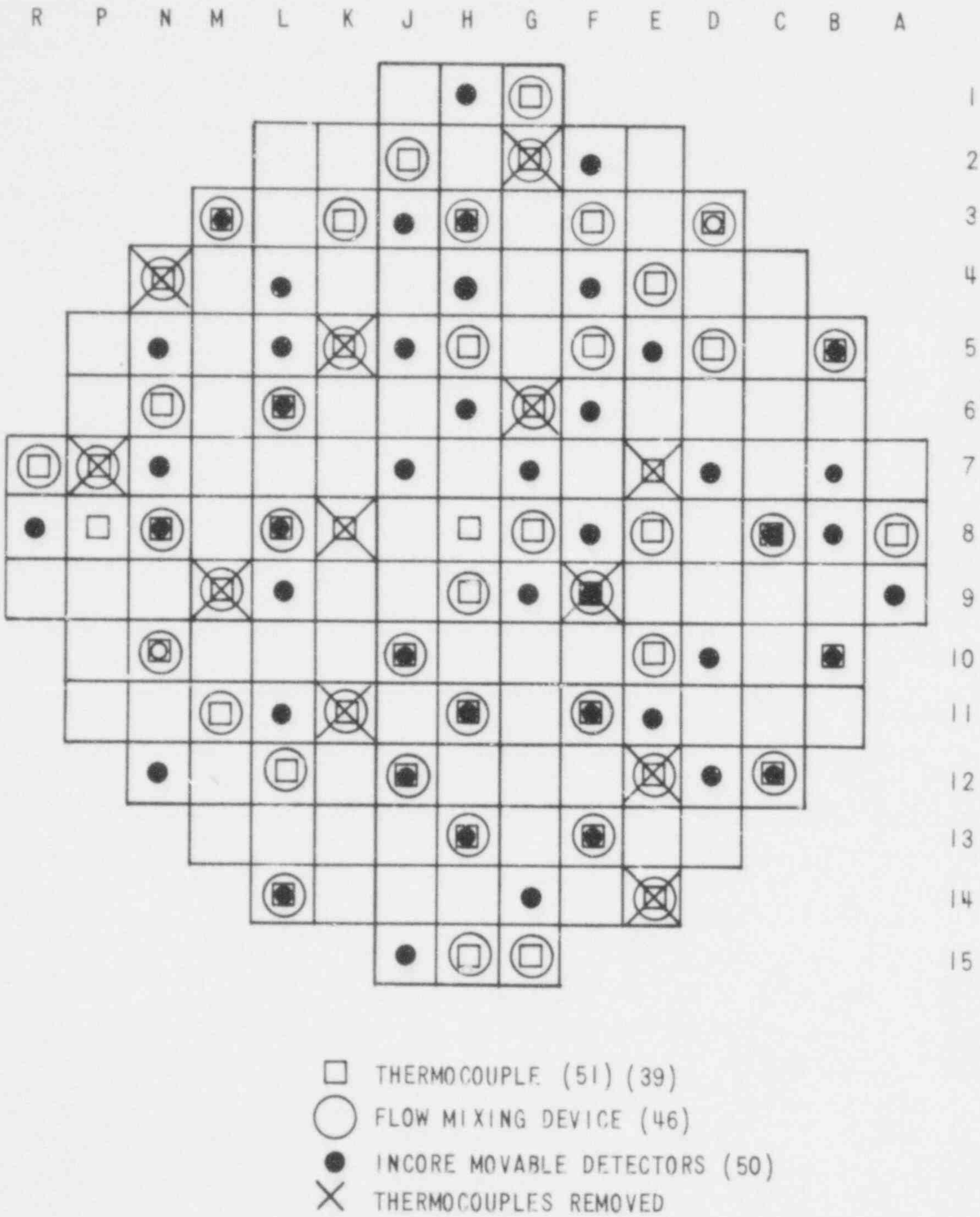

Figure 4-7. J. M. Farley 1 Flow Mixing, Thermocouples and Incore Movable Detector Locations

468 170

13465-49

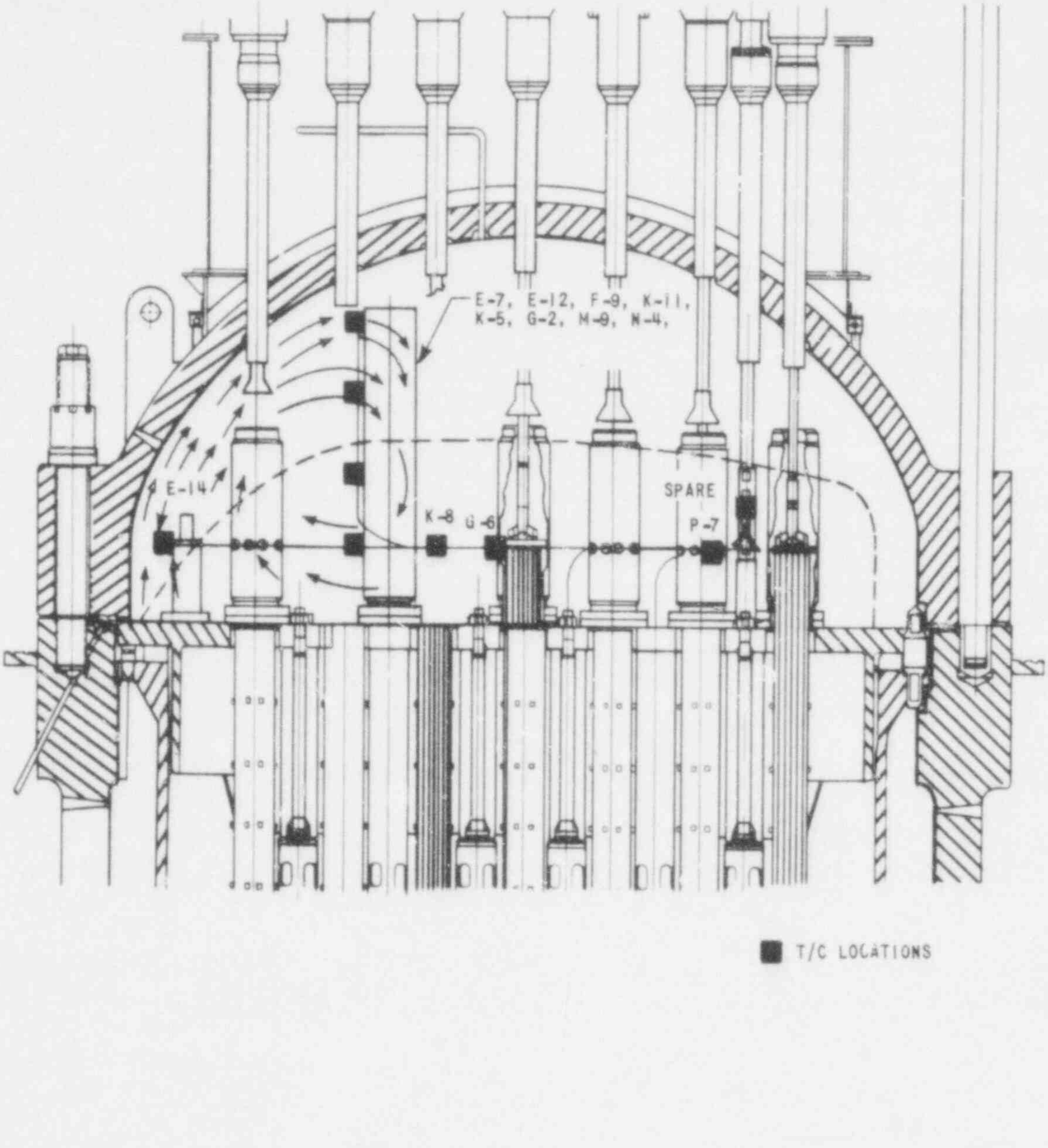

Figure 4-8. Farley Unit 1, 3-Loop Upper Head Region Momentum Controlled Flow Pattern

468 171

than those in region 2 (F-9, K-11, M-9, N-4, G-6, K-8, etc.). Conversely, an alternate flow pattern, which is controlled by density gradients, would exist if the hot guide tube exit flow was of sufficiently low density to rise or stratify in the top of the upper head, shown in figure 4-9. In this case, the temperature of the two groups of T/C's, indicated above, would be reversed, i.e., the E-7, E-12, K-5, and G-2 would record the higher temperatures. In this case, a region of low velocity flows would exist directly above the support plate in which significant radial temperature variations could develop. In such a situation, the variation in temperature would be detected by T/C's E-14, N-4, K-8, G-6, K-11, and P-7.

The computer readout program was modified to reflect 39 core monitoring thermocouples and 13 vessel head region thermocouples.

The following data were obtained for zero-power hot standby at 25, 50, 75, and 100 percent power. (It should be noted that the zero-power hot standby data served as a T/C calibration point.)

- Hot leg temperature of all three loops, °F.
- Cold leg temperature of all three loops, °F.
- Core power level, MWt.
- System pressure, psia.
- Upper head region thermocouple readings (13), °F.
- Number of steps which control banks are inserted.
- Core exit thermocouple map.
- Relative fuel assembly power map.

In addition, any knowledge of anomalies were to be reported in the following:

- Primary and secondary side heat balances.
- Any other known variations in calculations regarding hot and cold leg temperatures.
- Any spurious behavior of the thermocouples.

The raw data both from the computer and toggle switches was analyzed by the Nuclear Operations Group to assure that the data were consistent. Based on the information provided by the Nuclear Operations, the local and volume weighted mean upper head region fluid temperature was computed.

468 172

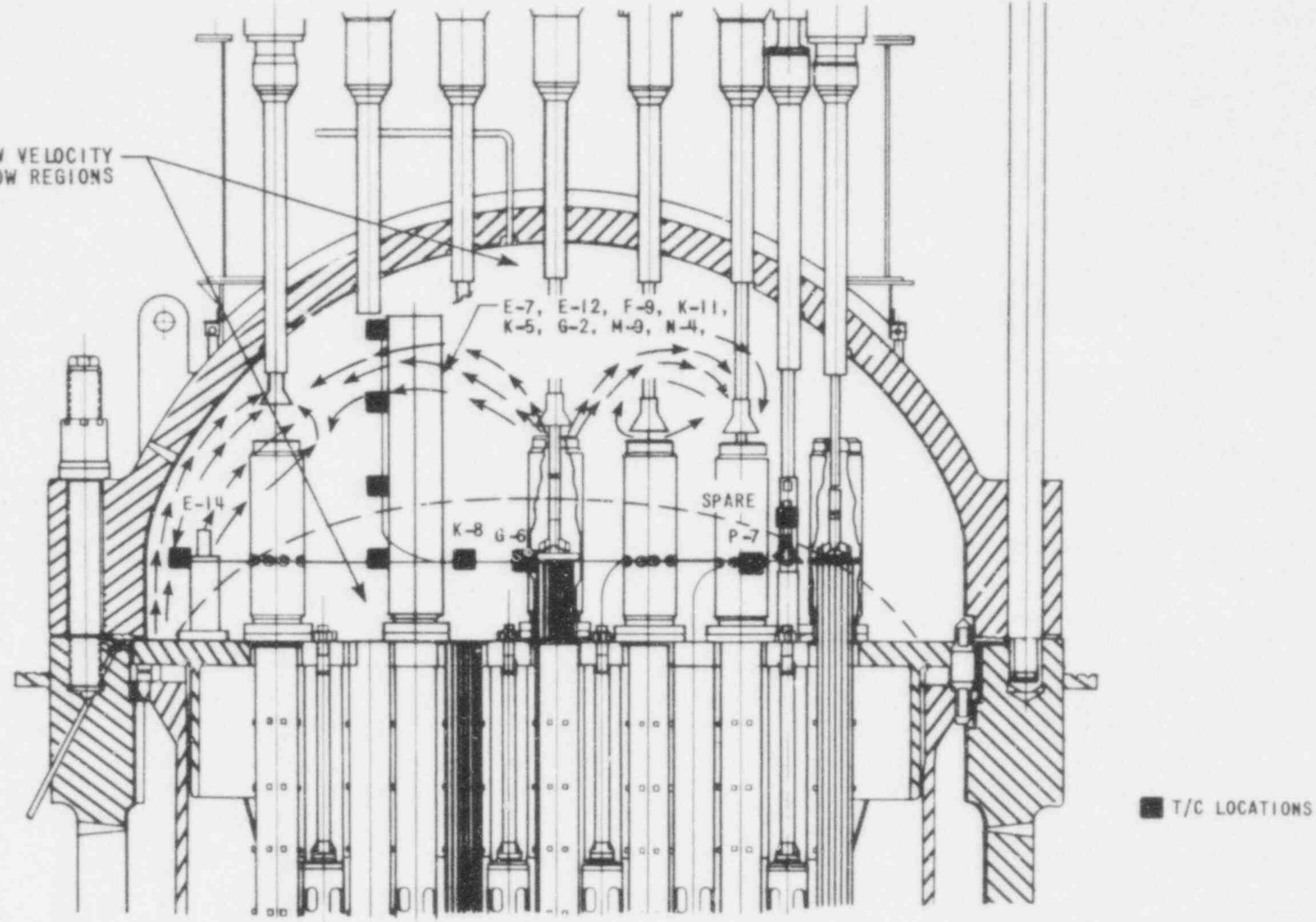

13465-49

Figure 4-9. Farley Unit 1 3-Loop Upper Head Region Density Controlled Flow Pattern

468 173

With respect to the UHI plants, the in-plant measurement program objective is to verify that the upper head temperature corresponds to T_{cold}. As a result of the initial assumption that the vessel upper head region fluid temperature was maintained at T_{cold}, all NRC licensing reviews for the UHI design were based on the premise that no flashing occurred in the upper head prior to injection. The NRC indicated that if flashing occurred in the region before injection, it would probably be necessary to submit a revised UHI ECCS model for approval by the staff; this would have a major impact on the plant schedule. It was concluded that sufficient excess flow was present in the UHI plants to "return" the upper head temperature to T_{cold}. By committing the excess flow, it would not be necessary to submit a revised model to the NRC for approval. Based on the results of the 1/5-scale model test (see section 3), modifications were made to all domestic UHI plants such that approximately four percent of the total vessel flow enters the vessel upper head region. To verify that the upper head region of the UHI plant is maintained at T_{cold}, instrumentation has been provided in McGuire Unit 1 and Sequoyah Unit 1. Each plant is equipped with five T/C's located in the core exit thermocouple conduits between the upper support plate and upper support plate flange as shown in figure 4-10. As discussed in section 3, this region possesses the greatest likelihood of having a fluid temperature greater than T_{cold}. The in-plant measurements are to be obtained during plant startup according to the same format presented for the Farley plant.

4-5. PREDICTED UPPER HEAD REGION MEAN TEMPERATURE

Predictions of the mean upper head region fluid temperature, expressed as the percent of difference between T_{cold} and T_{hot} have been made for all plants included in the in-plant measurement program. The predictions were based on the results of the TORCH code as a function of the following parameters and uncertainties:

- Head cooling flow rate with an uncertainty of ±7 percent of the best-estimate value.
- The temperature of the fluid entering the upper head region via the guide tubes, on a best-estimate basis, is approximately equal to the vessel hot leg temperature (T_{hot}) plus 4.5°F. The minimum anticipated fluid temperature corresponds to T_{hot} and the maximum corresponds to a value which is 14 percent greater than the nominal vessel temperature rise.
- The hydraulic loss coefficients of the guide tubes with an uncertainty of ±10 percent of the best-estimate value.

468 174

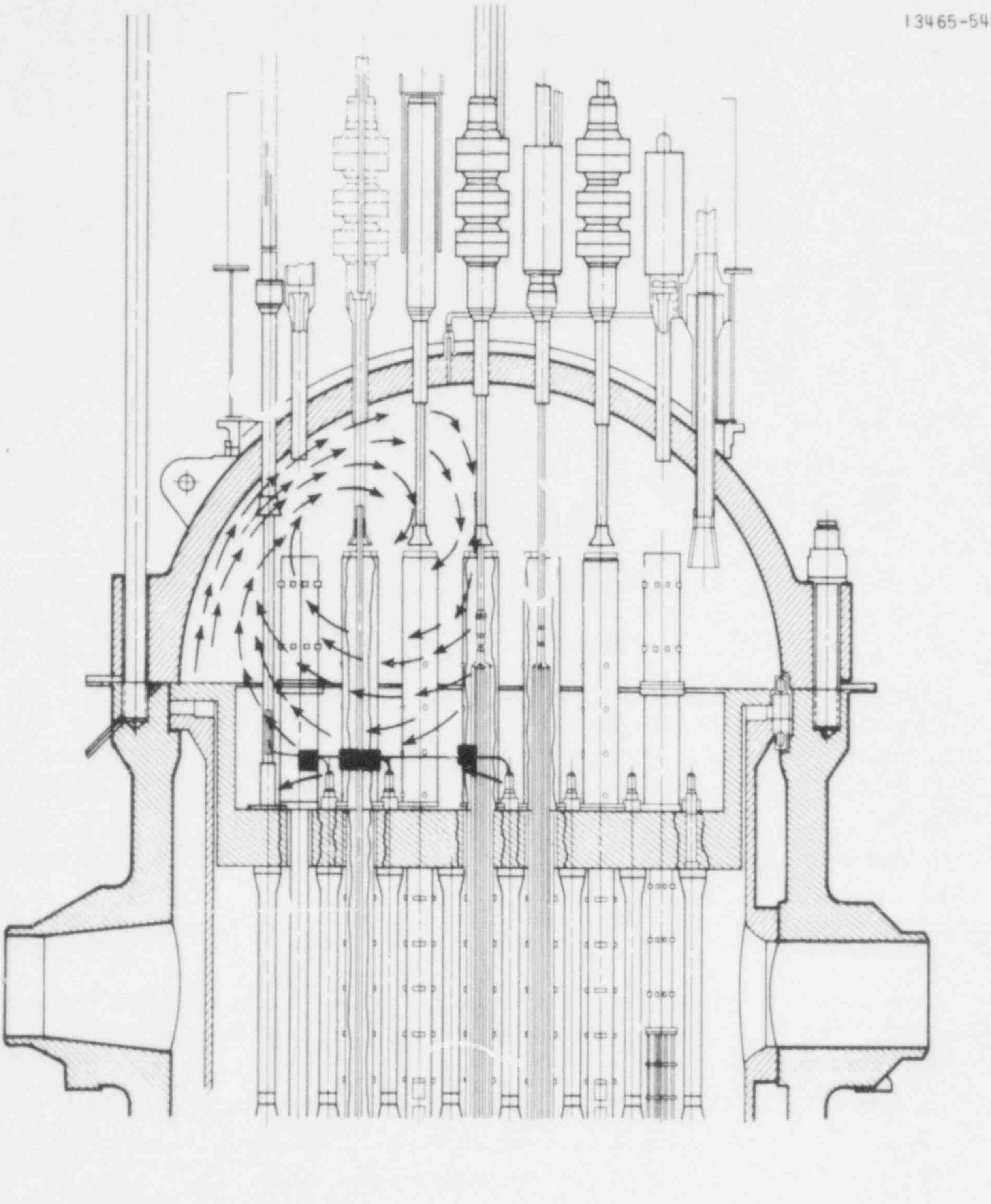

Figure 4-10. W. B. McGuire Unit 1 4-Loop Upper Head Thermoccuple Schematic

468 175

Tabie 4-2 presents a summary of the minimum, best estimate, and maximum anticipated mean vessel upper head region fluid temperature for each of the plants in the measurement program. Figures 4-11 through 4-15 graphically present the predicted relationship between the upper head temperature and the head cooling flow.

It can be seen from table 4-2 that on a best-estimate basis all plants, with the exception of McGuire and Sequoyah, have relatively "hot" heads and the variation around the best estimate is in the range of ±7 percent of the difference between T_{cold} and T_{hot}.

TABLE 4-2

PREDICTED MEAN UPPER HEAD REGION FLUID TEMPERATURE

Plant	Mean Upper Head Region Fluid Temperature (% of Difference Between T_{cold} and T_{hot})		
	Minimum	Best Estimate	Maximum
R. E. Ginna	[ ][c,e]	[ ][c,e]	[ ][c,e]
H. B. Robinson			
Surry 1			
Turkey Point 4			
J. M. Farley 1			
Zion 2			
McGuire 1			
Sequoyah 1			

As indicated by figures 4-11 through 4-15, the amount of flow required to "return the upper head region to T_{cold}" varies among plant types. The 2-loop 14 x 14 plant (figure 4-11) and 3-loop 15 x 15 plants (figures 4-12 and 4-13) contain guide tubes with significantly lower hydraulic resistance than the 3-loop 17 x 17 plant (figure 4-14) and 4-loop 15 x 15 plant (figure 4-15). The figures also depict the combined effect of uncertainties associated with the temperature of the fluid entering the head region via the guide tubes and the guide tube hydraulic loss coefficient.

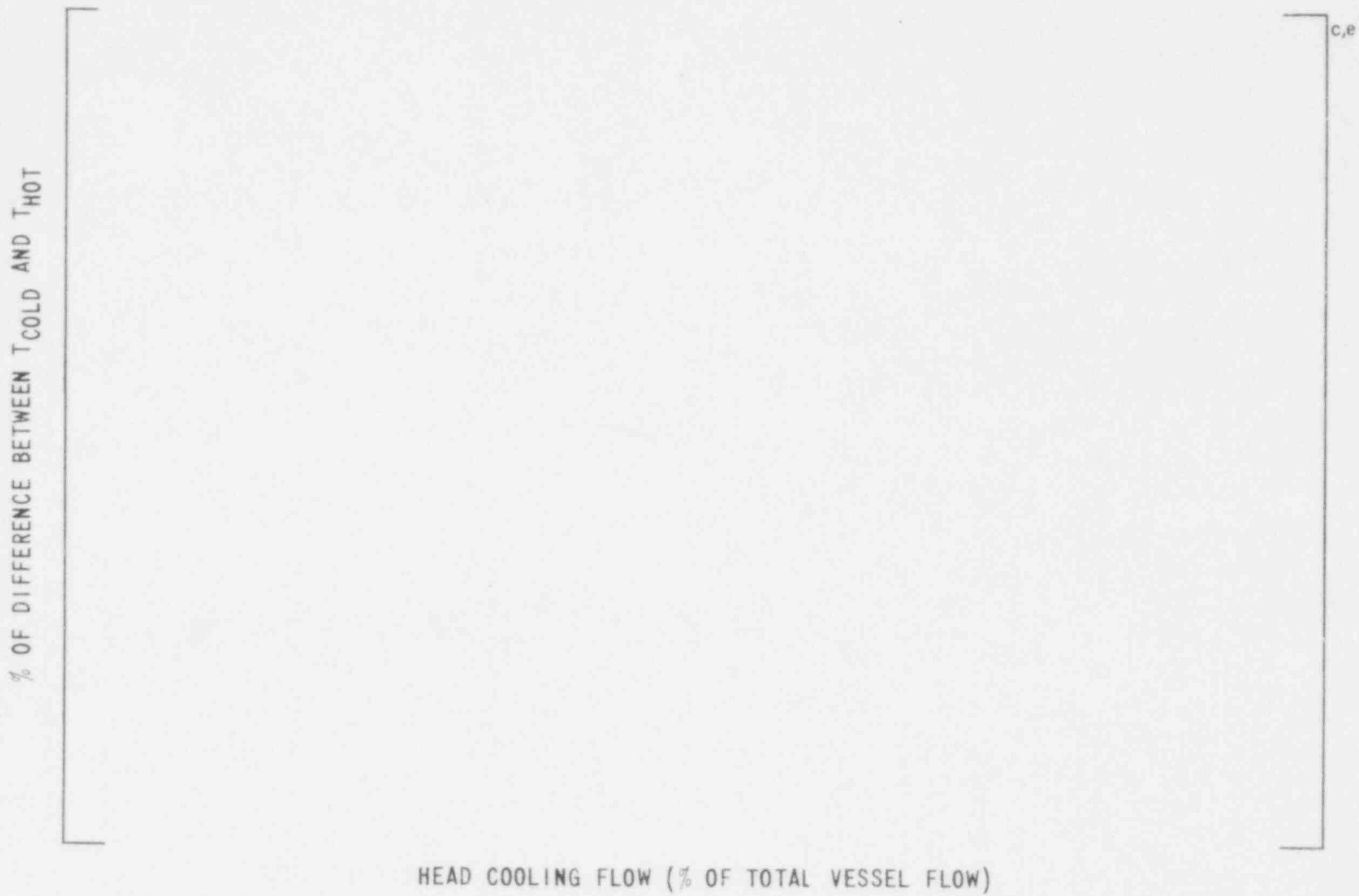

13465-55

Figure 4-11. R. E. Ginna Predicted Mean Upper Head Region Fluid Temperature Versus Head Cooling Flow Rate

468 177

13465-56

Figure 4-12. Turkey Point 4 and H. B. Robinson Predicted Mean Upper Head Region Fluid Temperature Versus Head Cooling Flow Rate

468 178

% OF DIFFERENCE BETWEEN T_{COLD} AND T_{HOT}

c,e

HEAD COOLING FLOW (% OF TOTAL VESSEL FLOW)

Figure 4-13. Surry 1 Predicted Mean Upper Head Region Fluid Temperature Versus Head Cooling Flow Rate

13465-57

468 179

Figure 4-14. J. M. Farley 1 Predicted Mean Upper Head Region Fluid Temperature Versus Head Cooling Flow Rate

13465-58

13465-59

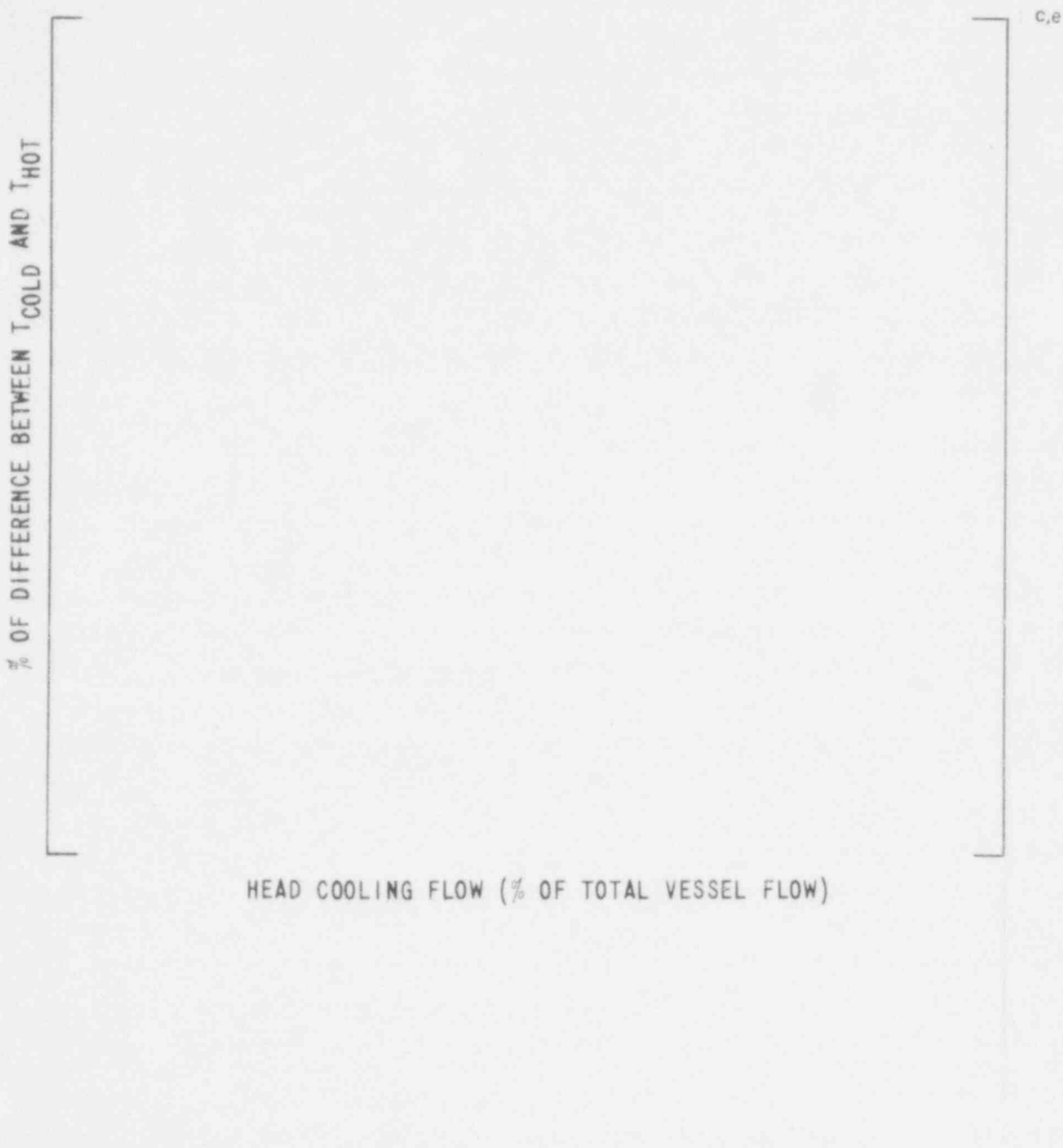

Figure 4-15. Zion 2 Predicted Mean Upper Head Region Fluid Temperature Versus Head Cooling Flow Rate

468 181

Based on uncertainties, there is a head-cooling flow difference of approximately one percent of total vessel flow between the amount of flow required to assure T_{cold} and the amount of flow which might result in T_{cold}. The head cooling flow rate, indicated by a triangle on each of the figures, corresponds to the value at which T_{cold} fluid will exit all guide tubes, accounting for all adverse uncertainties. The minimum head cooling rate which might result in T_{cold} for the upper head temperature is based on all uncertainties being favorable and no T_{hot} fluid entering the upper head region.

4-6. IN-PLANT UPPER HEAD TEMPERATURE MEASUREMENTS

Data have been obtained from all operational plants participating in the upper head temperature measurement program. Sequoyah 1 and McGuire 1 data will be obtained during the initial phases of plant operation. It should be noted that for the two upper head injection plants cited above, the temperature measurements will confirm that the upper head region fluid temperature corresponds to T_{cold}.

The in-plant data were obtained for power levels ranging from hot standby to full-power operation. Numerous sets of data have been received from each plant to verify consistency and to observe any apparent trends. The hot standby data were employed to cross-calibrate the upper head thermocouples, cold leg RTD's and hot leg RTD's under isothermal conditions. By determining the calibration factors at the hot standby conditions, the potential uncertainty in the T/C measurements is significantly reduced. The calibration factors were applied to each thermocouple measurement and the "% of the difference between T_{cold} and T_{hot}" was computed. Data for hot standby conditions have not been obtained at Surry 1. Therefore, it has not been possible to compute accurate upper head temperatures for this plant. For all plants except J. M. Farley 1 the mean upper head temperature was represented by determining the arithmetic average of all thermocouple measurements, primarily due to the limited number of upper head region thermocouples. With respect to J. M. Farley, the mean upper head temperature represents a volume-weighted value. Approximately 38 percent of the upper head fluid volume is located above the top of the upper guide tubes and 62 percent of the fluid volume is below the top of the upper guide tubes. As discussed previously, the Farley instrumentation is distributed both axially and radially in the upper head region and therefore each of the thermocouples can be associated with a fraction of the upper head fluid volume.

A summary of the in-plant measurements is presented in table 4-3. The table presents the maximum and minimum values measured, along with the mean of all the data for a given plant. In general, there is about a ±6 percent variation around the mean. The variation appears to be random. No trends regarding any influence of RCC insertion or burnup were apparent.

468 182

TABLE 4-3
MEASURED UPPER HEAD REGION FLUID TEMPERATURES

Plant	Upper Head Region Fluid Temperature (% of Difference Between T_{cold} and T_{hot})		
	Minimum	Mean	Maximum
R. E. Ginna H. B. Robinson Turkey Point 4 Surry 1 J. M. Farley 1 Zion 2	[ ] [b,c,e]	[ ] [b,c,e]	[ ] [b,c,e]

a. No data have been received at hot standby conditions. When the hot standby data become available, an addendum will be added to this report.

Figures 4-16 and 4-17 present the J. M. Farley upper head region temperature measurement at 50 and 100 percent power. Based on the data presented in figures 4-16 and 4-17 it can be seen that the upper section of the vessel head region (levels A and B) is slightly lower in temperature than the lower section of the upper head region (levels C and D). These temperatures are consistent with a momentum-controlled flow pattern as discussed previously. The temperature variation between the minimum and maximum measured upper head region fluid temperature is less than 10°F; i.e., 7.6°F or 11.6 percent of the difference between T_{cold} and T_{hot}, and is therefore judged to be essentially uniform.

4-7. COMPARISON OF MEASURED AND PREDICTED TEMPERATURE

A comparison of the measured and predicted mean upper head region fluid temperatures is presented in table 4-4. It can be seen from the table that on a best-estimate basis the maximum variation between the measured and predicted mean is 2.5 percent of the difference between T_{cold} and T_{hot} or approximately 1.6°F. In addition, all of the measured means are within the uncertainty range associated with the predicted mean. Based on the above in-plant data the analytical technique employed to estimate the mean upper head region fluid temperature compared favorably.

468 183

13465-49

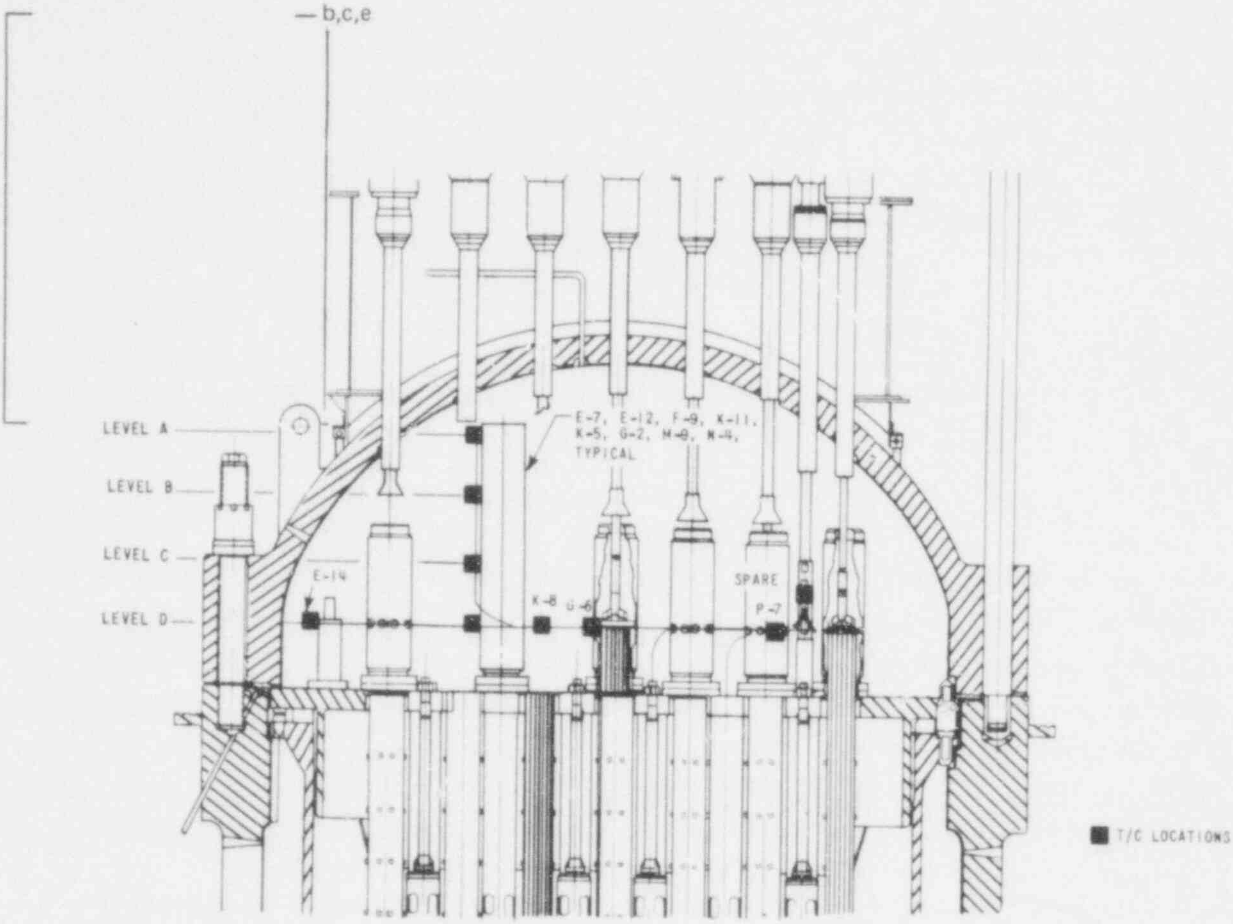

Figure 4-16. J. M. Farley Data at 50% Power

468 184

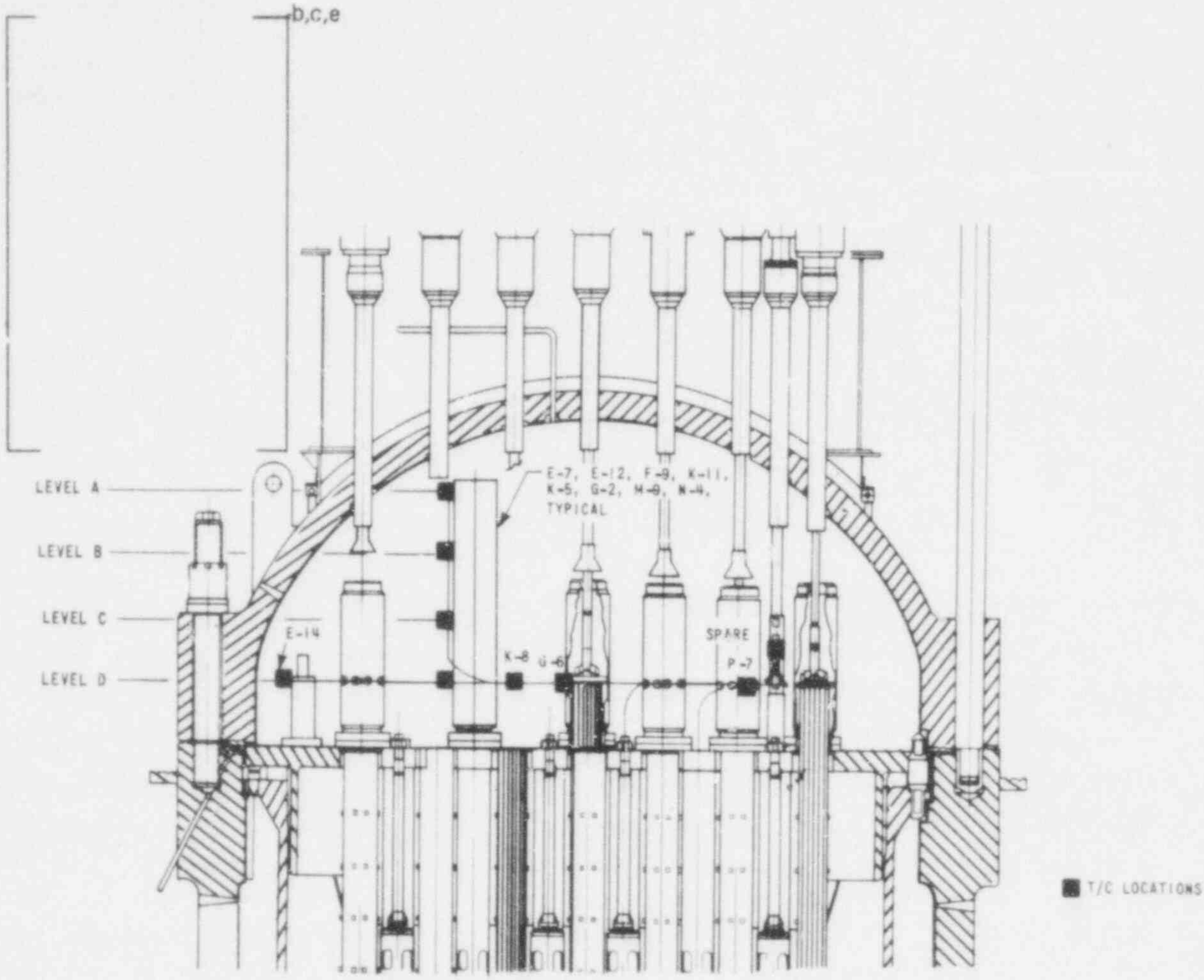

Figure 4-17. J. M. Farley Data at 100% Power

468 185

TABLE 4-4

COMPARISON OF IN-PLANT MEASURED AND PREDICTED MEAN UPPER HEAD REGION FLUID TEMPERATURES

Plant	Measured Mean (%)[a]	Predicted Mean, %[a]			Measured-Predicted Best Estimate (%)[a]
		Min	Best Est.	Max	
J. M. Farley	[ ] b,c,e	[ ] b,c,e	[ ] b,c,e	[ ] b,c,e	-0.1
H. B. Robinson					0.8
Turkey Point 4					0.8
R. Ginna					1.0
Zion 2					2.5

a. Percent of difference between T_{cold} and T_{hot}: $\frac{T_{head} - T_{cold}}{T_{hot} - T_{cold}}$ (100)

All discussions to this point have dealt with the mean upper head region temperature. The following discussion will address the maximum upper head region fluid temperature. Based on the results of the 1/5-scale model test (section 3) and the in-plant measurements, it is possible to estimate the upper head region maximum fluid temperature. The difference between the maximum and mean temperatures is primarily a result of the upper head region temperature variations associated with the flow pattern (spatial variations) and temperature fluctuations attributed to turbulence (variations in time).

Spatial variations in temperature were observed in both the Farley in-plant measurements and the 1/5-scale model test. Due to differences in the hydraulic characteristics of the plants it was necessary to determine a generalized relationship for spatial variations about the mean. The amount of head cooling flow required to return the upper head region to T_{cold} and the amount of head cooling flow entering the upper head region varies from plant to plant. However, the ratio of the head cooling flow divided by the amount of flow required to maintain the upper head at T_{cold} represents a value ranging from 0 to 1.0, which all plants have in common. By determining: (1) the ratio of head cooling flow to the head cooling flow required to maintain T_{cold}; and (2) the variation between the maximum averaged and overall mean upper head temperature observed at Farley and in the 1/5-scale model testing, it was possible to develop the generalized relationship depicted in figure 4-18.

468 186

13465-62

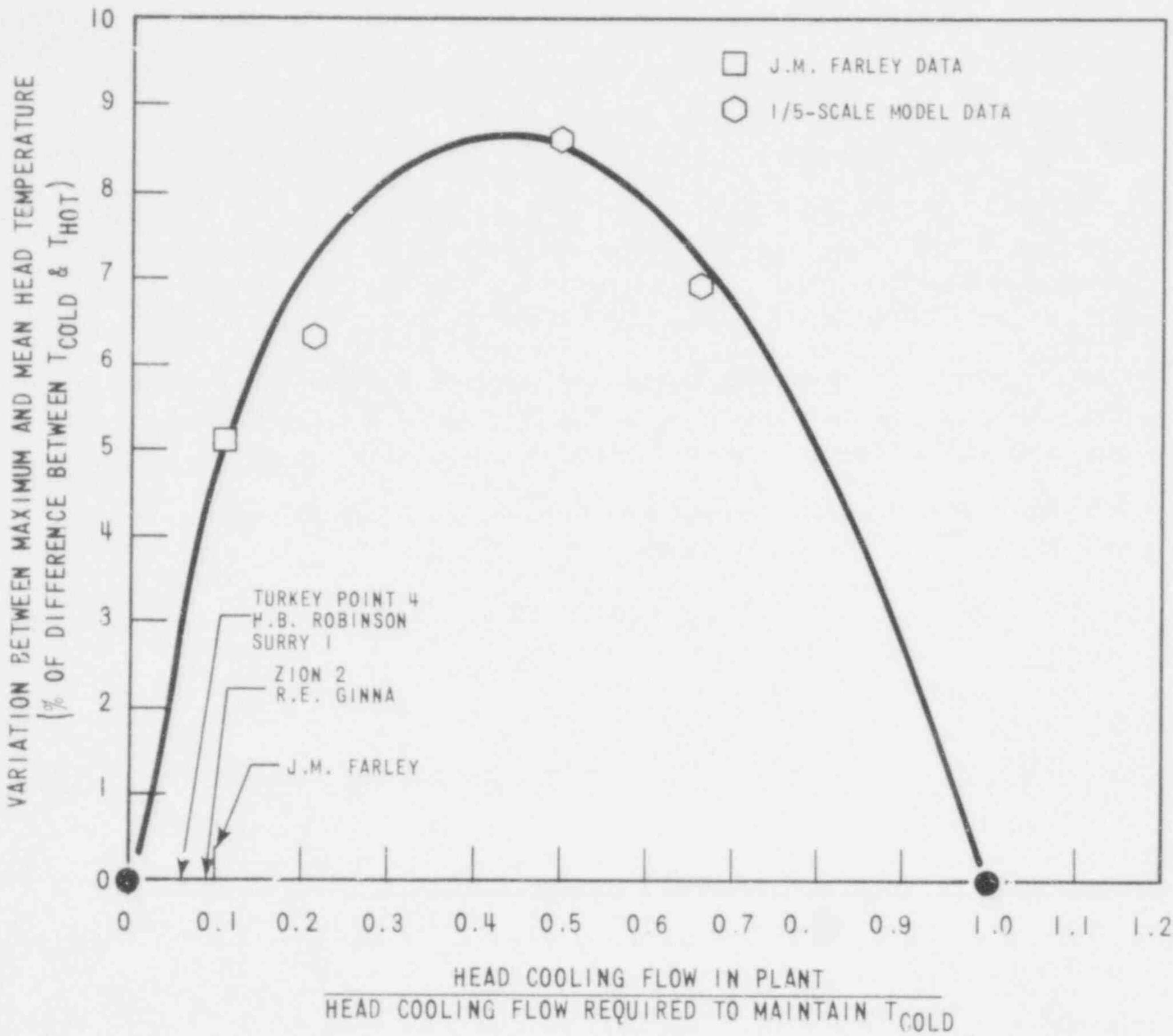

Figure 4-18. Spatial Variation Between the Maximum and Mean Upper Head Region Fluid Temperature

468 187

It can be seen from the figure that at the end points no variation exists and the maximum variation, 8.6 percent, exists at approximately the midpoint. As indicated by the figure, the spatial variation for the plants involved in the in-plant measurement program varies from 3.1 to 5.1 percent of the difference between T_{cold} and T_{hot}.

Temperature variations versus time, attributed to flow turbulence, were observed in the 1/5-scale model tests. The magnitude of these variations was typically ±1.7 percent of the difference between T_{cold} and T_{hot}.

In addition to the preceding variations in temperature, the potential error in the in-plant thermocouple must be accounted for. This variation could amount to 0.4 percent of the difference between T_{hot} and T_{cold}. This variation would be much larger if calibration data had not been at hot standby conditions.

Table 4-5 presents a comparison of observed and anticipated maximum upper head region temperatures. As indicated in the table, the observed maximum is always less than the anticipated maximum and the observed maximum is always less than T_{hot}.

In summary, all comparisons between the predicted and in-plant measurements, both the mean and maximum, show good agreement.

TABLE 4-5
COMPARISON OF OBSERVED AND ANTICIPATED MAXIMUM UPPER HEAT TEMPERATURE

Plant	No. of T/C's	Measured Mean (%)[a]	Spatial Variation Observed in 1/5-Scale Model and J. M. Farley (%)[a]	Timewise Variation Observed in 1/5-Scale Model (%)[a]	Potential T/C Variation (%)[a]	Anticipated Max. Upper Head T/C Temperature (%)[a]	Max. Measured T/C Temperature (%)[a]
J. M. Farley	13	[ ] b,c,e	5.1	1.7	0.4	[ ] b,c,e	[ ] b,c,e
H. B. Robinson	1		3.1	1.7	0.4		
Turkey Point 4	3		3.1	1.7	0.4		
R. Ginna	3		4.3	1.7	0.4		
Zion Unit 2	3		4.3	1.7	0.4		

a. Percent of different to T_{hot}: $\frac{T_{head} - T_{cold}}{T_{hot} - T_{cold}}$ (100)

SECTION 5
OVERALL CONCLUSIONS AND RESULTS

5-1. CONCLUSIONS

1. The TORCH code, which is employed to predict the mean upper head region fluid temperature of non-UHI and UHI plants, shows good agreement with the measurements.

2. The flow pattern in the upper head region is momentum-controlled. This implies that there is no significant flow stratification.

3. The upper head fluid temperature does not exceed the vessel hot leg temperature in non-UHI plants.

4. The upper head region fluid temperature in the UHI and non-UHI plants can be maintained at T_{cold} by providing sufficient head cooling flow to assure no core exit temperature fluid enters the head.

5-2. RESULTS

1. Standard plants (non-UHI) with 14x14 or 15x15 fuel assemblies have upper head region fluid temperatures ranging from 80 to 98 percent of the difference between T_{cold} and T_{hot} based on existing head cooling flow rates. Westinghouse LOCA analyses are conservatively based on the upper head region fluid temperature being 100 percent of the difference between T_{cold} and T_{hot}.

2. Standard plants (non-UHI) with 16x16 or 17x17 fuel assemblies have upper head region fluid temperatures ranging from 50 to 85 percent of the difference between T_{cold} and T_{hot} based on existing head cooling flow rates. Westinghouse LOCA analyses are conservatively based on the upper head region fluid temperature being 100 percent of the difference between T_{cold} and T_{hot}. Should it become necessary at some time in the future to account for an upper head region fluid temperature less than T_{hot}, Westinghouse would verify that the value employed is conservative.

3. Westinghouse has incorporated the capability to maintain the vessel upper head region fluid temperature at the cold leg value in all reactor internals fabricated after November 1976. In addition the technology has been developed to incorporate the T_{cold} capability for reactor internals in the field. In the future Westinghouse may exercise the option of maintaining a cold leg fluid temperature in the vessel upper head. Should this occur, the LOCA analyses would be based on the cold leg temperature (as is the case currently for domestic UHI reactor internals).

APPENDIX A
THE TORCH COMPUTER CODE

[ ][c,e]

468 192

APPENDIX B
PROPERTIES OF AQUEOUS SODIUM CHLORIDE SOLUTIONS

AQUEOUS SODIUM CHLORIDE SOLUTIONS

HEAT CAPACITY

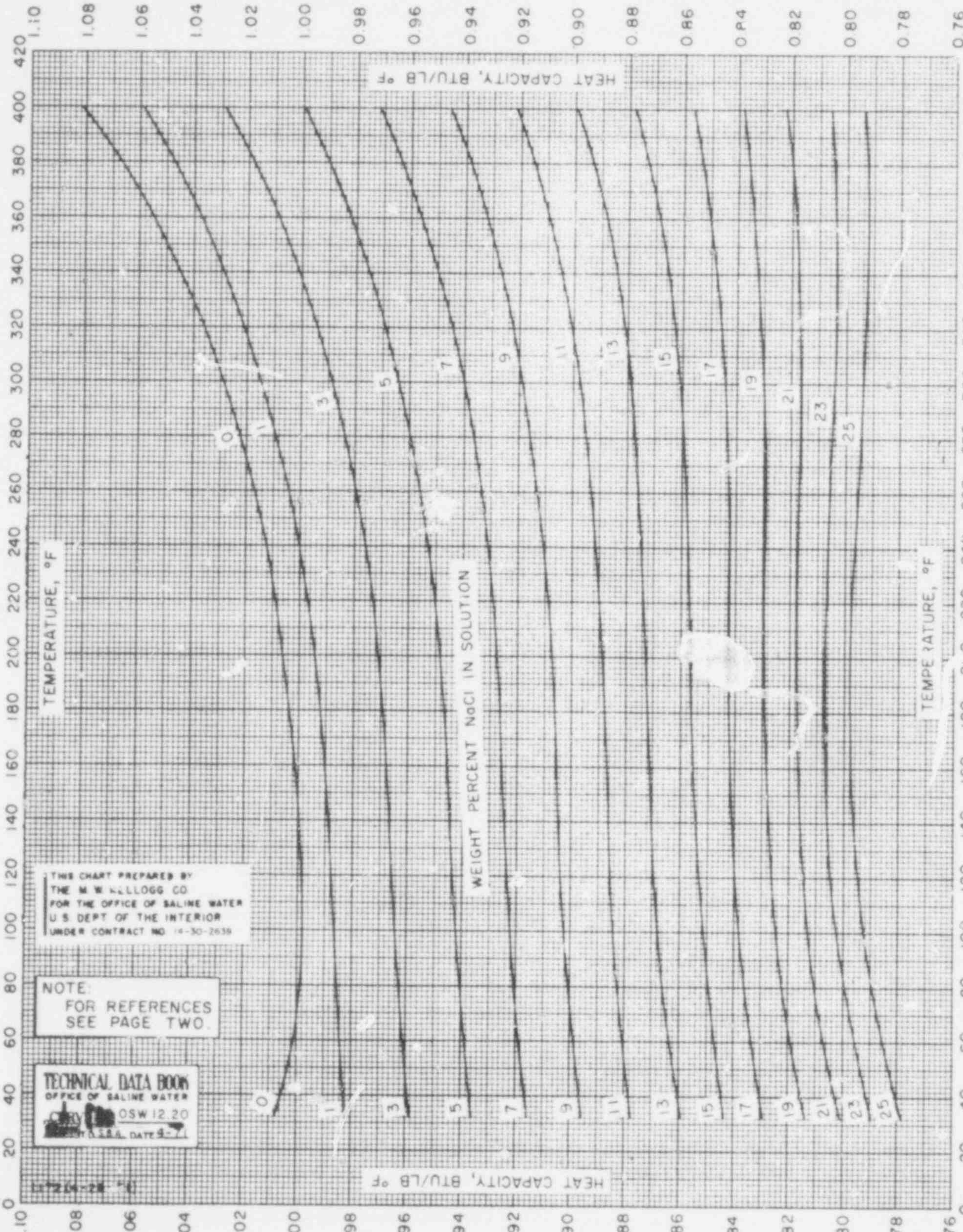

AQUEOUS
SODIUM
CHLORIDE
SOLUTIONS

HEAT CAPACITY

REFERENCES:

1. *Air Conditioning Refrigerating Data Book*, 9th Ed., p. 8-07, The American Society of Refrigerating Engineers, New York, N.Y. (1955).
2. Badger, W.L., and Baker, E.M., *Inorganic Chemical Technology*, p. 221, McGraw-Hill Book Co., Inc., New York (1928).
3. Dorsey, N.E., *Properties of Ordinary Water-Substance*, p. 258, Reinhold Publishing Corp., New York (1940).
4. *International Critical Tables*, 2, 328 (1927); 5, 115 (1929), McGraw-Hill Book Co., Inc., New York, N.Y.
5. Jessup, R.S., *Refrig. Eng.*, 40, 100 (1940).
6. Keenan, J.H., and Keyes, F.G., *Thermodynamic Properties of Steam*, John Wiley and Sons, Inc., New York, N.Y. (1936).
7. Lipsett, S.G., Johnson, F.M.G., and Maass, O., *J. Am. Chem. Soc.*, 49, 1940 (1927).
8. Parker, V.B., *Thermal Properties of Aqueous Uni-Univalent Electrolytes*, NSRDS-Nat. Bur. Stand. 2, Table XIV A (April 1, 1965).
9. Randall, M., and Rossini, F.D., *J. Am. Chem. Soc.*, 51, 323 (1929).
10. Rutskov, A.P., *J. Applied Chem. (U.S.S.R.)*, 21, 820 (1948).
11. Sverdrup, H.U., Johnson, M.W., and Fleming, R.H., *The Oceans*, p. 61, Prentice-Hall, Inc., New York (1946).
12. U.S. Dept. of the Interior, Office of Saline Water Research and Development Progress Report No. 227, p. 31 (Dec. 1966).
13. U.S. Dept. of the Interior, Office of Saline Water Research and Development Progress Report No. 522 (March 1970).
14. University of California, C.A. Bromley to H. Ozkardesh, The M.W. Kellogg Co., *Heat Capacity of Sodium Chloride Solutions*, letter dated Oct. 27, 1970.
15. Unterberg, W., Report No. 64-21: *Thermophysical Properties of Aqueous Sodium Chloride Solutions*, Univ. Calif. Dept. of Engg., Los Angeles, Calif. (May 1964).

172(4-29-71)

THIS SHEET PREPARED BY
THE M.W. KELLOGG CO.
FOR THE OFFICE OF SALINE WATER
U.S. DEPT. OF THE INTERIOR
UNDER CONTRACT NO 14-30-2639

THE USE OF ENTHALPY CHARTS IN THE CALCULATION OF HEAT AND MATERIAL BALANCES

Fresh water may be obtained from sea water by evaporation from the sea water, after which concentrated saline solution is discharged. Such a system is shown diagrammatically in Figure 1, wherein evaporation is effected by means of condensing steam in a coil, tube bank, or other suitable structure. The solution of a sample problem in which a steam rate is to be determined is illustrated.

The overall heat and mass balances for the depicted system will be set by certain fixed or required conditions, which in this case are set as:

1) System pressure = 14.7 psia
2) Fresh brine rate = 1000 gph
3) Fresh brine chlorinity = 19.0
4) Spent brine chlorinity = 100.0
5) Available steam pressure = 25.0 psia
6) Fresh brine temperature = 80°F

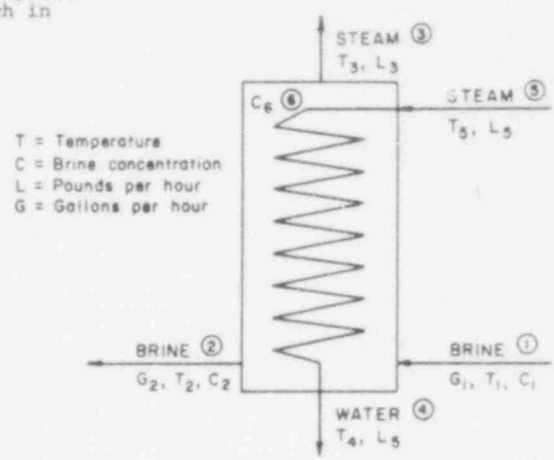

FIGURE 1

The following calculation then illustrates the derivation of overall heat and material balances:

Concentration C_1 is equivalent to 3.44 wt. % NaCl (OSW 0.021)

Concentration C_2 is equivalent to 18.0 wt. % NaCl (OSW 0.021)

Concentration C_6 is equivalent to 18.0 wt. % NaCl.

Since the system pressure = 14.7 psia,

Temperature T_3 = 220°F (OSW 12.50)

Temperature T_2 = 220°F (OSW 12.50)

Density of Stream 1 = 63.7 lbs/cu ft. (OSW 12.60)

Therefore, mass flow rate of Stream 1 = 8,515 lbs/hr

Therefore, by mass balance, $0.18\ L_2 = 0.0344\ L_1$

Therefore L_2 = 1,627 lbs/hr

and L_3 = 6,888 lbs/hr.

Enthalpy of Stream 1 = 47 Btu/lb (OSW 12.30)

Enthalpy of Stream 2 = 161 Btu/lb (OSW 12.30)

Enthalpy of Stream 3 = 1154 Btu/lb (OSW 10.31)

Enthalpy of Stream 4 = 208 Btu/lb (OSW 10.31)

Enthalpy of Stream 5 = 1161 Btu/lb (OSW 10.31)

Therefore, by enthalpy balance,

$$L_5 \times 1161 + 8515 \times 47 = 1627 \times 161 + 6888 \times 1154 + L_5 \times 208$$

From which the steam rate = 8196 lbs/hr.

THIS SHEET PREPARED BY
THE M. W. KELLOGG CO.
FOR THE OFFICE OF SALINE WATER
U.S. DEPT. OF THE INTERIOR
UNDER CONTRACT NO 14-30-2639

1169 (4-29-71)

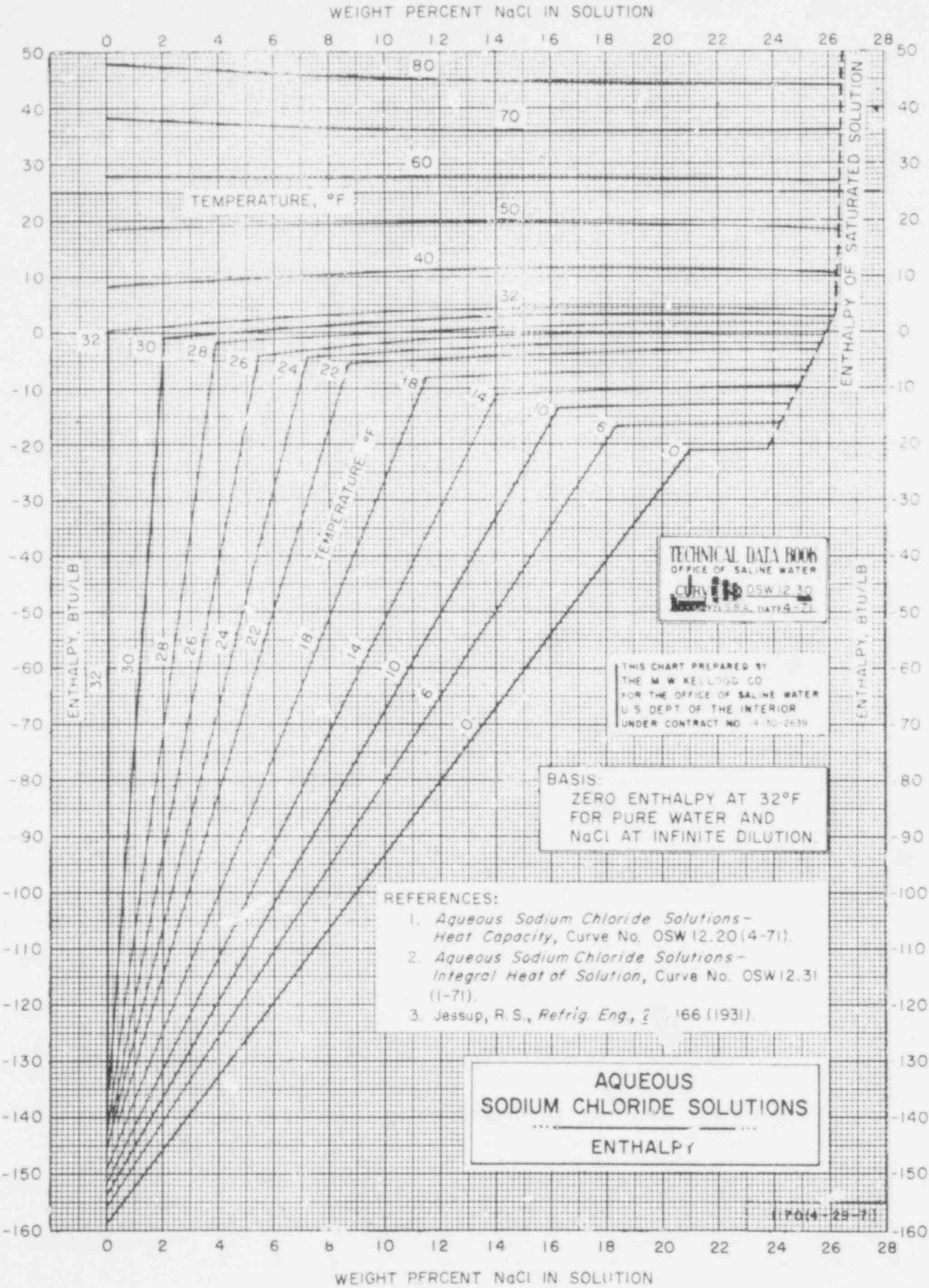
WEIGHT PERCENT NaCl IN SOLUTION
ENTHALPY, BTU/LB
TEMPERATURE, °F
ENTHALPY OF SATURATED SOLUTION
80
70
60
50
40
32
30
28
26
24
22
18
14
10
6
0
TECHNICAL DATA BOOK
OFFICE OF SALINE WATER
OSW 12.30
DATE 4-71
THIS CHART PREPARED BY
THE M. W. KELLOGG CO.
FOR THE OFFICE OF SALINE WATER
U.S. DEPT OF THE INTERIOR
UNDER CONTRACT NO. 14-30-2639
BASIS:
ZERO ENTHALPY AT 32°F
FOR PURE WATER AND
NaCl AT INFINITE DILUTION.
REFERENCES:
1. Aqueous Sodium Chloride Solutions - Heat Capacity, Curve No. OSW 12.20 (4-71).
2. Aqueous Sodium Chloride Solutions - Integral Heat of Solution, Curve No. OSW 12.31 (1-71).
3. Jessup, R.S., Refrig. Eng., 2 , 166 (1931).
AQUEOUS
SODIUM CHLORIDE SOLUTIONS
ENTHALPY
1 PG(4-29-71)

468 197

AQUEOUS SODIUM CHLORIDE SOLUTIONS

ENTHALPY

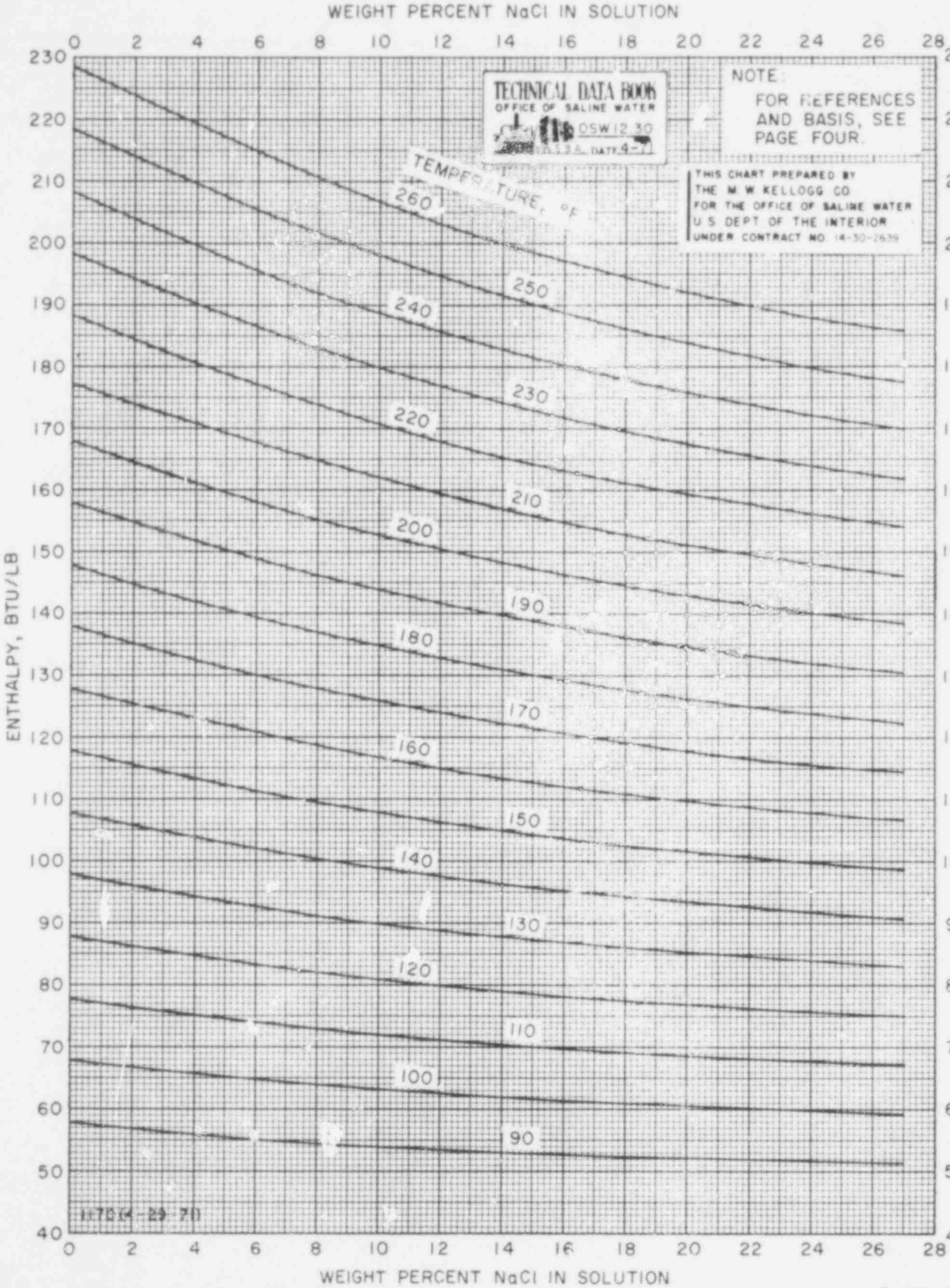

468 198

AQUEOUS SODIUM CHLORIDE SOLUTIONS

ENTHALPY

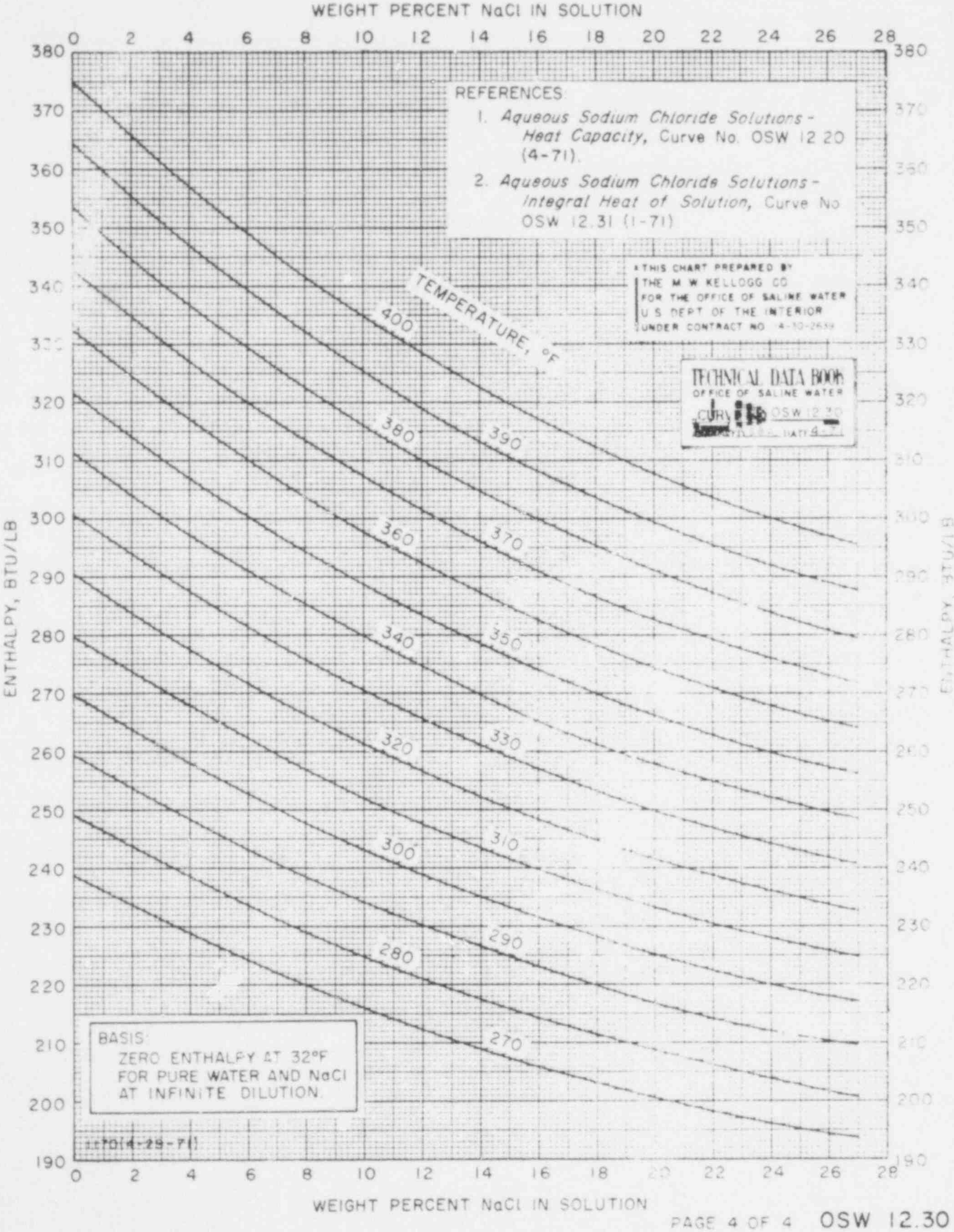

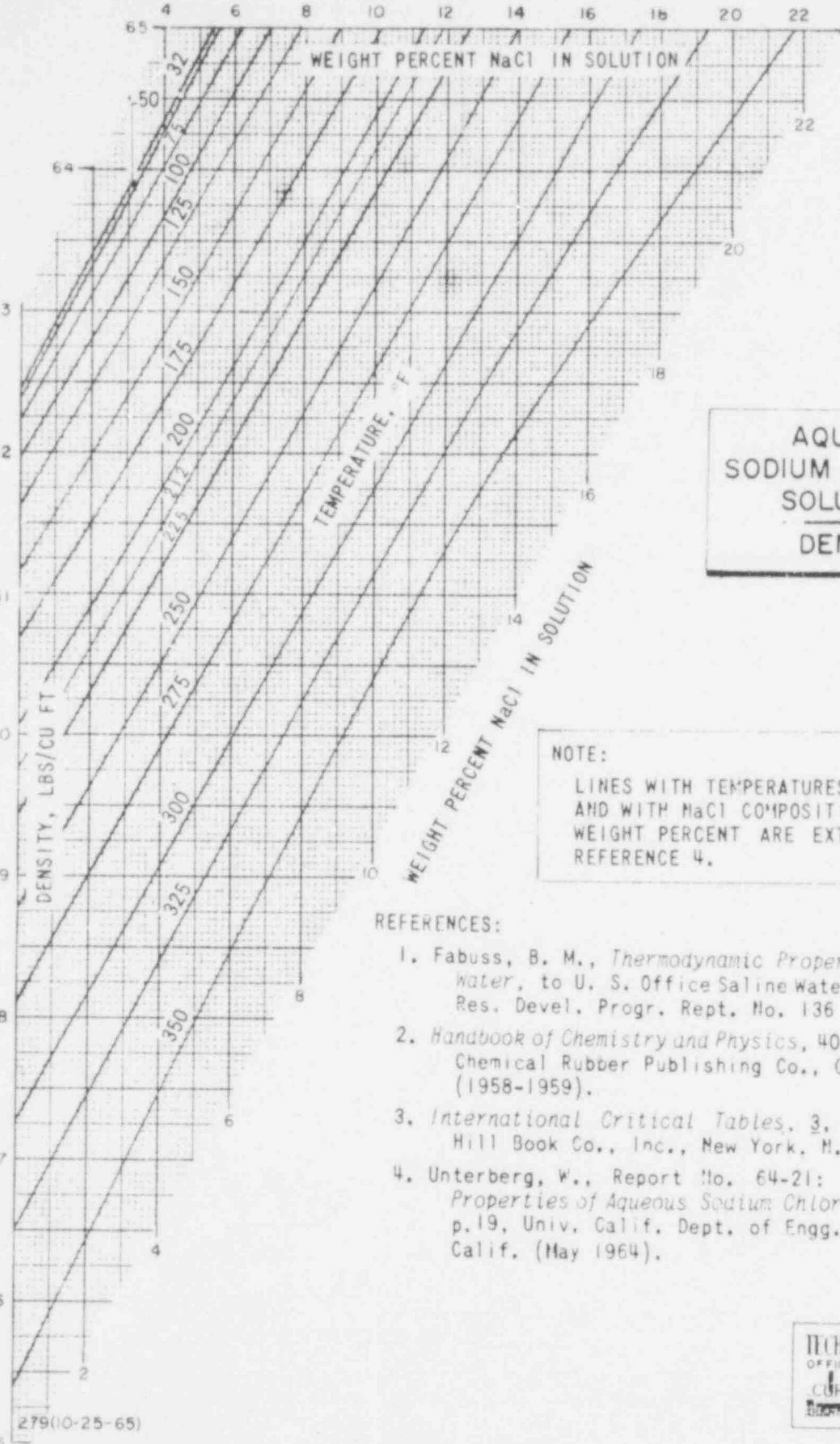

AQUEOUS SODIUM CHLORIDE SOLUTIONS

DENSITY

NOTE:

LINES WITH TEMPERATURES ABOVE 212 F AND WITH NaCl COMPOSITIONS ABOVE 12 WEIGHT PERCENT ARE EXTRAPOLATED BY REFERENCE 4.

REFERENCES:

1. Fabuss, B. M., *Thermodynamic Properties of Saline Water*, to U. S. Office Saline Water, Saline Water Res. Devel. Progr. Rept. No. 136 (July 1965).
2. *Handbook of Chemistry and Physics*, 40th Ed., p.2114, Chemical Rubber Publishing Co., Cleveland, Ohio (1958-1959).
3. *International Critical Tables*, 3, p. 79, McGraw-Hill Book Co., Inc., New York, N. Y. (1928).
4. Unterberg, W., Report No. 64-21: *Thermophysical Properties of Aqueous Sodium Chloride Solutions*, p.19, Univ. Calif. Dept. of Engg., Los Angeles, Calif. (May 1964).

TECHNICAL DATA BOOK
OFFICE OF SALINE WATER
CURVE NO. OSW 12.60
APPROVED W.C.S. DATE 1-66

AQUEOUS SODIUM CHLORIDE SOLUTIONS

DENSITY

NOTE:
LINES WITH TEMPERATURES ABOVE 212°F AND WITH NaCl COMPOSITIONS ABOVE 12 WEIGHT PERCENT ARE EXTRAPOLATED BY REFERENCE 4.

FOR REFERENCES SEE PAGE ONE.

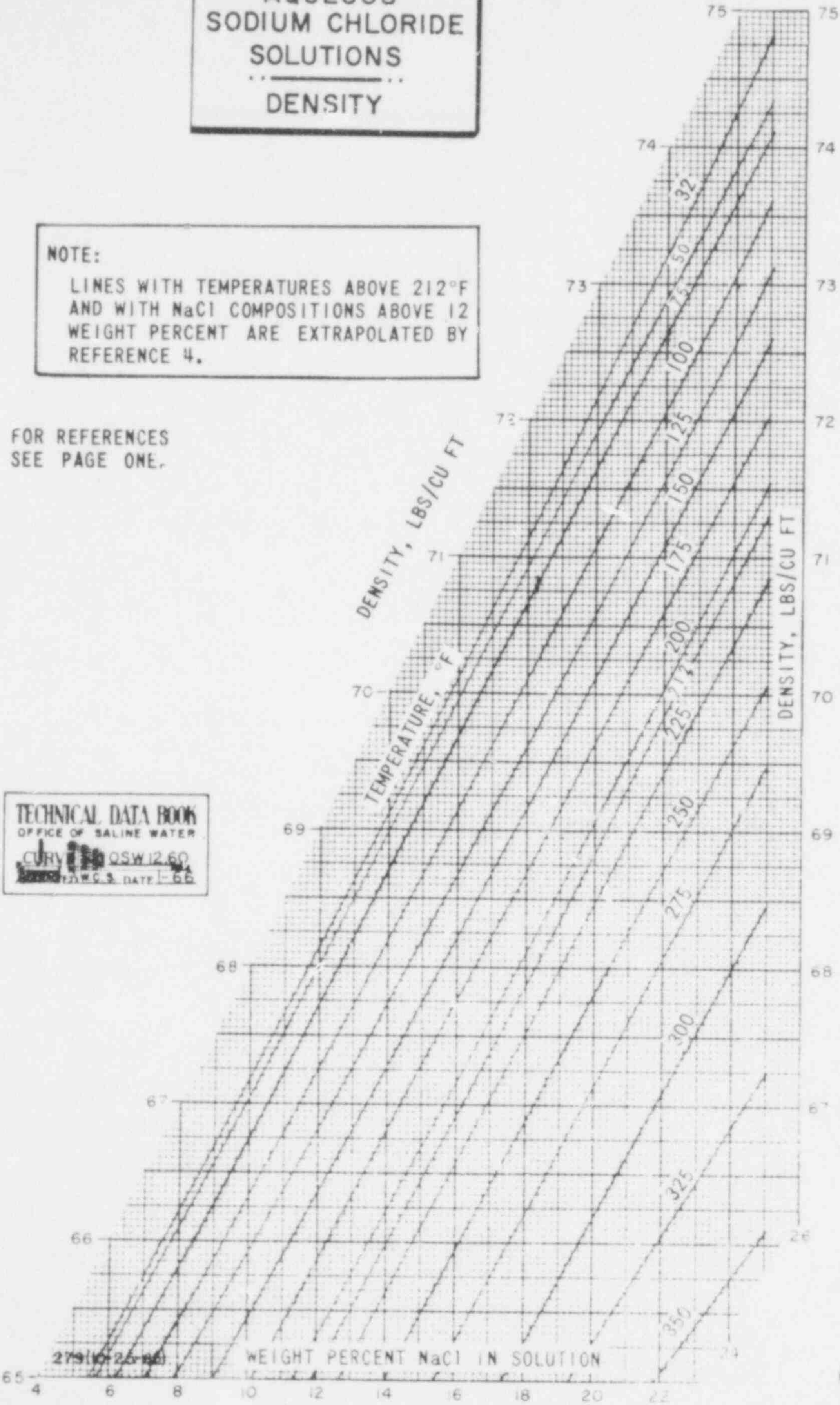

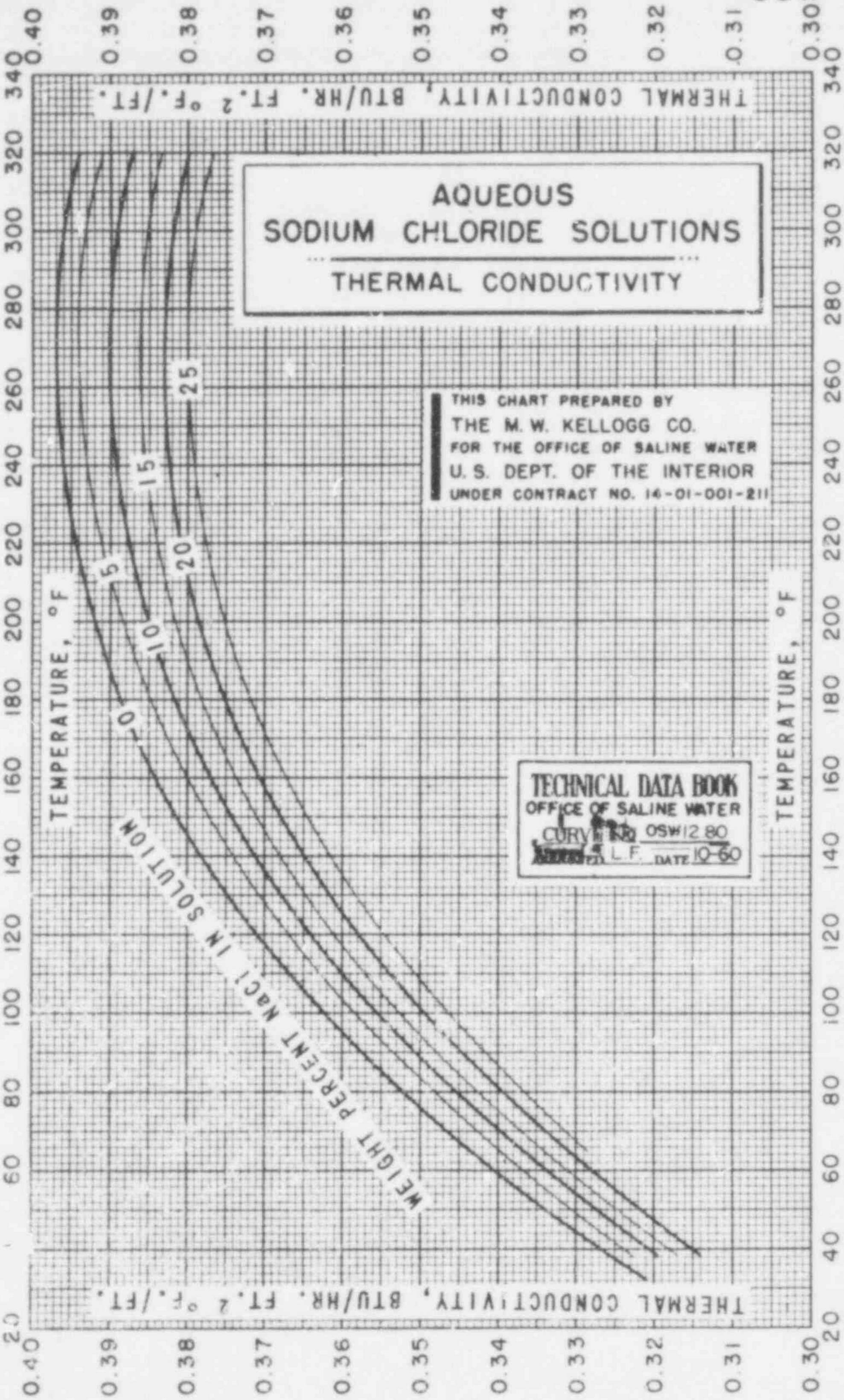

REFERENCES:

1. Dorsey, N.E., *Properties of Ordinary Water-Substance*, p. 273, Reinhold Publishing Corp., New York (1940).
2. Kaufmann, D.W., *Sodium Chloride*, pp. 620, 622, Reinhold Publishing Corp., New York (1960).
3. Riedel, L., *Chem.-Ingr.-Tech.*, 23, 59 (1951).

AQUEOUS SODIUM CHLORIDE SOLUTIONS

VISCOSITY

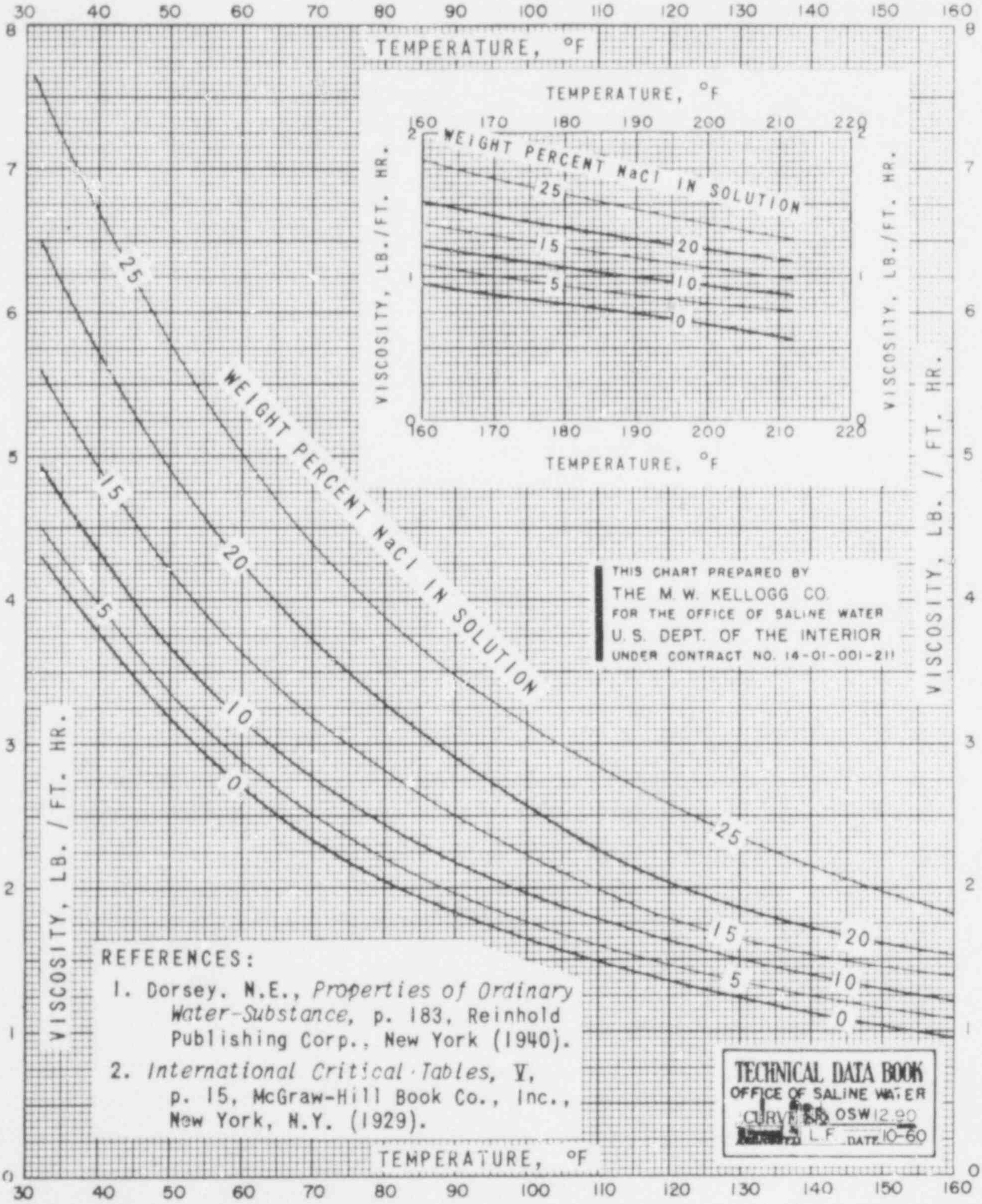

468 203

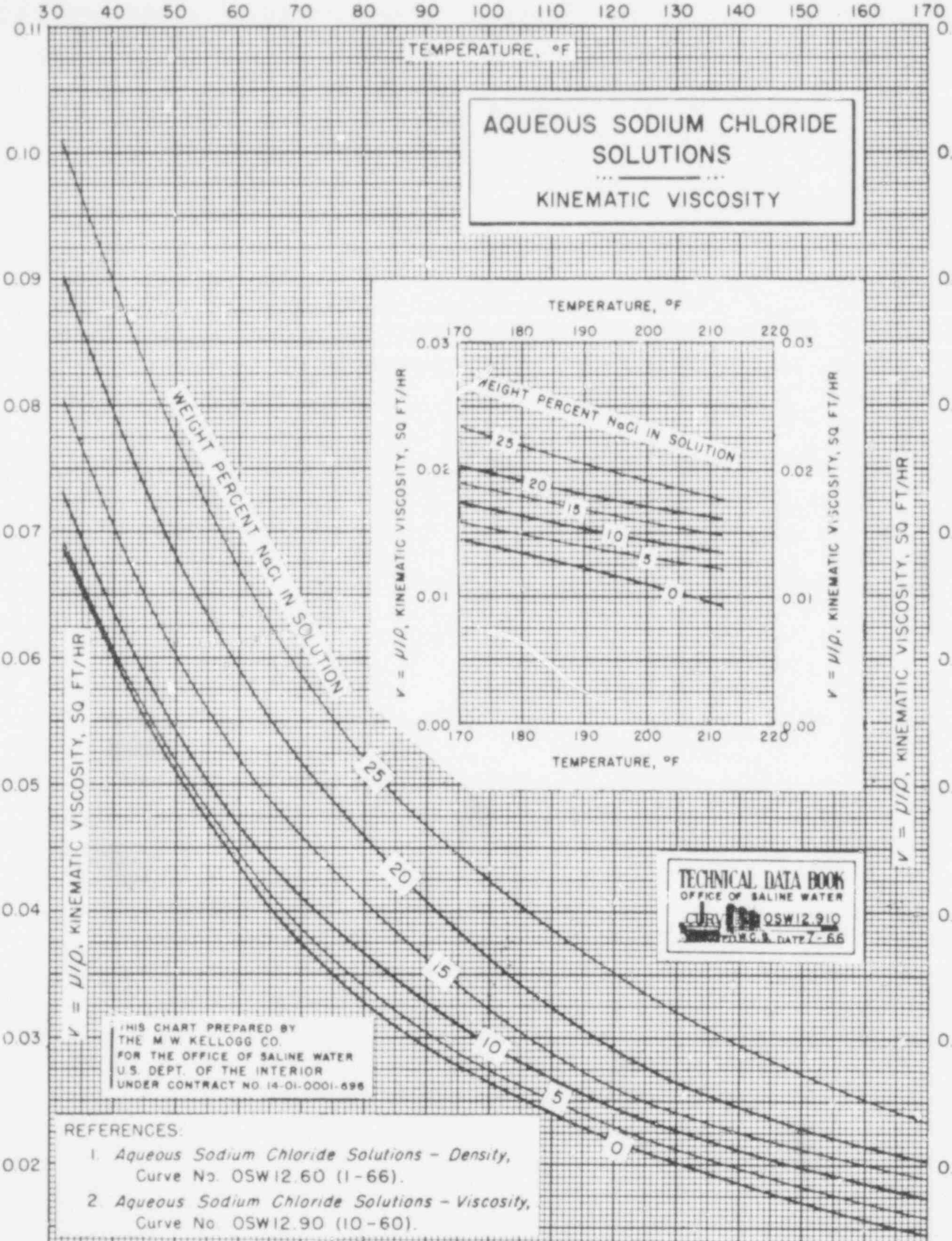
TEMPERATURE, °F
AQUEOUS SODIUM CHLORIDE SOLUTIONS
KINEMATIC VISCOSITY
WEIGHT PERCENT NaCl IN SOLUTION
25
20
15
10
5
0
ν = μ/ρ, KINEMATIC VISCOSITY, SQ FT/HR
TECHNICAL DATA BOOK
OFFICE OF SALINE WATER
OSW12.910
DATE 7-66
THIS CHART PREPARED BY
THE M. W. KELLOGG CO.
FOR THE OFFICE OF SALINE WATER
U.S. DEPT. OF THE INTERIOR
UNDER CONTRACT NO. 14-01-0001-696
REFERENCES:
1. Aqueous Sodium Chloride Solutions - Density, Curve No. OSW12.60 (1-66).
2. Aqueous Sodium Chloride Solutions - Viscosity, Curve No. OSW12.90 (10-60).
239 (6-7-66)